4-29-2016 12:00 AM

Mechanical Properties of Poly (vinyl alcohol) Based Blends and Composites

Nazanin Afghan
The University of Western Ontario

Supervisor
Dr. Andrew Hrymak
The University of Western Ontario

Graduate Program in Chemical and Biochemical Engineering
A thesis submitted in partial fulfillment of the requirements for the degree in Master of Science

Abstract

One of the most important product specifications in design of materials for different applications is to closely match desired mechanical properties of the target. The soft tissue could be very elastic such as blood vessels and skin, whereas others are soft and non-elastic such as fat tissue. Soft human tissue has a diverse structural component that give them the different feel, texture, shape, and mechanical properties.

Poly (vinyl alcohol) (PVA) as hydrophobic polymer has outstanding features such as very good physico-mechanical properties, nontoxicity and biocompatibility, and high swelling properties which makes them favorable for biomaterial and biomedical applications. By physically crosslinking PVA, one can eliminate residual amount of toxic crosslinking agent compared to chemically crosslinking. Moreover, by adding fillers (particle or fibers) to PVA and making PVA based blends, desirable mechanical properties can be achieved which, consequently can mimic the different human tissue texture and properties.

Different naturally based fillers such as chitosan, micro crystalline cellulose (MCC), and cotton fibers were added to improve the mechanical properties. Also, PVA was blended with xanthan gum and sorbitol to improve the elasticity of the material.

Keywords

Hydrogel, cryogel, PVA hydrogels, PVA-based composites, PVA based blends, cryogenic treatment, freeze-thawing, tissue phantoms.

Acknowledgment

I would like to acknowledge and show my gratitude to people who support, help, and guided me throughout my academic career:

I would like show my sincere gratitude my supervisor Dr. Andrew N. Hrymak for his guidance, support, and professional behavior during my academic career. I would also like to thank my co-supervisor Dr. Leonardo E. Millon for his help and advice on my research.

I would like to thank Primex Co., Iceland and Pharmacel Company for providing me with chitosan and MCC. I would like to thank all our laboratory members and research group for providing respectful environment for work.

I would like to thank my lovely parents Nasrin and Masoud, my brother Nima for their continuous support and unconditional love during my life. I would like to acknowledge the care and love of my grandmother. They have been great encouragement for me during my life.

I would also like to thank my dear friends Arash Sharif, Ehsan Ghiasi, Fatemeh Ferdosian, Gleb Meirson, Inès Griffoux, Daniel Park, Hojat Seyedy, Shengtai Zhou, Bilal Barakat Al-Bataina, Huda Herati, and Fabricio Guayaquil for their help, care, and support during my studies.

Table of Contents

List of Figures

List of Tables

Chapter 1 – Introduction

1.1. Background

Poly (vinyl alcohol) (PVA) is a hydrophilic polymer which is widely used due to: very good physico-mechanical properties, nontoxicity, biocompatibility, ease to form, and high swelling properties [1], [2]. Covalent, and physical crosslinking are the two different mechanisms for gelation of PVA [1], [3]–[8]. Physical crosslinking has the advantage of not leaving residual amount of toxic crosslinking agent. Therefore, it is more desired for biomedical applications. Physically crosslinked PVA cryogels have higher mechanical strength compared to chemically cross-linked PVA cryogels. Mechanical properties of PVA cryogels such as elasticity and strength are similar to soft tissue [9]–[12]. These characteristics can be controlled by degree of deacetylation, molecular mass of polymer, initial concentration of polymer in the solution, chain tacticity, chemical structure of gel-forming polymer material, thawing rate, duration of storing in frozen state, and repetition of freeze-thawing [1], [7], [8], [13]–[15].

Currently there are different ways for surgical training, such as: physical models, organs of animals and cadaver, and virtual reality [16]. Due to low availability and high cost of cadaver and moral values in use of animals as specimen, tissue phantoms can be used in medical training and education. The use of tissue phantoms for surgical training has the possibility of repeat or replay training with lower cost [17], [18]. Virtual reality provides a realistic simulation; but state of technology in software and hardware does not provide a realistic simulation of the tissue and all situations which may happen during the surgery [16]. Tissue-mimicking phantoms can be used in education, research, training residents, and surgical planning [17], [18]. Simulation training helps interns and surgical residents become familiar with standardized settings and learn in a non-risk environment and effective way [19]. In addition, realistic tissue phantoms are necessary for surgical trainings, which as for now only simple skills on these phantoms can be studied. Therefore, improving the mechanical properties of PVA hydrogels, that it is trying to imitate the properties and feel of target soft tissue, to make tissue-like phantoms is a better platform to train versus training on real humans in the operating room [16].

PVA hydrogels can give "feel" and "texture" of human tissue. This soft tissue could be very elastic such as blood vessels and skin, whereas others are soft and non-elastic such as fat tissue and other extracellular connective tissue around organs. Soft human tissue has a diverse structural component such as: elastin, collagen, glycosaminoglycans, proteoglycans, polysaccharides, and many others. The amount and structural arrangements of these components give them the different feel, texture, shape, and mechanical properties [20].

1.2. Objective

The objective of this research is to create new composites and blends, using PVA hydrogel as the main matrix material, and investigating the effect of different types of fillers (particulate or fibrous) and blends as to come up with improved feel and mechanical properties that match the most human-like soft tissue. Chitosan was chosen to be added to main matrix to increase the stiffness of the material. Chitosan is a popular and safe additive. Cotton fibers were added to PVA in order to improve the strength of the hydrogel. Cotton fibers are natural source of cellulose. It was expected that blending PVA with sorbitol give the elastic behavior to the hydrogel. Sorbitol is a food grade material, which is safe to use as additive.

Mechanical testing procedure for uniaxial tensile test, elongation at break, and suture tension pull through test was developed for testing PVA-based hydrogels. The goal of this research was to increase the elasticity and suture retention of final material.

1.3. Thesis Outline

Chapter 2 is a literature review of all relevant topics of this research. Polymeric gels, physically cross-linked cryogels is discussed followed by PVA hydrogels, influential factors of formation of PVA hydrogels their mechanism, and their applications. Particulate-reinforced fibrous-reinforced and hydrogel blends are discussed. In Chapter 3, materials, experimental procedure and test protocols are discussed. In Chapter 4, fitted models for mechanical testing of samples including: uniaxial strain-stress, elongation at break, and suture-tension pull through force are discussed. In

addition, a brief explanation of the statistical analysis is given in this chapter. Chapter 5 discusses the results achieved form all tests for the PVA-based hydrogel composites and PVA-based hydrogel blends. In Chapter 5 strain-stress data of all samples were compared with porcine aorta. Chapter 6 provides conclusions and recommendations.

Chapter 2 – Literature Review

2.1. Overview

The aim of this study is to investigate mechanical properties of PVA based blends and composites. PVA with particulate and fibrous fillers as reinforcing agents was investigated in biomedical applications. In addition, other polymer additives are also explored. Therefore, this chapter gives some information about polymer gels, more precisely Poly (vinyl alcohol) (PVA), cryogenic treatment, application of PVA cryogels, and PVA composites.

2.2. Polymeric Gels

Gels are systems containing polymer and immobilized solvent forming a 3D network by chemical and physical bonds connecting macromolecular chains [7], [8]. Polymeric gels form in a cycle with moderate freezing, hold in the frozen state and subsequently thawing the solution monomeric or polymeric precursors lead to polymeric cryogels [13]. The term cryogel was made by combining "cryo" (in Greek *kryos* means frost or ice) and "gel", emphasizing the specific formation of the gel [1]. The term hydrogel is used if the immobilized solvent is water. Hydrogels are hydrophilic polymer networks that exhibit the ability to swell in the presence of water, shrink in the absence of water, and absorb a large portion (up to 3000 times by weight) by weight of water in its network [7], [8], [14], [15].

Polymeric gel is a flexible network of crosslinked chains. There are two different mechanisms in gelation of gels: covalent, and physical crosslinking [3], [4]. Covalent crosslinking gel ("permanent" or "chemical" gel) is a good method to control crosslinking density. However, non-degradable crosslinking formation and toxicity of crosslinking agent should be taken into account [5]. "Physical" or "reversible" gels are formed when the network is held together by molecular entanglement or secondary forces such as H-bonding or hydrophobic forces, van der Waals forces, and ionic interactions [6]. Although, ionic crosslinking is a simple way to form gels, ions could be exchanged with other ions in aqueous environment and weaken the original properties of gel [15]. Calcium alginate is an example of this type of hydrogel [7], [14]. Gels formed under cryogenic

treatment (cryogels) are classified as physical gels. All these interactions in physical gels can be disrupted by changes in physical conditions (ionic strength, pH, temperature, and application of stress), whereas chemical gels are stable [8]. Chemical and physical gels are not homogenous due to clusters of molecular entanglement, and contain regions of low water swelling and high crosslink density, respectively [14]. Figure 2.1 provides physically and chemically synthesized hydrogels schematically.

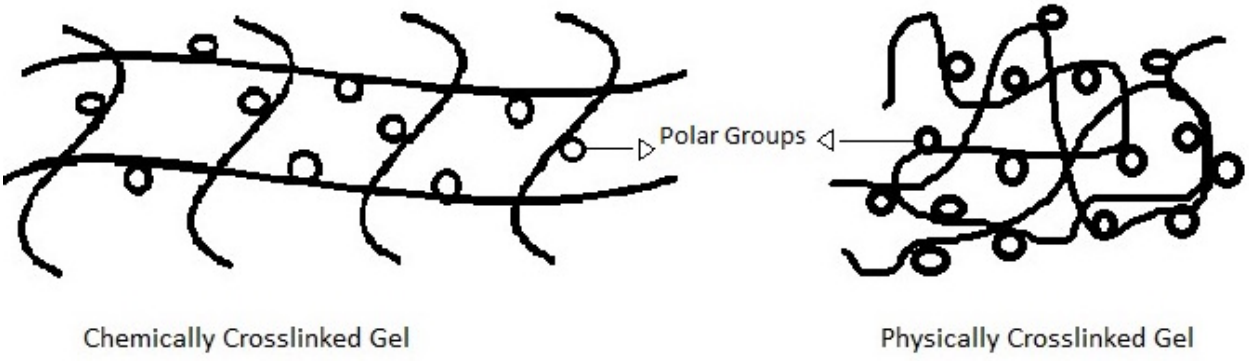

Figure 2.1 - Chemically and physically synthesized hydrogels.

Several studies on cryotropic gelation phenomena showed that cryogels can be made from precursor systems falling into five categories: colloidal dispersion (freezing of colloid sols leading to the arrangement of particle-to-particle contact), solutions of monomeric precursors (polycondensation in moderately frozen aqueous/organic solvent or chemically or radiation0induced crosslinking polymerization), solutions of high molecular weight precursors (curing the macromolecule by adding chemical agent or irradiation), solutions of self-gelling polymers (forming a non-covalent and physical gels), and solutions of polyelectrolytes containing low molecular weight or polymeric crosslinking counter ions (creating stable ionic bridges in between the polyelectrolytes) [13], [21]. The solvent must crystallize under freeze-thaw cycles. If the solvent goes through a glass transition state, unfrozen liquid micro phase is not established, hence, cryogel is not formed [1].

Hydrogels are widely used with potential applications as biomaterials in tissue engineering. Their structural similarity to macromolecular-based components in the body, biocompatibility, biological performance parameter (e.g. cell adhesion), controlled degradation, and swelling characteristic has been found a suitable option for tissue engineering applications [14], [22]–[25]. Hydrogels provide chemical balance between hydrogel and tissue, enabling water, ion, and metabolites exchange [25]. Moreover, elastic nature and viscoelastic behavior makes hydrogels suitable for tissue replacement [5].

Based on their natural or synthetic origin, hydrogels are divided into two categories. Hydrogels from natural polymers such as collagen and gelatin, hyaluronate, fibrin, alginate, agarose, and chitosan have been utilized in reconstruction of skin and liver, wound healing, skeletal muscle cells, dental impression, enable cell proliferation, and to assist bone formation [26]–[31]. Collagen is the most popular natural-derived polymer and can be formed as gel either physically or chemically. However, these gels are expensive and have low physical strength [32]. Poly (acrylic acid) and its derivatives, poly (ethylene oxide) and its copolymers, Poly (vinyl alcohol), polyphosphazene, and polypeptide are classified as synthetic hydrogels. PVA has been used in cartilage replacement, drug delivery applications, cardiovascular tissue replacement, skeletal tissue regeneration, and artificial extracellular matrices in tissue engineering [31]–[33].

2.2.1. Physical (non-covalent) Polymeric Cryogels

In general, non-covalent physical gels include a wide class of polymeric gels either formed in aqueous or organic media [34]–[38]. Polymer gel phase can be formed in one of the stages of cryogenic treatment:

- during freezing of initial structure (colloid dispersion of gelatinized starch),
- storage in the frozen condition (mostly formation of chemically crosslinked cryogels),
- thawing the frozen system (mainly non-covalent cryotropic gelation, for example, PVA in aqueous solution) [13].

Poly Vinyl alcohol (PVA) solutions (in water or DMSO) [39], [40], amylopectin, starch are some examples of non-covalent formation of cryogels. They can be cooled, stored at specific negative temperature, and then thawed to obtain the desired cryogel [13], [41], [42]. These cryogels are

thermally reversible: they can be dissolved in high temperatures and repeated freeze-thaw cycles form again a cryogel [2], [43].

The majority of studies in physical polymeric cryogels are related to PVA cryogels. This popularity of PVA based cryogels is due to outstanding features such as: availability, very good physico-mechanical properties, nontoxicity and biocompatibility, easily produced compared with other physical cryogels, and high swelling properties [1], [2]. PVA cryogels are formed when PVA solutions (organic or inorganic) are exposed to repeated freeze-thaw cycles [39], [44]. High swelling properties, blood compatibility, similar mechanical properties with natural tissue, compatible with human tissue, high dimensional stability, and being stable at room temperature make them favored in biomedical and biomaterial application. The main areas that PVA cryogels are used as biomaterials are wound dressing, contact lenses, biosensor, drug delivery, biosensors, and tissue replacement [5], [10], [14], [45]–[49].

2.3. Poly (vinyl alcohol) (PVA)

PVA has a quite simple chemical network with a pendant hydroxyl group. The monomer cannot be found in stable form. Therefore, it cannot be produced directly. PVA is obtained by radical polymerization of vinyl acetate to poly (vinyl acetate) (PVAc) followed by hydrolysis of PVAc to PVA. Since the hydrolysis reaction does not go to completion, PVA is always a copolymer of PVA and PVAc. PVA with high degree of hydrolysis (99%) is commercially available. Figure 2.2 shows the chemical reaction for producing PVA [5], [7], [10].

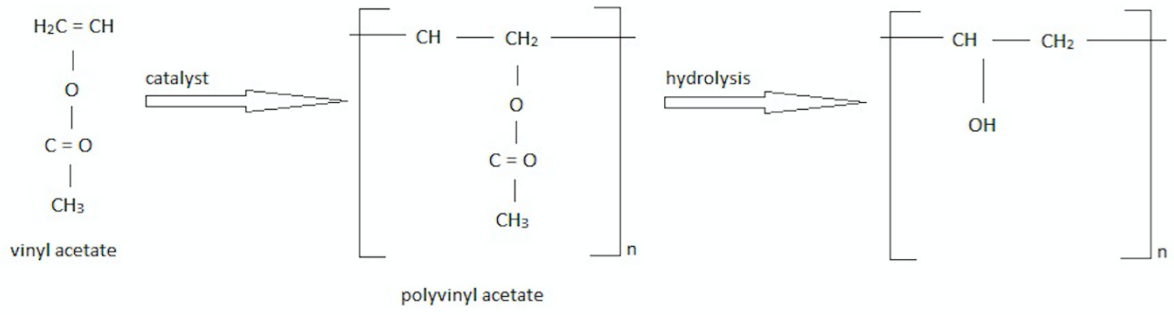

Figure 2.2 - Chemical reaction of producing PVA.

Degree of hydrolysis, which is an indicator of the presence of acetate groups in the polymer, affects polymer properties. It has been reported that PVA with high degree of hydrolysis (above 95%) has lower solubility in water. Due to hydrophobic acetate groups, the temperature must be raised to 70 °C in order to be dissolved in water. Also PVA grades with high degree of hydrolysis are harder to crystalize. Radical polymerization of PVAc and subsequent hydrolysis of PVAc to PVA, provides a wide molecular weight distribution. Since the molecular weight distribution affects crystalinization, mechanical strength, and diffusivity, the degree of the hydrolysis has great importance in different grades of PVA [7], [10].

PVA can be crosslinked either chemically or physically [6], [9], [45], [50], [51]. Formaldehyde, glutaraldehyde, acetaldehyde and other monoaldehydes are some crosslinking agents used to crosslink PVA [5], [7], [10], [45], [50]. As with any crosslinking agent, residual amounts must be removed for biomedical application. If the residue has not been removed, it may cause displeasing effects. γ-irradiation has the advantage over using chemical crosslinking agent, as it does not leave behind any undesired residue [7], [10]. Physical crosslinking is another method to form PVA gels. Due to the formation of crystallites during cryotropic treatment a 3D network is formed [5], [10], [52]. Since physically crosslinking PVA through freeze-thawing thermal cycles have higher mechanical strength, do not require presence of crosslinking agent (lack of toxic residues), able to preserve their original shape, and high water content, it is more desired technique to form a 3D network for biomedical applications [10], [51], [53]–[56].

2.3.1. Influential Factors in Formation of PVA Cryogels

There are several factors determining properties and structure of PVA cryogels: degree of deacetylation, molecular mass of polymer, initial concentration of polymer in the solution, chain tacticity, chemical structure of gel-forming polymer material, thawing rate, duration of storing in frozen state, and repetition of freeze-thawing [2], [10], [13], [39], [42], [50], [52], [57]–[59].

In a study done by Lozinsky et al. [42], PVA solutions with lower degree of deacetylation than 90% did not form gel in any conditions in range of -10 to -20 temperature (neither by storing the

specimen in frozen state up to 10 days nor increasing concentration of PVA from 10% to 20%). In the case of 5% O-acetyl group residues very weak gel is formed. O-acetyl groups inhibit the formation of several intermolecular hydrogen bonds by interfering with the establishment of contacts. Therefore, no gel is formed [2], [6], [13], [42], [50], [52].

PVA cryogels formed with molecular mass lower than 70,000 g/mol yield weak gels without the ability to retain their original form [42]. There is a minimum chain length needed in order to crystalize PVA. In other words, higher molecular mass is preferred for formation of strong and more elastic PVA cryogels [57]. With the increase of chain length of the polymer, the degree of overlap of the coil, number of topological entanglement, and number of intermolecular interactions increases. Therefore, denser physical network in PVA cryogel is formed which is harder with higher melting point. It was reported that as molecular mass increases the size and number of crystallites increases [2], [6], [10], [13], [50], [52], [57].

By varying the initial concentration of polymer in solution in cryogenic treatment spongy cryostructurates having moderate strength or elastic non-spongy cryogels (PVA cryogels) can be obtained [42], [57]. It was shown that thermoreversible PVA gels formed in cryogenic treatment with higher initial concentration of PVA in solution were more elastic with higher melting temperature [2]. By increasing the concentration of PVA a decrease in size of macropores were observed which confirms more elasticity of higher concentrated samples [13]. The degree of crystallinity increased by varying the concentration on initial solution from 7 to 15 wt.% [57]. However, at high concentration of PVA (20%), when the molecular mass is over 60-70 kDa, a very viscous PVA solutions are obtained, which are difficult to process [6], [50].

Tacticity of PVA can also interfere with intermolecular hydrogen interactions. Intermolecular hydrogen bond mainly appears by participation of hydroxyl groups in syndiotactic PVA blocks; whereas, isotactic fragments participate in intramolecular interactions. Therefore, PVA cryogels formed with enriched syndiotactic fragments have higher a degree of crystallinity than PVA cryogels yielded based on atactic polymers with approximately the same molecular mass [2], [6], [50], [52].

The junction knots in 3D polymer networks of cryogels are stabilized by the chemical nature of intermolecular bonds (hydrogen bonds or hydrophobic interactions). When PVA solution freezes, solvent crystalizes and solute will remain in still liquid region of the solution. Polymer-polymer interaction is enhanced in cryoconcentration leading to strong junction knots in 3D cryogel network [2], [50], [58]. In cryoconcentration, which is a natural phenomenon happening during thawing, the concentrated phase is separated from the initial solution [60]. Hydrogen bonds are the main contact between chains in PVA thermally reversible cryogels. Cryogenic treatment causes the formation of microcrystalline regions functioning as junction knots in PVA cryogels. In addition, the degree of physical crosslinking density is related to the number of thermal cycles [58], [59]. More stable networks are formed by increasing the number of freeze-thaw cycles. This can be explained by intensification of the interactions between water molecules and hydroxyl groups in PVA [57].

The most important parameter influencing PVA cryogels is defrosting rate [50]. It was claimed that with slow thawing rates (0.01-0.05 K min^{-1}) very elastic cryogels are formed. While only viscous and turbid colloid solution was observed with high thawing rates (10 K min^{-1}) [2]. In sufficiently wide range of freezing rate (0.1 to 17.0 °C min^{-1}) the effect of physical characteristics is small. However, with fast freezing rates (in liquid nitrogen) cracks are formed in the system [52]. In addition, the longer samples were held in frozen state more viscous, turbid, rigid cryogels were formed. Number of freeze-thaw cycles also affect characteristics of PVA cryogels [42], [61].

2.3.2. Mechanism of Formation of PVA Cryogels

In a study made by Yokoyama et al. [10], it was concluded that PVA cryogels consist of three different phases: aqueous phase with low concentration of PVA, PVA amorphous phase, and PVA crystalline phase. As the temperature of the homogenous solution decrease, molecular movements of polymer chain will be reduced. As a result, intermolecular interactions of PVA (mostly hydrogen bonds) increase which, forms crystalline nuclei. These crystallites function as crosslinks in forming a 3D PVA cryogel network. The crystallization process continues if the system is held in the frozen state for a longer period of time. It has also been suggested that the porous structure of PVA cryogels has been derived from the first stage of freezing due to incomplete crystallization of water. When the system thaws, ice crystals melt, leaving pores behind. These pores are

stabilized due to formation of PVA crystallites which act as junction knots in forming 3D network. In amorphous phase, each PVA polymer chain is associated with water. Crystalline phase hinders movements of PVA chains in amorphous phase [1], [40], [43], [62], [63]. Figure 2.3 shows a basic diagram of cryotropic gelation.

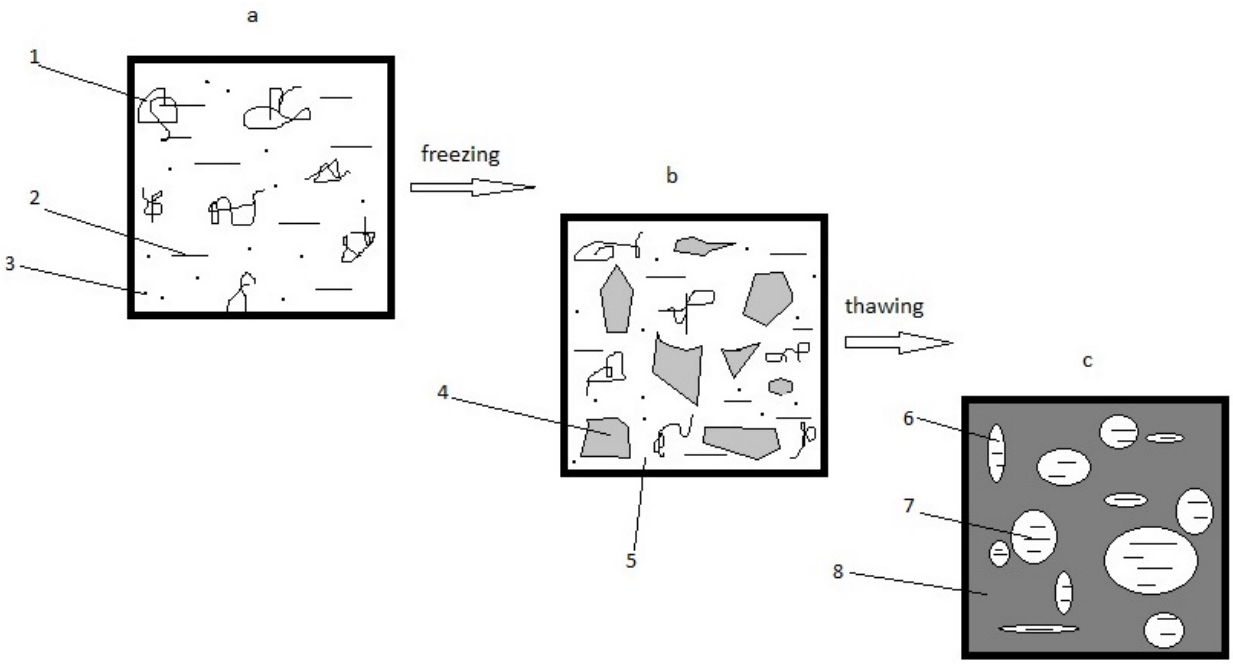

Figure 2.3 - Cryotropic gelation.

(a) Initial sample, (b) sample after freezing, (c) cryogel.

(1) Polymer chain, (2) solvent, (3) low molecular weight compounds or monomers, (4) poly crystal of frozen solvent, (5) unfrozen liquid micro-phase (6) macro-pores, (7) solvent, (8) polymer network of gel phase of hetero-phase cryogel.

2.4. Composite Material

A composite material is made by combining two or more materials with different physical and mechanical properties. Usually one of the materials has very different properties. The continuous phase is called the matrix, while the discontinuous phase is called reinforcement or filler. Composite materials have been widely used in different areas of science. By combining a selection of material properties, and filler orientation, aspect ratio, volume fraction, with the matrix material

mechanical and physiochemical characteristics of a particular application can be achieved. In general, for the performed study, based on materials geometrics, composites are classified in two categories: particulate-reinforced composites and fibrous-reinforced composites. Dispersion of particles and fibers in the composite plays an important role in determining the mechanical properties of composite. Composites with properly dispersed reinforcing agent can improve mechanical properties. On the other hand, with poorly dispersed reinforcement agent, composite mechanical properties are weakened [7], [64], [65].

There has been attention in nanocomposite materials. In nanocomposite materials, at least one of the characteristic lengths is nanoscale. Nanoscale materials typically have a higher surface to volume ratio. Therefore, low concentrations of reinforcement agent is typically needed in nanocomposites to improve mechanical properties [7], [65].

2.4.1. PVA-Chitosan Particulate Composite Hydrogel

Chitosan is derived from the alkaline deacetylation of chitin [66]. After cellulose, chitin is the most abundant polysaccharide in nature which is obtained from animal sources (shellfish, shrimp, and crab) [66], [67]. Chitosan is a copolymer of N-acetyl-D-glucosamine and D-glucosamine [66]. Proportions of N-acetyl-D-glucosamine and D-glucosamine residues give distinct structural changes. Therefore, chitosan is distinguished by molecular weight and degree of deacetylation [66]–[68]. Blend systems with PVA-chitosan hydrogel can enhance compatibility and cell adhesion. Therefore, they have been widely used in biomedical and tissue replacement applications mainly because of non-toxic, non-carcinogenic, and bio-adhesive characteristics of these gels [66], [67], [69]. As a result, because of formation of hydrogen bonds chitosan is potentially miscible in dilute acidic solutions below pH 6.0 [66].

Blends of PVA and chitosan were explored to make hydrogels by freeze-thawing method. PVA-chitosan hydrogels were characterized by differential scanning calorimetry (DSC). Results for DSC revealed independent nature of PVA melting point showing that structure of PVA crystallites does not change because of the presence of chitosan. Moreover, value of glass transition goes up because of presence of chitosan compared to pure PVA hydrogel. In dynamic mechanical thermal

analysis (DMTA) it was shown that the modulus value was decreased by increasing chitosan content. This showed that chitosan perturbs the formation of PVA crystalline network [70].

Mathews et al. [71] explored the effect of cryogenic treatment on PVA-chitosan blends. Uniaxial mechanical test showed decrease in elasticity for successful freeze-thaw cycle within a range comparable to porcine aorta tissue. Liu et al. [72] also studied the number of freeze-thaw cycles followed by coagulation bath immersion and type of additive on structure and mechanical properties of PVA blended with chitosan. It was claimed that the modulus increased by 2-5 times when the number of thermal cycles increased from 1 to 3.

In a study by Costa Junior et al. [73], PVA and chitosan mixture was crosslinked chemically by glutaraldehyde. Mechanical properties of the blend were investigated by stress-strain tensile test. It was found that by increasing chitosan content of hydrogel, the swelling index and toughness decreased. The tested hydrogel showed good mechanical properties, cell viability, and non-toxicity for potential skin engineering application. Arvanitoyannis et al. [74] also examined PVA and chitosan blends with the addition of sorbitol (as a plasticizer) to modify mechanical properties. Yong et al. [75] examined PVA and chitosan hydrogels prepared with γ-irradiation, followed by free-thaw cycles. They reported an increase in mechanical strength and decrease in swelling ratio when content of PVA in these hydrogels increased.

PVA and chitosan blends have also been investigated for the food packaging. Chitosan films were less stretchable compared to pure PVA films. These films also showed plastic behavior. However, the plastic deformation was decreased by increasing content of chitosan in the films. Elongation at break and degree of crystallinity for chitosan and PVA blends decreased by increasing ratio of Chitosan in the blends; however, the addition of chitosan improved rigidity and resistance fracture [66], [76].

In previous works, either PVA and chitosan mixtures was crosslinked chemically or by freeze-thaw cycling method followed by special treatment such as coagulation with water immersion. In this work, the mechanical properties of PVA-chitosan hydrogel composites, which chitosan being

used as particulate-reinforcing agent, using freeze-thaw cycles without any treatment was investigated.

2.4.2. PVA-Cellulose Fibrous Composite Hydrogel

Cellulose fiber materials are a very favorable alternative in bio-nanocomposite applications because of their characteristics: abundantly present in environment, high strength and stiffness, high aspect ratio, low weight, and biodegradability [77]. Cellulose is the world's most abundant polysaccharide. Cellulose can be extracted from plant sources such as wood, cotton, hemp, and other plant-based materials. Cellulose can be biosynthesized by algae, tunicates, fungi, and some types of bacteria [7], [78], [79]. The term "micro-fibril" is used to define cellulose fibers with 2-10 nm diameter, with length of several tens of microns. A noteworthy feature of nanofiber cellulose is hydrophilicity compatible with matrices such as PVA. Table 2.1 shows a three subcategories of cellulose nanofibers based on their function, preparation method, and processing condition [80].

Type of Nano-cellulose	Sources	Formation	Average size
Micro-fibrillated cellulose (MFC)	Wood, sugar beet	Delamination of wood by mechanical action	Diameter: 5-60 nm Length: several micrometers
Nano-crystalline cellulose (NCC)	Wood, cotton, hemp, wheat straw	Acid hydrolysis of cellulose	Diameter: 5-70 nm Length: 100-250 nm
Bacterial Nano-cellulose (BNC)	Low molecular weight sugars and alcohols to support bacterial synthesis	Bacterial synthesis and acid hydrolysis	Diameter: 20-100 nm

Table 2.1 - The family of nano-cellulose material.

Abitbol et al. [81] studied PVA hydrogels reinforced with cellulose nanocrystals (CNCs) prepared from repeated freeze-thaw cycles. It was reported that these hydrogels have improved structural stability. Moreover, water sorption of these hydrogels increased with CNC content because of the

hydrophilic nature of cellulose and reduction in PVA crystallinity. Elastic moduli and confined compression of PVA-CNC increased compared to pure PVA hydrogels. Millon et al. [79] formed PVA-bacterial cellulose hydrogel system from cryogenic treatment. The bacterial cellulose fibers had an average diameter of 50 nm, which were produced by a fermentation process of bacterium *Acetobacter xylinum*. It was reported that the resulting composites had a wide range of mechanical properties which can be used in biomedical and tissue engineering applications.

Mihranyan [82] studied reinforced PVA hydrogels formed by chemical crosslinking of surface modified micro-crystalline cellulose (MCC) with PVA. It was reported that viscoelastic behavior of resulting hydrogels was improved which is favorable for biomedical orthopedic applications.

Cotton fibers and MCC were added to PVA solution followed by freeze-thaw cycles in order to form a 3D network. Cotton is natural source of cellulose and is abundantly available in nature. Based on other studies which was done by others, they have not studied the mechanical properties of PVA-cotton and PVA-MCC hydrogels using freeze-thaw cycles (crosslinking agent free).

2.5. Polymer Blends

Mixtures of at least two different polymer species are described as polymer blends. Polymer alloy is an immiscible polymer blend, with modified interphase and morphology. By blending polymers, a desired set of chemical or mechanical properties can be generated. In this thesis, PVA blends with xanthan gum and sorbitol are studied [83].

2.5.1. PVA-Xanthan Gum Hydrogel Blend

Xanthan gum is a microbial polysaccharide produced by bacterium *Xanthomonas campestris* [84], [85]. The structure of the main chain is chemically identical to cellulose [84]. By altering fermentation conditions in production, xanthan gum with different molecular weights is derived. Xanthan gum is used as a stabilizer and thickener in the food industry [85], [86].

Giannouli and Morris [87] claimed that stronger and more cohesive network is produced when xanthan gum is frozen and then thawed. Microcrystals were formed in gel structure because of freeze-thaw cycles [88].

Alupei et al. [89] studied swelling properties of PVA and xanthan gum hydrogels chemically crosslinked by epichlorohydrin. It was concluded that crosslinking PVA and xanthan gum in the presence of epichlorohydrin resulted in a hydrogel with high swelling rate. Moreover, it was claimed that swelling ratio increases with increasing temperature and time of crosslinking reaction for a xanthan gum blend. In another study by Ray et al. [90], xanthan gum and PVA were used to make pH-sensitive interpenetrating network (IPN) in the presence of glutaraldehyde as a crosslinking agent. These hydrogels were investigated to optimize drug encapsulation efficiency and release rate. Bhattacharya et al. [91] examined swelling kinetics and water retention ability of Poly (acrylic acid)/Poly (vinyl alcohol) – xanthan gum IPN through a chemical crosslinking process. The IPN polymer exhibit a more porous surface, water absorbency, and water retention. Bhunia et al. [92] investigated physical and mechanical properties of PVA and xanthan gum blends with different molecular weight under a low dose electron beam. At low molecular weight, PVA and xanthan gum blend showed similar physical properties under dry and wet condition. But for high molecular weight PVA and xanthan gum systems, mechanical properties were superior under a wet condition.

In this study PVA was blended with xanthan gum and formed 3D network hydrogel without chemically crosslinking using freeze-thaw cycles and the mechanical properties of prepared gels were investigated. Based on previous studies made by researchers, they did not form crosslinking agent free 3D network in PVA-xanthan gum system. Moreover, tensile properties of physically crosslinked PVA-xanthan gum gels were not studied.

2.5.2. PVA-Sorbitol Hydrogel Blend

Sorbitol is a 6-carbon sugar alcohol metabolized slowly in the human body. It can naturally be found in apples, pears, peaches, and some dried fruits such as dates and raisin [93], [94]. Sugar alcohols are carbohydrates, which are synthesized by substituting an aldehyde group with a

hydroxyl group. Sorbitol is used as a bulking agent, stabilizer, and thickener. It can be used in the food industry, pharmaceutical and cosmetics products [93].

Loughlin et al. [95] claimed that adding polyol sugars, such as sorbitol, prevent borate physically crosslinked PVA hydrogels to separate into two distinct phases. Arvanitoyannis et al. [96] studied PVA and chitosan blends plasticized by sorbitol. Melting point and heat transfer decreased with increasing plasticizer content. The percentage of elongation, CO_2 and water permeability increased by addition of sorbitol. In another study by Lazaridou et al. [97], the effect of polyols in β-glucan solutions crosslinked with freeze-thaw cycles was investigated. The tensile strength decreased while the percentage of elongation increased by increasing the content of sorbitol. Yun et al. [98] examined the effect of hydroxyl and carboxyl functional groups in PVA blends. It was claimed that by adding sorbitol, with 6 hydroxyl groups, the percentage of elongation increased. Based on previous studies by researchers, they have not investigated the mechanical properties of PVA-sorbitol hydrogels using freeze-thaw cycles.

Chapter 3 – Materials and Experimental Methodology

3.1. Overview

This chapter covers experimental method and procedure used in the preparation of different composites and blends. For all blends and composites, the effect of concentration of filler and number of freeze-thaw cycles on mechanical properties of samples were investigated. Three different mechanical tests were performed: uniaxial tensile test, elongation at break test, and suture-tension pull through test.

3.2. Material Preparation Procedure

3.2.1. PVA Solution Preparation

Poly vinyl alcohol M_w 146,000-186,000 g/mole with 99+ % hydrolyzed (Sigma-Aldrich). At PVA 10 wt. % was set as the control. The main reasons for choosing 10 wt.% PVA as control was high viscosity, problems with transferring high viscous solutions into molds, and eliminating presence of air bubbles in solutions [9], [50]. Therefore 10 wt.% PVA was kept constant in all blends and composites and it is set to be the control [9], [52]. The 10 wt. % PVA with distilled water was added to a one liter Pyrex resin flask. The batch was supplied with mechanical mixing, temperature control, and reflux column (preventing excess vapor pressure build-up and water loss). The PVA solution was heated for approximately 3 hours at 90 °C until the PVA was fully dissolved and clear jelly like solution was obtained [12].

3.2.2. PVA-Chitosan Solution Preparation

Chitosan with 95% degree of deacetylation, 8 mPa.s viscosity, and 110-150 kDa molecular weight Premix Company, Iceland was used. The provided Chitosan was in white powder. PVA with M_w 146,000-186,000 g/mole, 99+% hydrolyzed (Sigma-Aldrich) was used. The equations for calculating mass of filler is addressed in Appendix A.

In solutions with higher concentration of filler, the high viscosity of solution and presence of air bubbles in the solution were problems. In order to transfer high viscosity solutions into molds; and the solutions were moved into appropriate containers and covered. Then, each container was heated in a warm water bath until the solution was able to flow easily. Air bubbles are created during mechanical mixing, and were allowed to degas by standing overnight [56]. Four (4) systems were prepared with 10 wt. % PVA and 1.5, 3, 4.5, and 6 wt. % chitosan, respectively.

3.2.3. PVA Microcrystalline Cellulose (MCC) Solution Preparation

Microcrystalline cellulose (MCC) with aspect ratio of 3.19 Pharmacel 101 (DFE Pharma Company) was used. Scanning electron microscopy (SEM) of MCC fibers is shown in Figure 3.1. Average length and diameter of used MCC is 68.91 μm and 21.62 μm, respectively.

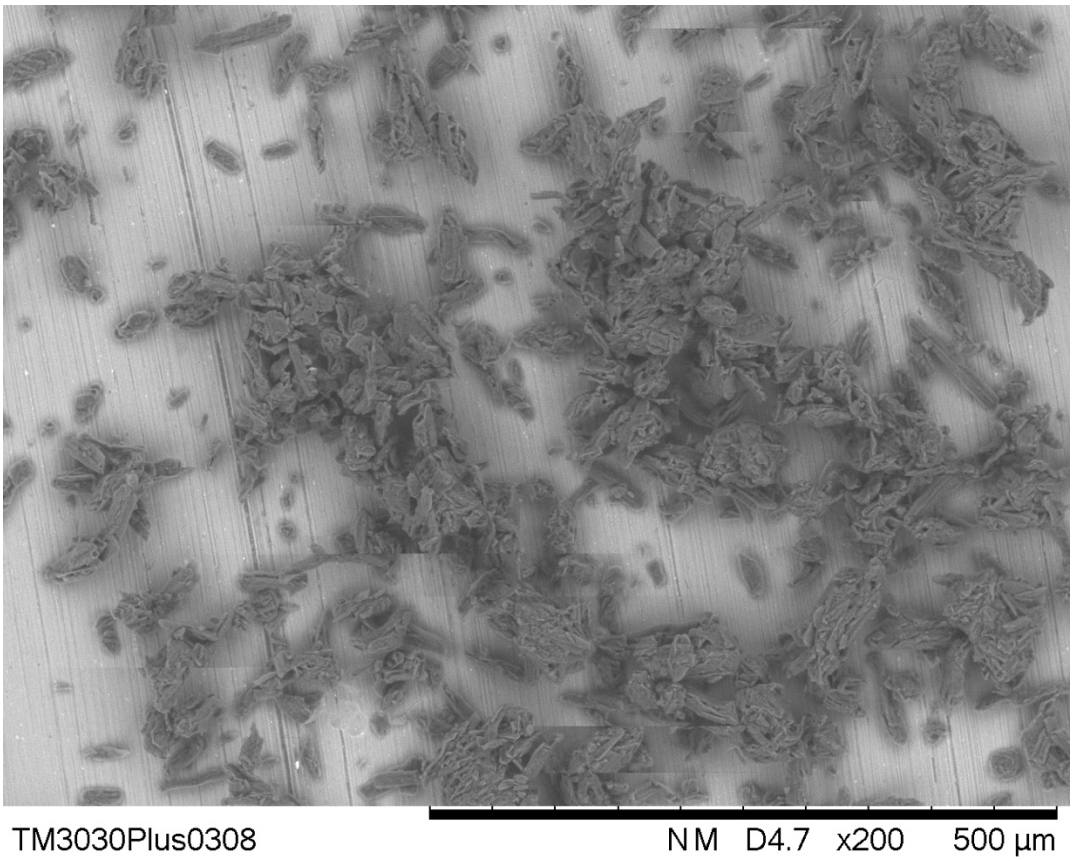

Figure 3.1 - SEM of MCC.

Cellulose nano-fibers were obtained from MCC dispersed fibers and distilled water, sonication (Bransonic Ultrasonic Cleaner model 5510MTH). The jars with MCC suspensions were put in a water bath with controlled temperature, as described by Frone et al. [99]. The temperature was set at 50 °C, and samples were sonicated for 20 minutes with 200 W power.

After sonication, the suspension of cellulose in distilled water was added to the initial 15 wt. % PVA solution. The solution was mixed well in order to obtain a homogenous finial solution. The solution was allowed to stand overnight to release air bubbles. Final solution was transferred into molds for cryogenic treatment. Four (4) systems were prepared with 10 wt. % PVA and 1.5, 3, 4.5, and 6 wt. % cellulose, respectively.

3.2.4. PVA-Cotton Solution Preparation

PVA powder was mixed with cotton flock (Miapoxy). The average length and diameter of fibers were measure by confocal microscope. The aspect ratio of cotton fibers was 10.9 with average length of 233.3 μm and average diameter of 21.4 μm. Figure 3.2 shows Cotton fibers under focal microscope. Four (4) systems were prepared with 10 wt. % PVA and 1.5, 3, 4.5, and 6 wt. % cotton flock, respectively.

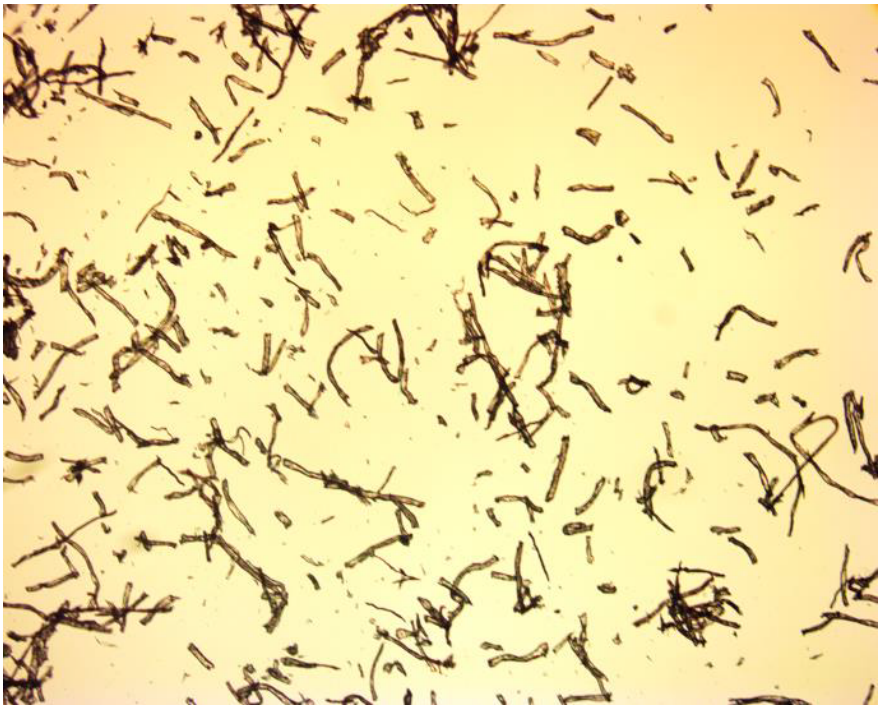

Figure 3.2 - Cotton fibers under confocal microscope.

3.2.5. PVA-Xanthan Gum Solution Preparation

PVA powder was mixed with xanthan gum (Duinkerken Food, Charlottetown) powder. PVA powder and xanthan gum powder were mixed and then distilled water was added slowly to mixture of powders in a one-liter Pyrex resin flask. The solution was heated for about 4 hours to obtain a clear jelly like solution, with the powders fully dissolved. Four (4) blends were prepared with 10 wt. % PVA and 0.5, 1, and 1.5 wt. % xanthan gum. The highest concentration of xanthan gum was 1.5 wt. %. Solutions with higher concentration of xanthan gum had very high viscosity, which was not easily processed.

3.2.6. PVA-Sorbitol Solution Preparation

D-sorbitol ≥ 98% (Sigma-Aldrich) and PVA with M_w 146,000-186,000 g/mole, 99+% hydrolyzed (Sigma-Aldrich) were used. PVA and D-sorbitol powders with distilled water were added to one-liter Pyrex resin flask. Clear jelly like solution was obtained after three hours. Four (4) blends were prepared with 10 wt. % PVA and 2.5, 5, 7.5, and 10 wt. % sorbitol.

3.3. Sample Preparation Procedure for Mechanical Testing

Mechanical testing required flat and tube specimens. Prepared solutions were transferred to flat molds with flat steel plates (20cm·17cm) and rubber spacers of approximately 2.30mm of thickness. The tube-like mold contained one hollow plastic tube with outer diameter of 32mm and one solid steel tube with diameter of 22.2mm. The solid steel tube was placed inside the hollow plastic tube and fixed with rubber O-ring spacers with 1.5mm thickness.

The molds were placed in an environmental chamber, following the procedure of Millon et al. [7]. For comparison purposes, the freeze-thaw rate was kept constant at 0.1 °C/min [9], [50]. Consequently, in one cycle the chamber started at 20°C and cooled the molds to -20°C, held the molds at -20°C for one hour, heated them back to 20°C, and kept the temperature at 20°C for forty minutes before starting another cycle (if needed). Figure 3.3 shows temperature versus time graph for one thermal cycle. A mold was taken out of the chamber after cycles 1, 3, 5, and 7, respectively.

Cycle 7 was the last cycle that hydrogels were tested. In a work done in our research group by Daniel Park, the mechanical properties of hydrogels after cycle 7 did not change. For each cycle sample, five material samples were cut.

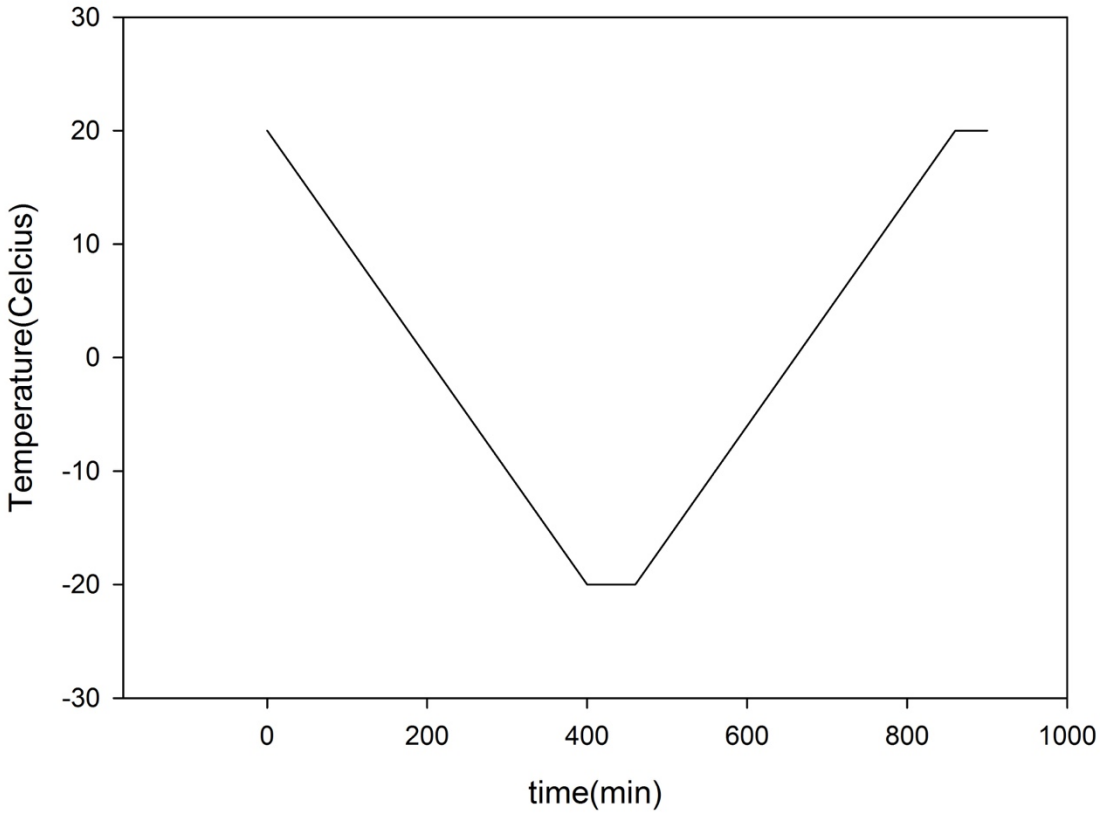

Figure 3.3 - Temperature versus time in one cycle.

3.4. Mechanical Testing

3.4.1. Uniaxial Mechanical Testing

The strain-stress behavior of polymers was investigated with a MARK-10 ESM301L motorized test stand, using MARK-10 Series5 force gauge model M5-10 (2,000 lbF capacity) load cell. The ESM301L are highly configurable motorized test stands for tension and compression testing applications up to 300 lbF (1.5 kN) for laboratory and production environments. For all systems, a guideline for testing procedure was established based on experience and procedure reported by

Millon [7]. All tests were conducted at room temperature approximately 20 °C. This mechanical testing machine was also provided with a custom design Plexiglas water bath if experiments were needed to be done in water (shown in Figure 3.4).

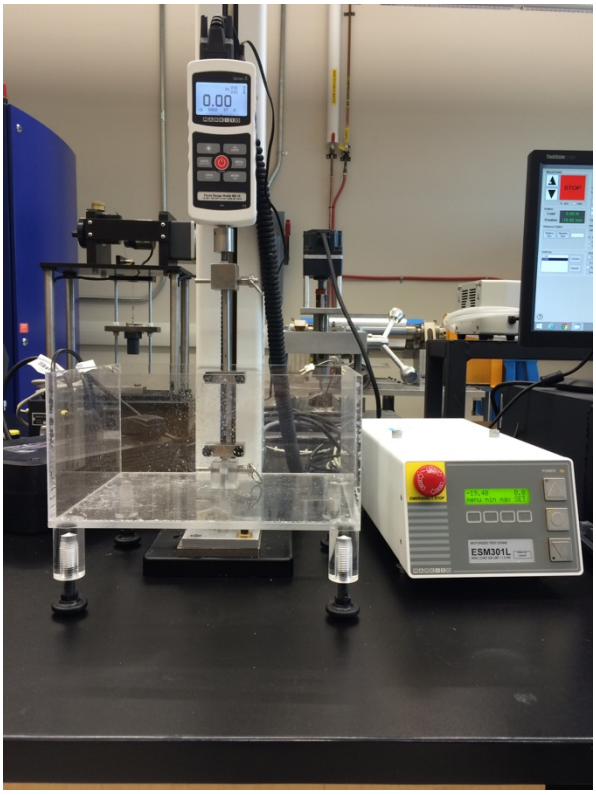

Figure 3.4 - MARK-10 ESM301L motorized test stand.

Custom designed grips were employed to hold the samples while testing. Contact surface of the grips and sample was roughened in order to reduce probability of sample slippage while testing. Figure 3.5 shows a sketch of custom designed grips. Metallic sheets were placed on top of the sample's gripping surface so that the sample stays fixed during the test. A black stabilizing frame was used for proper alignment, keeping upper and lower grip in place (spacing the grips) while the sample was fastened onto the grips. Figure 3.6 shows a sample while was fastened to lower and upper grips.

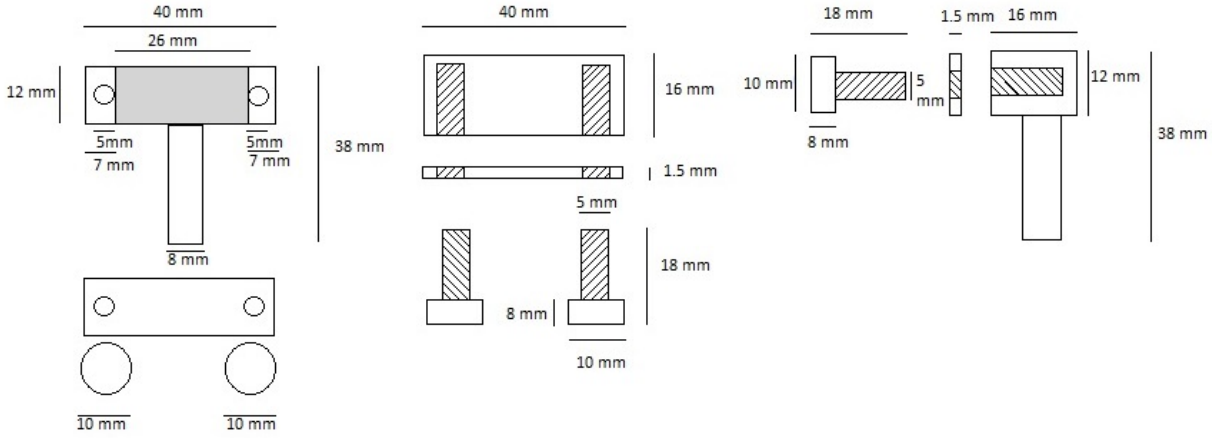

Figure 3.5 - A sketch of custom designed grip.

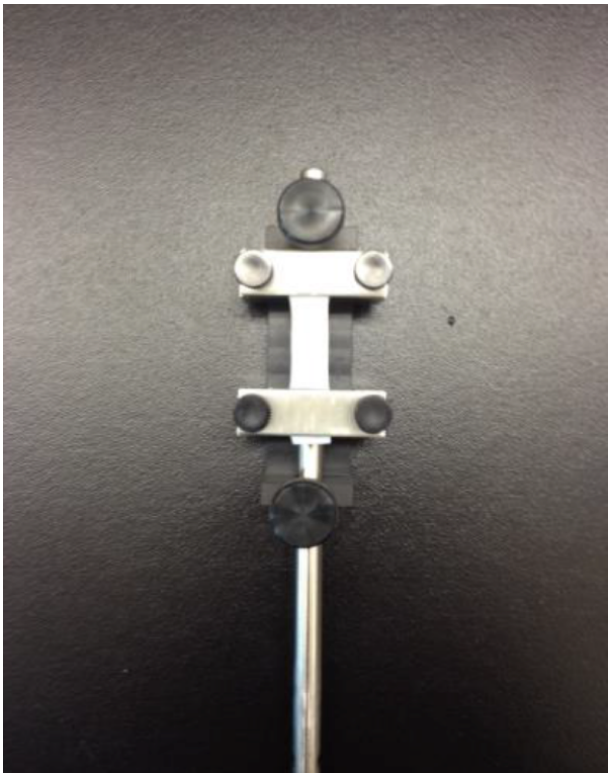

Figure 3.6 - A polymeric sample fastened to lower and upper grip with stabilizing frame on.

Samples were cut in rectangular shape with utility knife from approximately 2 mm sheet and then measured. Width, length, and thickness of samples were 10mm, 50mm, and 2mm respectively, and measured values were recorded. Each sample was fastened from the top and the bottom with custom designed grips.

Based on testing procedures reported by Hui [49], Gordon [9],and Millon [7] an updated testing procedure was obtained.

The first step is to zero the position in MARK-10. This was done by placing upper grip and lower grip (with metal sheets tightened with screws on them) in load cell. The one-inch black block, with width, length, and thickness respectively 16.5mm, 25.4mm, and 10mm, was located in between lower grip and upper grip. The load cell was connected to upper grip's rod and lower grip was fitted to bottom of Plexiglas water tank. The upper grip was lowered until it touched the one-inch black block and a jump in value of load was monitored by load cell. Value for travel was zeroed. For safety reasons and damage prevention of load cell, a red button was designed to stop the operation during any time of running the experiment. By zeroing the machine, any time during the experiment, it was possible to determine the position when the sample was under compression or tension. This process was done once in set of experiments (not after each test).

The original procedure applied by Gordon [9] and Hui [50] was based on determining the maximum reading. The maximum reading was determined either by stretching out the sample up to a load reading of 500 g, or until the sample reached to threshold of failure (without paying attention to the strain). The procedure was similar used by Millon [7]. In this procedure, all samples were strained to 80%. The crosshead speed was kept constant at 480 mm/min. All specimens were preconditioned with 10 loading and unloading cycles, 0% to 70% of strain. The final strain used for data acquisition in stress-strain test was up to 80%. The preconditioning was required to remove any residual stress in the specimen [9], [50].

The gauge length was grip-to-grip space after preconditioning, before conducting stress-strain test. The value of gauge length was changing by moving the actuator and monitored the load cell reading display. The load cell was able to read both compression and extension, from 0 gr to 5000

gr. The tensile test was carried out at crosshead speed 480 mm/min up to 80% strain when the gauge length was reached and sample was relaxed (load display showed zero). Gauge length, the loading and unloading of sample were automatically recorded as load versus extension data in an Excel file.

3.4.2. Elongation at Break

A test fixture as shown in Figure 3.6 was made to test the O-ring specimen. Figure 3.7 was taken from ASTM D412 [100]. Bench drill press and cutter were also used for cutting the samples in O-ring shape. The samples were cut uniformly when the blades were sharp and new. Mastercraft Digital Caliper (model 58-68004) and ring sizing stick were used to measure sample dimension. A guideline for testing procedure was obtained from ASTM D412 O-ring specimen type II. All tests were done at room temperature (approximately 20 °C). The purpose of this test is to measure maximum elongation of composite before rupture.

Using O-ring specimen in the above mentioned test fixture avoided sample to slip while testing ultimate elongation. Ring specimens allows elongation to be measured by grip separation. The elongation across the radial width of the ring specimens is not uniform. To minimize this effect, the width of the ring specimens must be small compared to the diameter.

The test was started when the distance between the centers of the two test fixture rods was 20 mm. O-ring samples were suspended vertically and symmetrically from the grips after zeroing the machine.

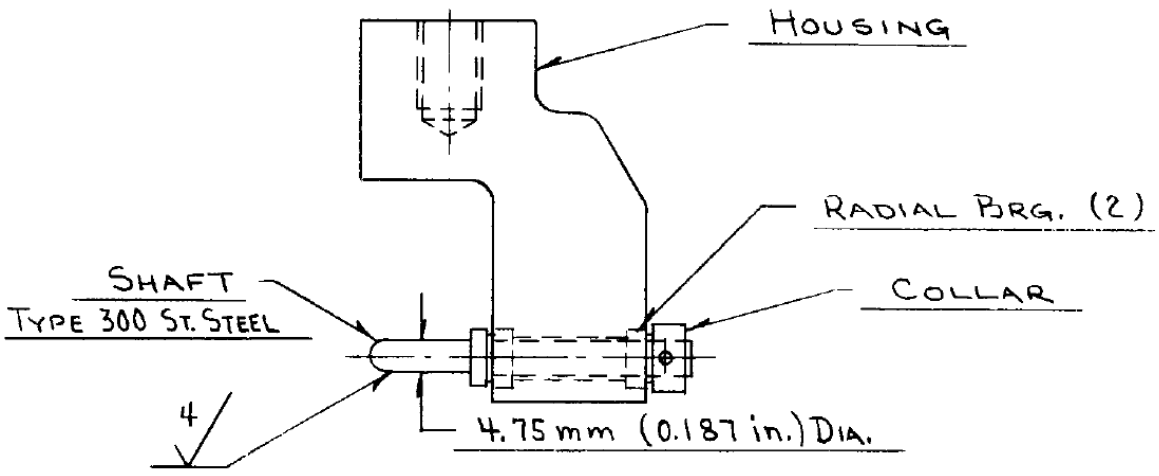

Figure 3.7 - Assembly, ring tensile test fixture - from ASTM D412.

Samples were cut in O-ring shape by using bench drill press and cutter. Cutter was set on driller press. Samples were placed on metal mandrel attached to bench driller press. The cutter was made of two parallel razor blades. The distance between holding plate and blade holder was adjustable. The width and thickness of O-ring samples was measured with a caliper, and the diameter of O-ring samples ring sizing stick was used. Width and thickness of samples were constant 5, 1.5 mm respectively. The diameter of samples varied from 20 mm to 24 mm. This was due to shrinkage of samples after each cycle. Width, thickness, and diameter of samples were recorded.

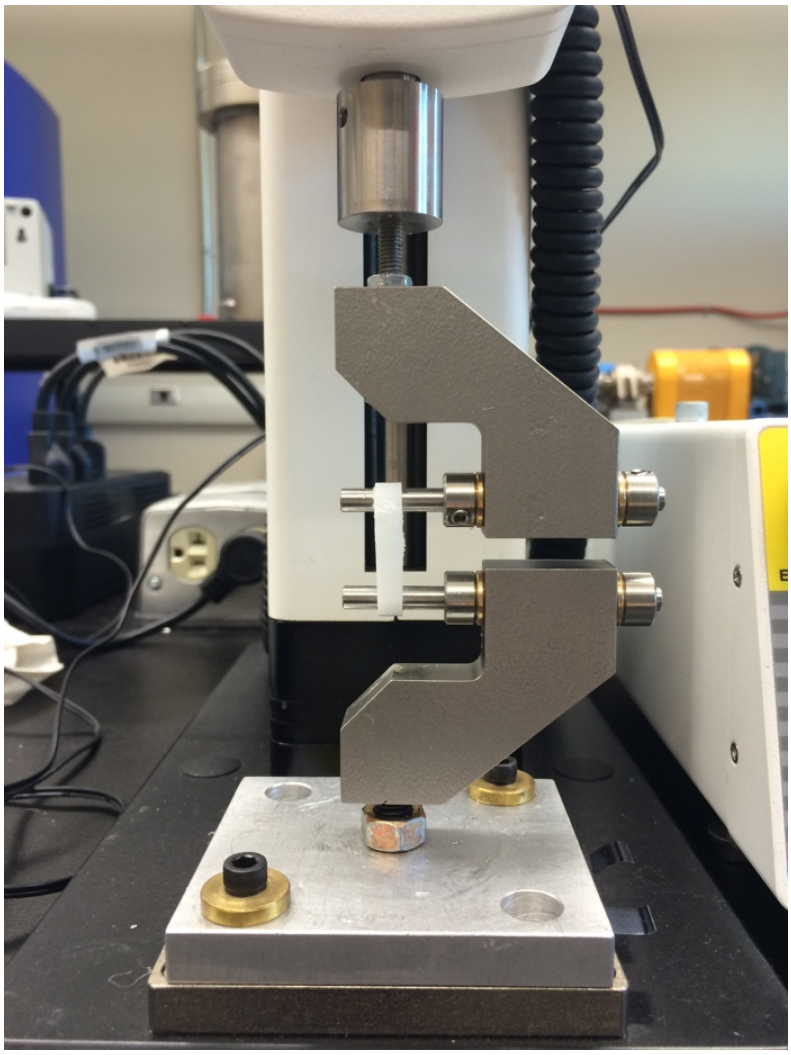

Figure 3.8 - Test fixture with sample hung.

Test procedure was drawn from ASTM D412. Tensile testing machine was zeroed when the distance between the centers of two test fixture rods was 20 mm. At this point, no sample was suspended from the fixtures. After the value for position and load were zeroed, samples were hung vertically and symmetrically to distribute tension uniformly over the cross section (Figure 3.8). The test machine could be stopped by pressing a red button on motorized test stand anytime of experiment because of safety reasons and avoiding load cell damage.

The test machine was started after zeroing the load cell, position, and suspending the samples. Samples were suspended vertically from test fixtures (see Figure 3.8). The crosshead speed was

constant at 480 mm/min during the test. Force and corresponding distance between grips were recorded until rupture. The data was automatically saved in an Excel file.

3.4.3. Suture-Tension Pull through Test

The objective of this test is to evaluate the influence of fibrous fillers and their weight loading on the tearing characteristics of hydrogel. Composite/hydrogel's resistance to initiation and propagation of a tear caused by suture under tension was studied in this test. In suture-tension pull through test the MARK-10 ESM301L was operated as the mechanical testing machine. Instruction was developed based on experience, testing procedure applied by Burkhard [101]. Common suture for cardiovascular tissue, 1238 vascular suture Nylon 4-0 suture 3/8 reverse cutting, was used in this test.

All tests were performed at room temperature approximately 20 °C. The same grip used in the uniaxial mechanical testing was used in order to hold suture and specimen while testing. The load cell was zeroed when lower grip and upper grip with suture were attached to the mechanical testing machine.

Five samples were cut by utility knife from sheet with approximately 2 mm thickness. Length and width of samples were 25mm and 5 mm respectively. All samples were punctured in suture puncture point shown in Figure 3.9. Length, width, and thickness of each sample was recorded.

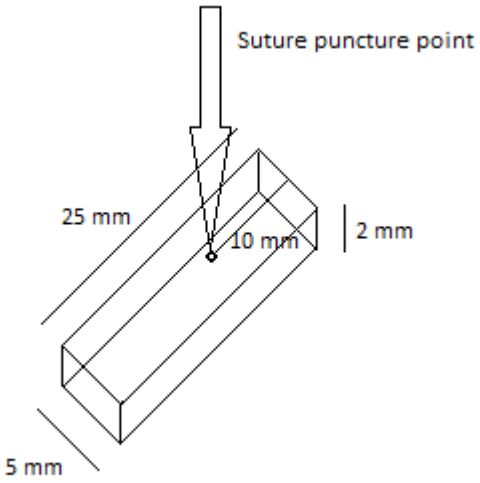

Figure 3.9 - Schematic of sample in suture-tension pull through test.

An update of testing procedure was attained based of testing procedure implemented by Burkhardt [101]. The main difference was the upper grip attached to mechanical testing machine.

The suture was turned to a loop and tied to the upper grip and fixed to the mobile arm of the mechanical testing machine. The suture has to be attached to the upper grip in a way that keeps the thread parallel to each side and with the direction of the pull. To eliminate slippage of the thread during pulling, a knot with at least once extra square knot was created. The sample was connected to the machine with its lower end to the grip. Upper grip should be set approximately 70 mm above lower grip in order to give sufficient room to tie the suture to the sample.

The upper grip was raised until there was minimum tension on the sample. The value for position was zeroed. The test was started at this point with 10 mm/min crosshead speed. Load corresponding to position was collected until the sample was completely torn. The data was saved in an Excel file. The maximum force, initiation of tear, and the average sustained force, propagation of tear, was recorded. Also for the evaluation type of failure was recorded. Three different types of failure event can be observed: (a) sample failure (starting at penetration hole), (b) sample failure at attachment grip, and (c) thread failure.

Chapter 4 – Data Analysis

4.1. Overview

This chapter covers the theory and equations used to analyze the data for stress-strain, elongation at break, and suture-tension test. The methods of statistical analysis are also covered in this chapter.

4.2. Uniaxial Tensile Testing

Tensile test is popular mainly because it allows us to get intrinsic properties of the material, specifically elastic modulus or stiffness as a function of strain and be able to compare between other materials and soft tissue targets. In this test, resistance of material to an applied force is measured. A specimen is placed in mechanical testing machine and force or load is applied. The amount of displacement is measured when specimen is under tension and it stretches. Thus, the change of length of specimen corresponding to original length of specimen can be calculated. Load (force) as a function of change in length is recorded. Therefore, information regarding to strength, Young's Modulus, and ductility of material can be obtained [102].

4.2.1. Stress and Strain

In the uniaxial tensile test, load versus position is recorded. Engineering strain and engineering stress are defined by following equations [9], [50], [102]:

$$\varepsilon_E = \frac{l - l_0}{l_0} = \frac{\Delta l}{l_0} = \frac{l}{l_0} - 1 \qquad \text{Eq.10}$$

$$\sigma_E = \frac{F}{A_0}, \qquad \text{Eq.11}$$

$$A_0 = W_0 \times t_0$$

Where:

ε_E engineering strain,

l final extension length, mm,

l_0 gauge length, mm,

σ_E engineering stress, N/m^2,

F applied force, N,

A_0 original cross-section area, m^2,

W_0 original width of sample, mm,

t_0 original thickness of sample, mm.

To be able to calculate the cross-sectional area corresponding to each value of force, it is assumed that the Poisson's ratio is 0.5 (sample is incompressible), which means that the volume of sample remains constant during the test [9], [102], [103]. The true stress and true stain explains the dimensional changes in uniaxial tensile test [9], [50], [102]. Based on this assumption, true stress and true strain can be calculated by following equations:

$$\sigma_T = \frac{F}{A}$$

$$\sigma_T = \frac{F}{A} \times \frac{A_0}{A_0}$$

$$A_0 \times L_0 = A \times L$$

$$\frac{A_0}{A} = \frac{L}{L_0}$$

$$\sigma_T = \frac{F}{A_0} \times \frac{L}{L_0} \qquad \text{Eq.12}$$

By substituting Eq. 10 in Eq.12:

$$\sigma_T = \frac{F}{A_0}(1 + \varepsilon_E)$$

$$\sigma_T = \sigma_E(1 + \varepsilon_E) \qquad \text{Eq.13}$$

$$\int_0^{\varepsilon_T} \partial\, \varepsilon_T = \int_{L_0}^{L} \frac{\partial L}{L}$$

$$\varepsilon_T = lnL + C$$

At $\varepsilon_T = 0$; $L = L_0$

$$0 = lnL_0 + C \longrightarrow C = -lnL_0$$

$$\varepsilon_T = lnL - lnL_0 = ln\frac{L}{L_0}$$

$$\varepsilon_T = ln(1 + \varepsilon_E) \quad \text{Eq.14}$$

Where:

σ_T	true stress, N/m^2,
F	applied force, N,
A	instantaneous cross-sectional area, m^2,
A_0	original cross-sectional area, m^2,
L_0	gauge length, mm,
ε_E	engineering strain, %,
ε_T	true strain, %.

There are number of possible equations reported in literature that can be used for fitting the data. For all PVA-based materials and soft tissues stress-strain curve is non-linear and has tendency towards stress axis. As a result, most of the equations used in literature have an exponential term. Following are some of the equations used in the literature to fit PVA data [7], [9], [12], [50], [104]:

$$\sigma = A + B\varepsilon + C\varepsilon^2 \quad \text{Eq.15}$$

$$\sigma = A\ exp(B\varepsilon) \quad \text{Eq.16}$$

$$\sigma = y_0 + A\ exp(B\varepsilon) \quad \text{Eq.17}$$

$$\sigma = y_0 + A\varepsilon + B\ exp(C\varepsilon) \quad \text{Eq.18}$$

$$\sigma = y_0 + A\ exp(B\varepsilon) + Cexp(D\varepsilon) \quad \text{Eq.19}$$

Where A, B, C, D, and y_0 are curve fitting factors.

Eq. 15 is not accurate; because strain-stress curve for PVA based materials show an exponential increase of stress corresponding to increased strain, Eq.15 is not accurate. Eq. 16 is the most popular as it is the easiest to use with only two parameters to characterize the stress-strain curve. However, it was shown that Eq.18 was a better fit because it has a linear trend at the beginning followed by exponential growth term [9], [50]. Millon reported that Eq. 17 has a closer fit to aortic

tissue. Eq.17 which is simpler form of Eq.18, was used for fitting the strain-stress data for PVA-based hydrogels [7].

The least square fitting parameters were found by using SigmaPlot (Systat Software Inc.) software program (Version 9.0).

4.2.2. Modulus

The slope of strain-stress curve in the elastic region is called Young's Modulus (E). The linear-relationship between strain and stress in elastic region of strain-stress curve is known as Hooke's law [7], [102]:

$$E = \frac{Stress}{Strain} \qquad \text{Eq.20}$$

Modulus is connected with binding energy of atoms. Steep slope in strain-stress curve indicates high elastic modulus, meaning high forces is needed to separate the atoms resulting the material stretch elastically. In composites, stiffness of composite is proportional to Young's Modulus. For example, in materials with higher Young's Modulus, smaller changes of dimension are observed under applied force compared to materials with lower elastic modulus [7], [102].

PVA-based hydrogels have non-linear strain-stress curve. Therefore, Young's Modulus was calculated by taking first derivative with respect to strain form Eq.17:

$$E = \frac{d\sigma}{d\varepsilon} = AB \exp(B\varepsilon) \qquad \text{Eq.21}$$

Where:

E, Young's Modulus or elastic modulus,

A and B fitting parameters,

ε, strain.

From Eq.21, Young's Modulus is a function of strain. Consequently, modulus of elasticity can be calculated in desired strain. In this study, the modulus of composites and blends were calculated up to 55% true strain.

4.3. Elongation at Break

For polymers, numerous mechanical properties can characterize their applicability. The ability of polymer to resist breaking under tensile stress is one of mechanical properties which is measured [105]. Elongation at break is defined as the increase of length until the last component of sample is broken. Materials with high elongation have capacity to handle force without failure. The data obtained from elongation at break should be reported at specific temperature and cross-head speed [106].

From values (load versus position) gathered by machine and test procedure described in ASTM D412 O-ring specimen type II, ultimate elongation, or elongation at break can be calculated from following equation:

$$Elongation = 200\times[\frac{L}{OC}] \quad \text{Eq.22}$$

Where:

Elongation	ultimate elongation or elongation at break, %,
L	increase in grip separation at break separation, mm,
OC	outside circumference of O-ring test specimen, mm.

4.4. Suture-tension Pull through Test

Wound closure is the most important requirement for healing after a surgery. An optimal wound closure can avoid infection and further complication in rehabilitation after surgery [101]. However, few studies have been made on tearing characteristics hydrogel; more precisely on initiation, and propagation of tear cause by suture under tension.

In this test, maximum force which is at initiation of tear, and average sustained force (propagation of tear), was recorded in Newton. In addition, type of failure for each sample was recorded.

4.5. Statistical Analysis

The standard deviation, true stress, true strain, ultimate elongation, stress at break, and maximum stress was calculated in Excel. Error bars in all Figures represent standard deviation for 5 samples. There were five replicates of each test. It was assumed that all the data sets were independent observations of normally distributed random variable. The test statistics was based on t-distribution and therefore, t-test was performed. SigmaPlot software version 3.0 was applied for t-test and ANOVA (one-way analysis of variance) where more than two groups were compared. Sigmastat makes sure that the assumptions for ANOVA test such as normality and equal variance is not violated before running the test. The program shows problem and options if these assumptions did not hold. For probability test the default p-value 0.05 was used. A report with relevant statistical information was given at the end of each test [7].

Chapter 5 – Results and Discussion

5.1. Overview

This Chapter covers the result and discussion of the experiments mentioned in Material and Experimental Methodology chapter. This includes four sections: 10% wt. PVA as the control, PVA-based particulate reinforced hydrogel composites, PVA-based fibrous reinforced hydrogel composites, and PVA-based hydrogel blends. PVA-MCC and PVA-cotton were considered as fibrous-reinforced hydrogel composites. Fibrous-reinforced composites improve the strength of the hydrogel. PVA-based blends such as PVA-sorbitol hydrogels give the elastic behavior to the hydrogel. For all samples stress-strain properties were investigated. Ultimate elongation and stress at break of PVA-sorbitol hydrogel blends was studied. The suture test was performed on an existing cotton fiber product. All the results were compared to the control and porcine aorta.

5.2. PVA-based Composites and Blends

The main purpose of this study is to prepare different PVA based composites and blends, investigate their mechanical properties, and explore their possible application in tissue phantoms. PVA based composite and blends were compared to target tissue porcine aorta. PVA-chitosan hydrogels as particulate-reinforced hydrogel composites, increases the stiffness of the final product. Fibrous-reinforced composites (PVA-MCC and PVA-cotton) improve the strength of the hydrogel. PVA-based blends such as PVA-sorbitol hydrogels give the elastic behavior to the hydrogel.

5.3. PVA Reference

5.3.1. Stress-strain

Figure 5.1 shows the stress-strain curve for 10 wt. % PVA as reference. The testing procedure was described in section 3.4.1. The data was fitted using Eq. 17. Following equation was utilized to fit the data:

Figure 5.1 displays a non-linear stress-strain relationship, and stiffness increases as the number of freeze-thaw cycles is increased (cycle 1 to cycle 7). In all samples, higher stress value was detected at higher strain. Cycle 7 was the last cycle in thermal cycling because after cycle 6 no difference in stress-strain curve was observed [9], [12]. The stress-strain data from porcine aorta was used for comparison as published by Millon et al. [79].

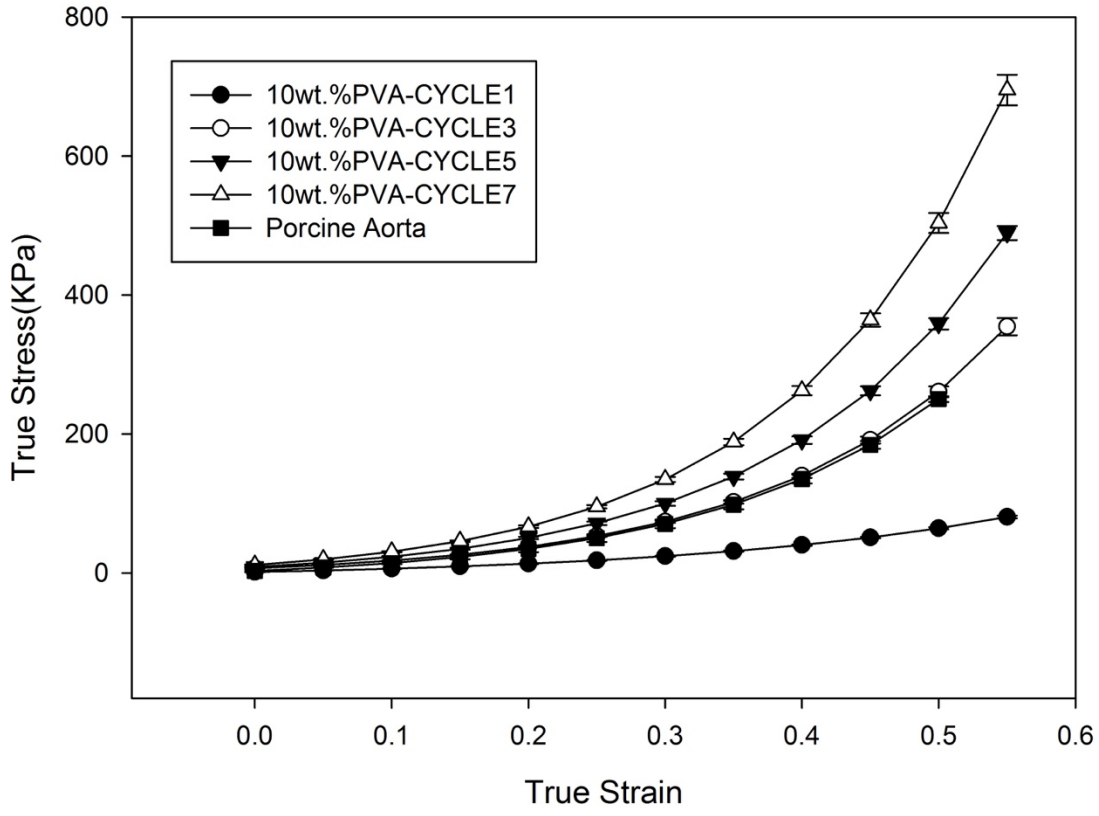

Figure 5.1 - Stress-strain curve for porcine aorta and 10 wt. % PVA hydrogel for cycles 1, 3, 5, and 7.

5.3.2. Modulus

Figure 5.2 presents the modulus-strain curve. Modulus is slope of stress-strain curve in elastic region [7], [102]. PVA hydrogels exhibit elastic behavior up to 55% true strain. As a result, Figure 5.2 shows the slope of the curves in Figure 5.1 corresponding to the true strain. Stiffness increases with increasing number of thermal cycles. Moreover, 10 wt. % PVA is stiffer in higher strain. After cycle 5, number of thermal cycling does not affect the stiffness of hydrogel as in lower cycles.

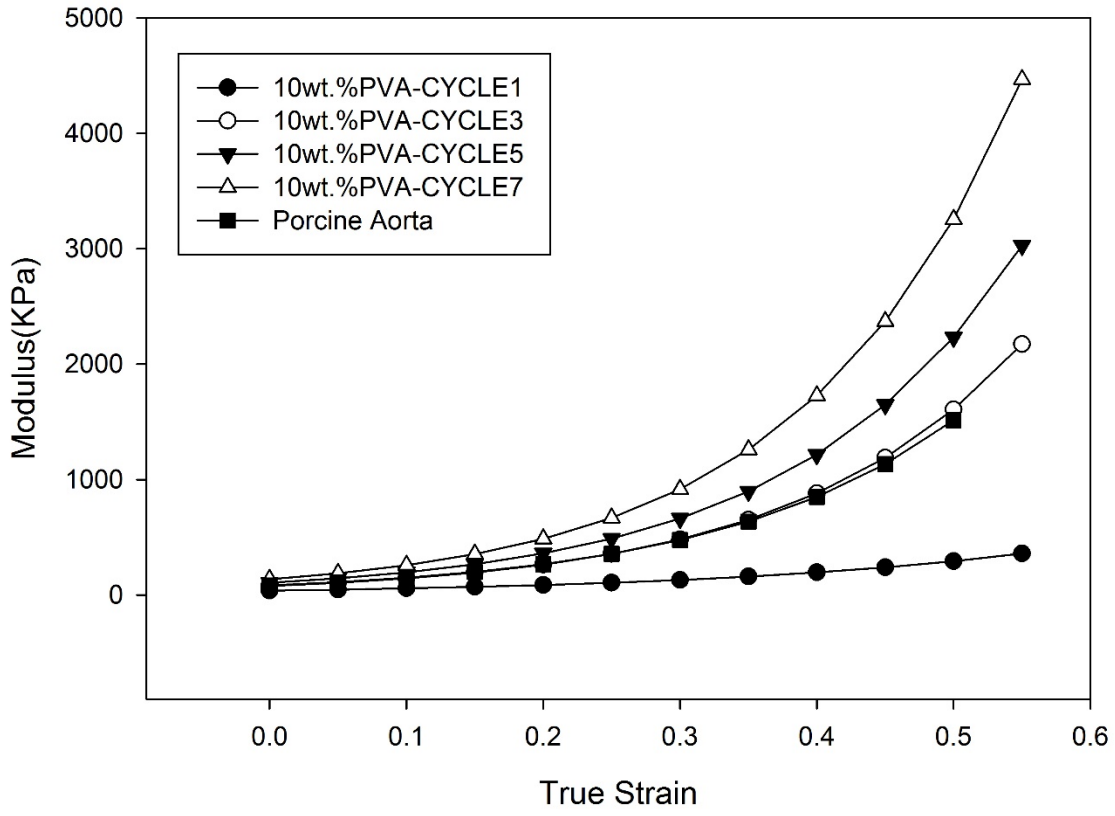

Figure 5.2 - Modulus-strain curve of porcine aorta and 10 wt. % PVA hydrogel for cycles 1, 3, 5, and 7.

5.3.3. Elongation at Break

5.3.3.1. Ultimate Elongation

Figure 5.3 displays ultimate elongation for 10 wt. % PVA at 1, 3, 5, and 7 thermal cycles. The testing procedure was described in section 3.4.2. At first cycle, PVA hydrogels show more elastic behavior. By increasing number of thermal cycles, PVA hydrogels become stiffer and less elastic. PVA hydrogels at first cycle are very soft. Therefore, cutting them in O-ring shape using bench drill press normally does not give clearly cut-samples. High standard deviations at cycle one compared to other cycles, were observed.

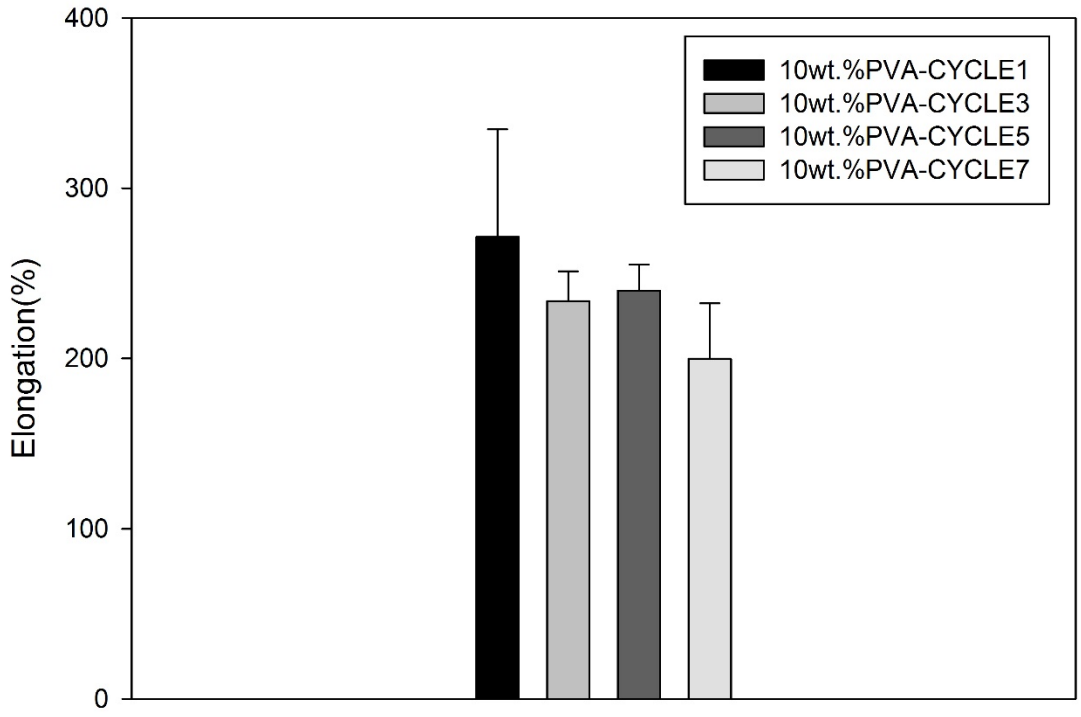

Figure 5.3 - Mean ultimate elongation for 10 wt. % PVA hydrogel in cycles 1, 3, 5, and 7.

5.3.3.2. Stress at Break

Figure 5.4 shows stress corresponding to the ultimate elongation. Stress at break surges from cycle 1 to cycle 5, although there is not any significant difference between cycle 5 and cycle 7 (P=0.45, P>0.05). This indicates that by increasing number of thermal cycles, PVA hydrogels become stiffer and less elastic, which requires higher force to break the hydrogel.

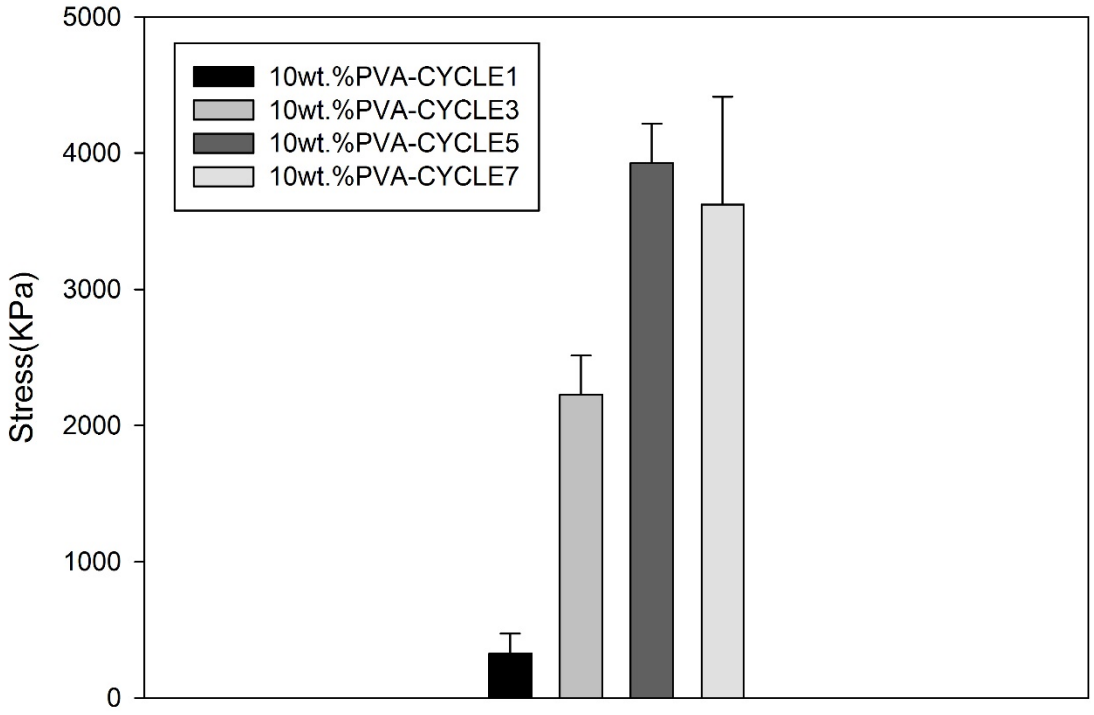

Figure 5.4 - Mean stress at break for 10 wt. % PVA hydrogel in cycles 1, 3, 5, and 7.

5.4. Particulate-reinforced PVA Hydrogel Composite

5.4.1. PVA-Chitosan Hydrogel

5.4.1.1. Stress-strain

In Figures 5.5, 5.6, 5.7, and 5.8 stress-strain curve of PVA-chitosan hydrogel composites compared to 10 wt. % PVA in cycles 1, 3, 5, and 7 is shown respectively. The weight loading of chitosan, as

well as number of thermal cycles, is varied in following Figures. Thermal cycling increased the stiffness of hydrogels.

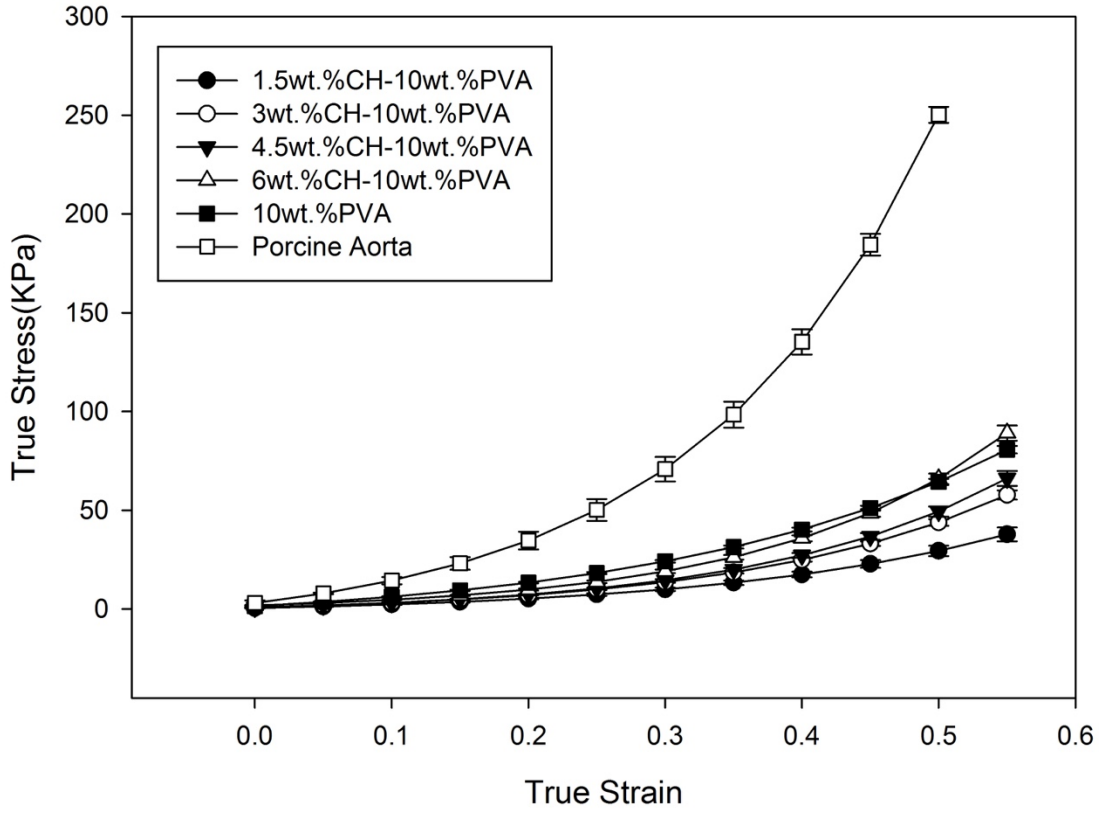

Figure 5.5 - Stress-strain curve for porcine aorta, PVA-chitosan hydrogel composite and 10 wt. % PVA hydrogel on cycle 1.

In cycle 1, there is statistically significant difference between the control and PVA-chitosan hydrogels. As shown in Figure 5.5, with increasing wt. % chitosan stiffness decreases. When ANOVA was applied at 30% strain, the stiffness of 10 wt. % PVA is statistically significantly higher than PVA-chitosan hydrogels ($P<0.001$). Statistical results at 50% strain show significant difference between PVA-chitosan hydrogels in 1.5, 3, and 4.5 weight loading of chitosan with the control ($P<0.001$). However, at 50% strain, the stiffness of 6 wt. % chitosan-PVA hydrogel is not

statistically different. Porcine aorta shows higher stiffness than PVA-chitosan hydrogels and 10 wt. % PVA in cycle 1.

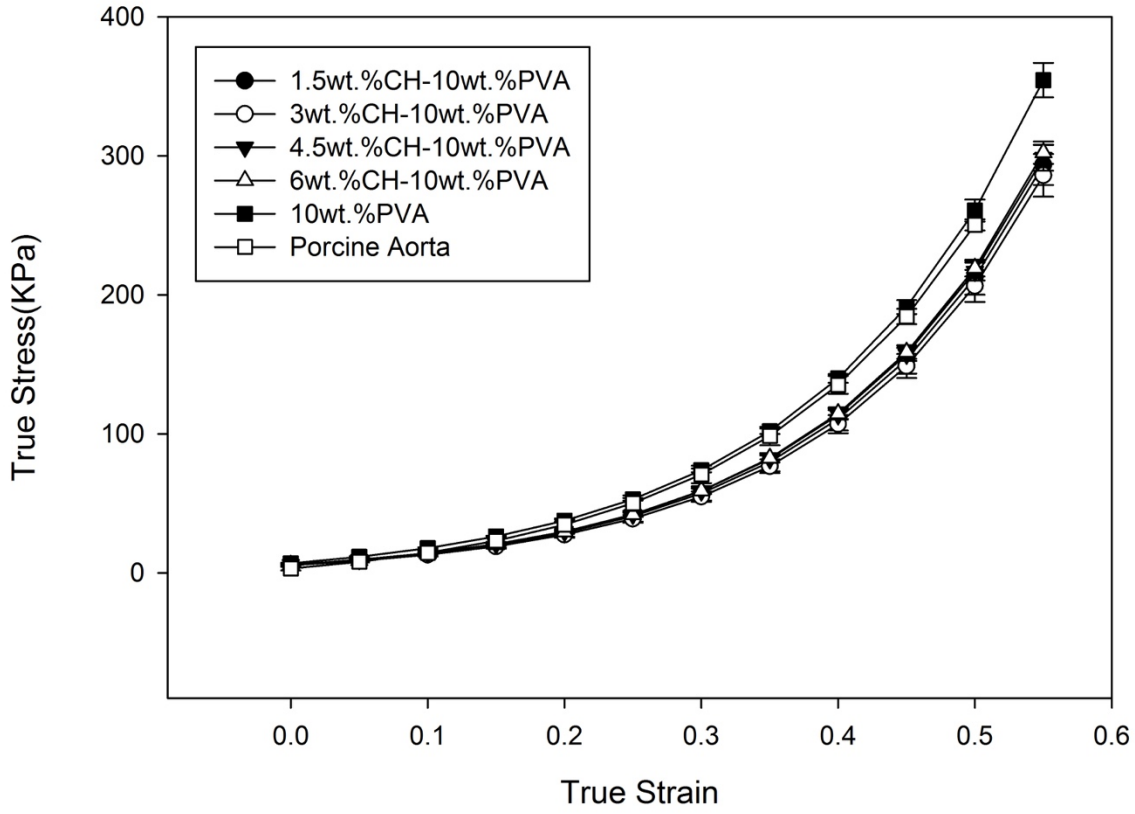

Figure 5.6 - Stress-strain curve for porcine aorta, PVA-chitosan hydrogel composite and 10 wt. % PVA hydrogel on cycle 3.

In cycle 3, stress-strain curves of PVA-chitosan hydrogels are overlapping. In other words, different weight loading of chitosan (from 1.5 to 6) did not affect the stiffness of material. By applying ANOVA at 30% and 50 strain, there is significant difference in stiffness of PVA-chitosan hydrogel with the control ($P<0.001$). Moreover, the load curve of PVA-chitosan hydrogels does not match with porcine aorta. (Figure 5.6)

As shown in Figure 5.7, the stiffness of PVA-chitosan hydrogels with 3 wt. %, 4.5 wt. %, and 6 wt. % filler loading are lower than the control in cycle 5. When ANOVA was applied at 30% and 50% strain, there was a statistically significant difference with the control ($P<0.05$). For PVA-chitosan hydrogel with 1.5 wt. % chitosan there is no statistically significant difference with 10 wt. % PVA ($P>0.05$). There is no statistically significant difference between porcine aorta and PVA-chitosan hydrogel with 4.5 wt. % chitosan.

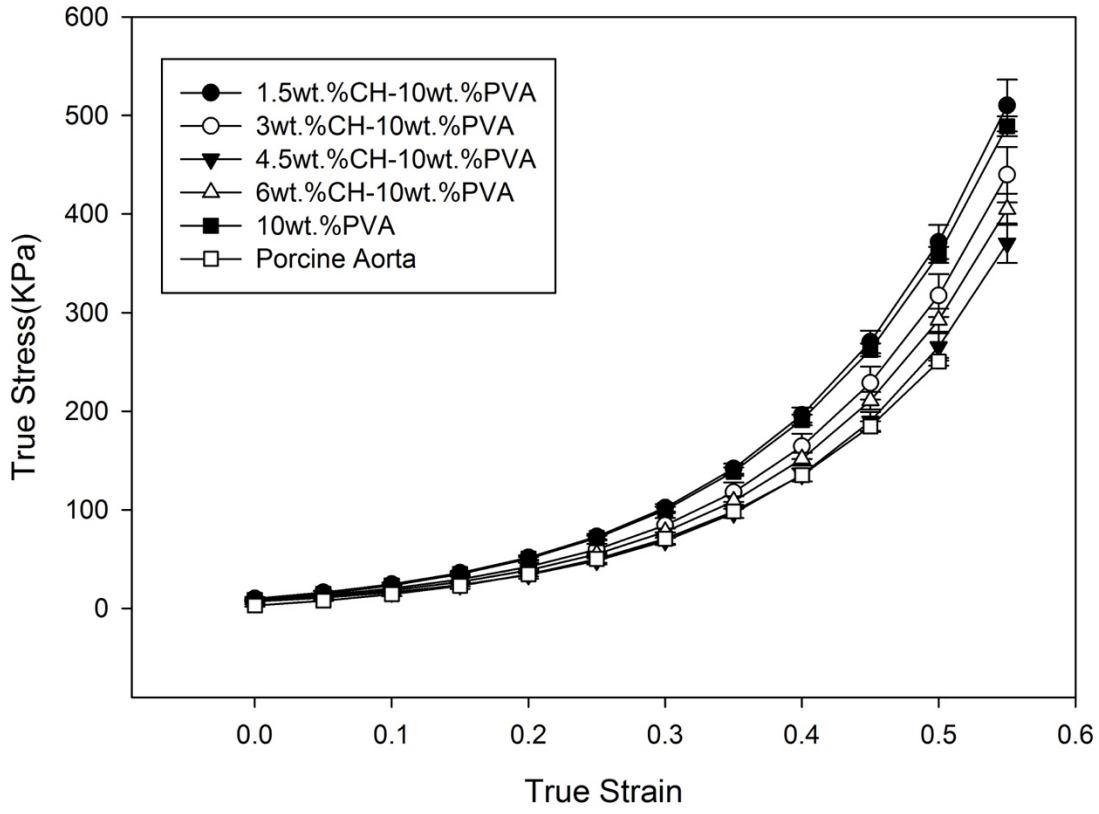

Figure 5.7 - Stress-strain curve for porcine aorta, PVA-chitosan hydrogel composite and 10 wt. % PVA hydrogel on cycle 5.

At cycle 7, the stiffness of PVA-chitosan hydrogels is lower than the control. When ANOVA was applied at 30% and 50% strain, there is statistically significant difference between 10 wt. % PVA. This indicates that by increasing the number of thermal cycles and addition of chitosan particles as reinforcing agent in hydrogel, no improvement was noticed. (Figure 5.8)

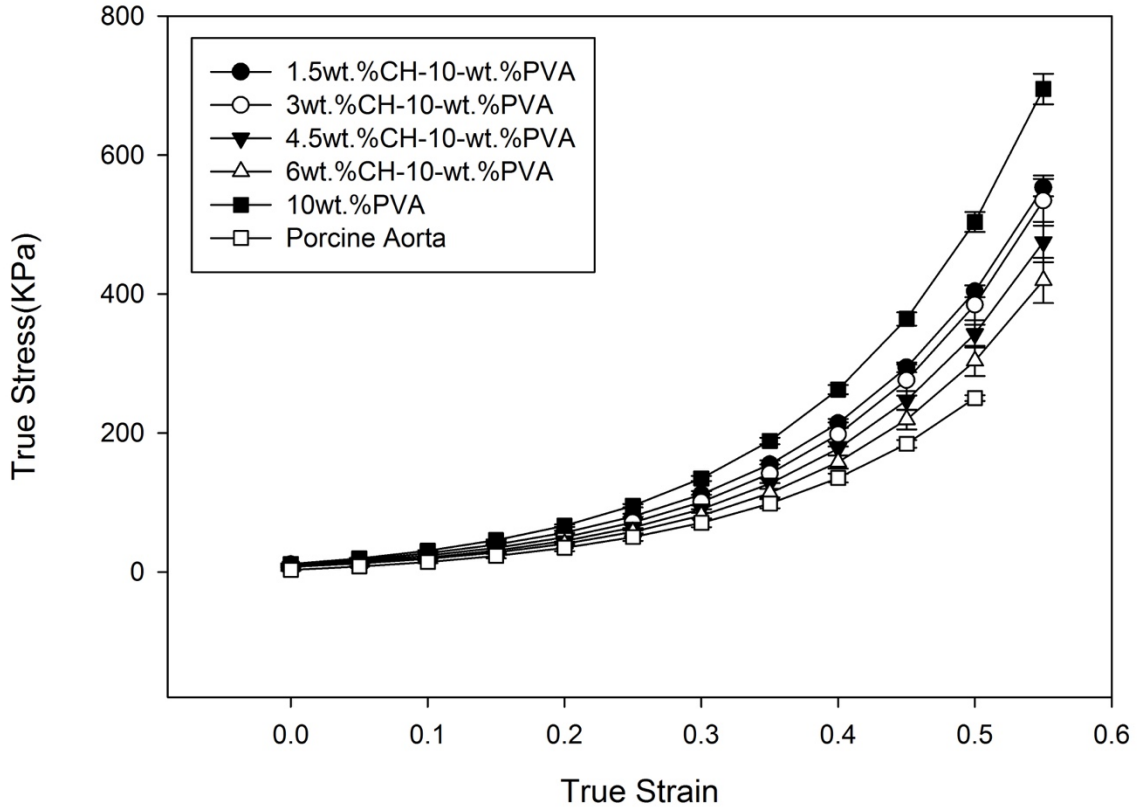

Figure 5.8 - Stress-strain curve for porcine aorta, PVA-chitosan hydrogel composite and 10 wt. % PVA hydrogel on cycle 7.

5.5. Fibrous-reinforced PVA Hydrogel Composite

5.5.1. PVA-MCC Hydrogel Composite

5.5.1.1. Stress-strain

The effect of adding microcrystalline cellulose (MCC) with different weight loadings to PVA hydrogels is investigated. Number of cycles was also varied for this study. Figures 5.9, 5.10, 5.11, and 5.12 presents stress-strain curve for PVA-MCC hydrogel composite with different weight loadings of MCC compared to 10 wt. % PVA for cycles 1, 3, 5, and 7, respectively.

In cycle 1, there is no statistically significant difference between PVA-MCC hydrogels with 3, 4.5, and 6 wt. % filler loadings at 30% strain (P>0.05). The stiffness of PVA-MCC with 1.5 wt. % MCC was lower than others. When ANOVA was applied at 30% and 50% strain, there is statistically significant difference for PVA-MCC hydrogels with 4.5 wt. % and 6 wt. % of MCC with the control (P<0.001). At higher weigh loadings of MCC stiffness increases. (Figure 5.9)

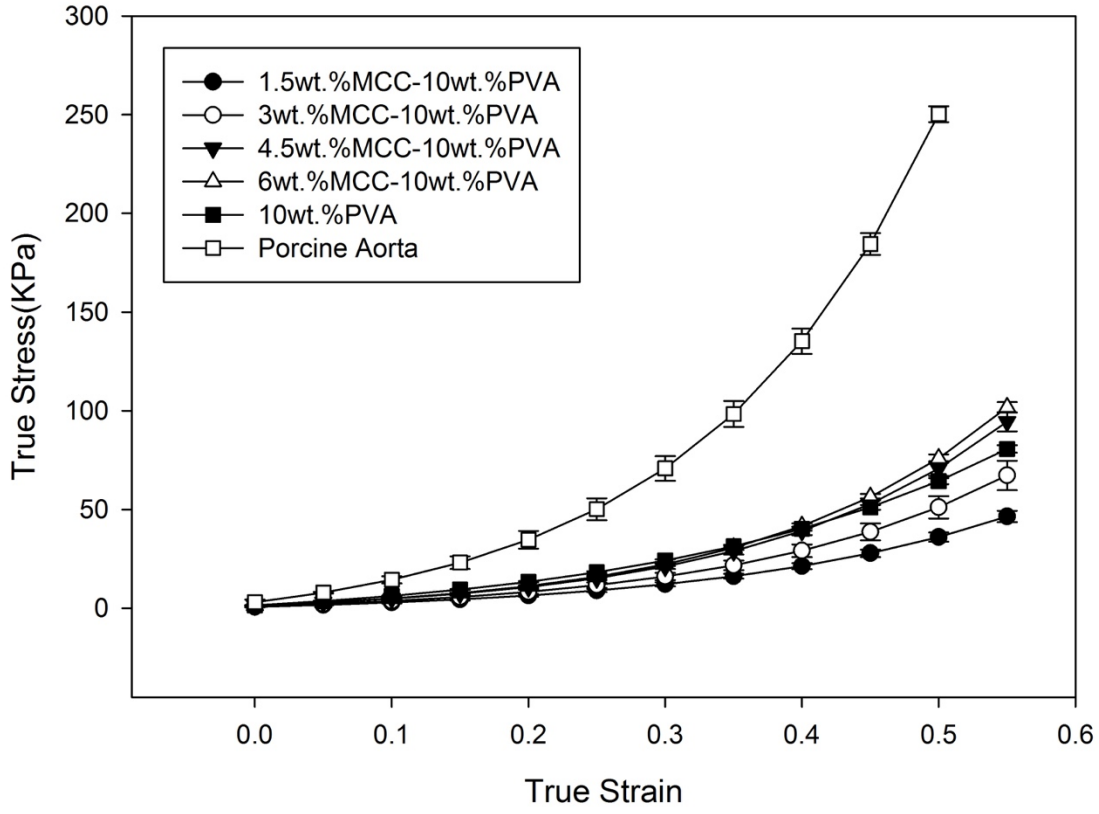

Figure 5.9 - Stress-strain curve for porcine aorta, PVA-MCC hydrogel composite and 10 wt. % PVA hydrogel on cycle 1.

Figure 5.10 displays PVA-MCC hydrogel composites for cycle 3. All PVA-MCC hydrogel composites almost overlay on each other. At 30 % strain, there is no statistically significant difference with the control (P>0.05). At 50 % strain, PVA-MCC with 6 % weight loading shows higher stiffness than the control (P=0.03, P<0.05). The load curve of porcine aorta and PVA-MCC with 4.5 wt. % are statistically the same.

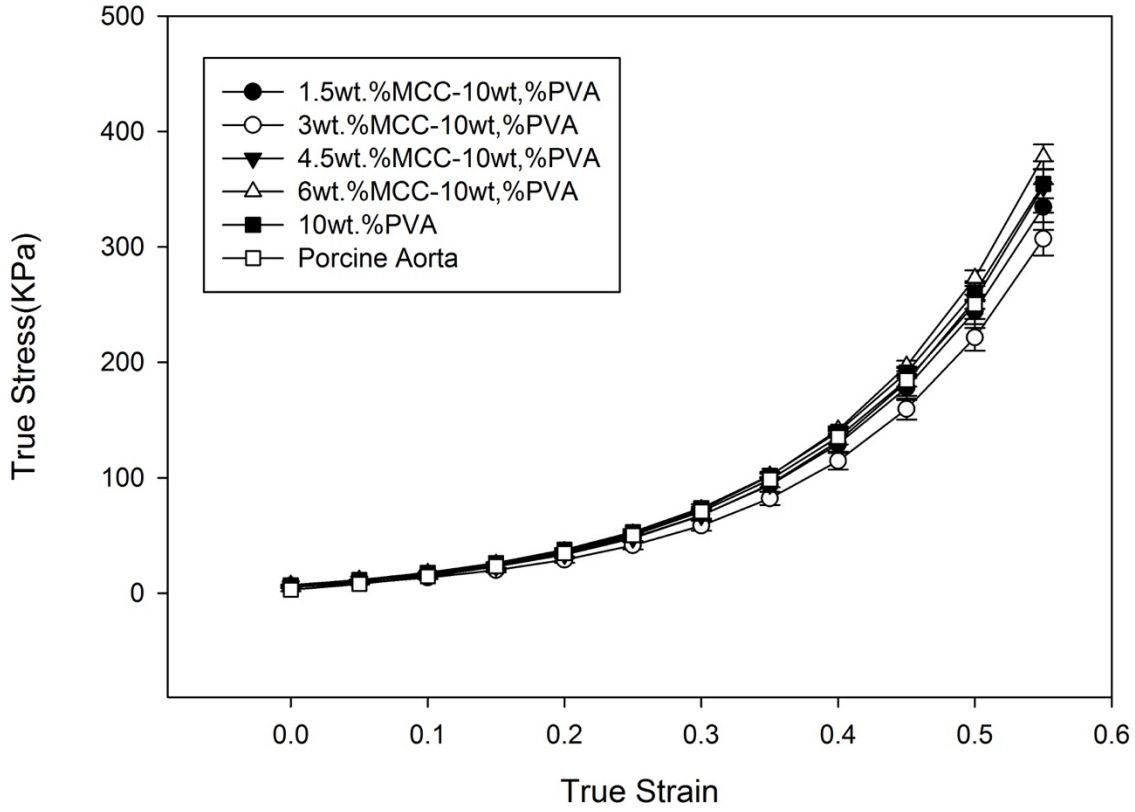

Figure 5.10 - Stress-strain curve for porcine aorta, PVA-MCC hydrogel composite and 10 wt. % PVA hydrogel on cycle 3.

In cycle 5, same pattern as cycle 3 is observed. At 30% strain, there is no statistically significant difference between PVA-MCC hydrogels and 10 wt. % PVA. However, at 50% strain PVA-MCC hydrogels show slightly higher stiffness than the control ($P \leq 0.05$). Figure 5.11 presents stress-strain curve for PVA-MCC hydrogel composite for cycle 5.

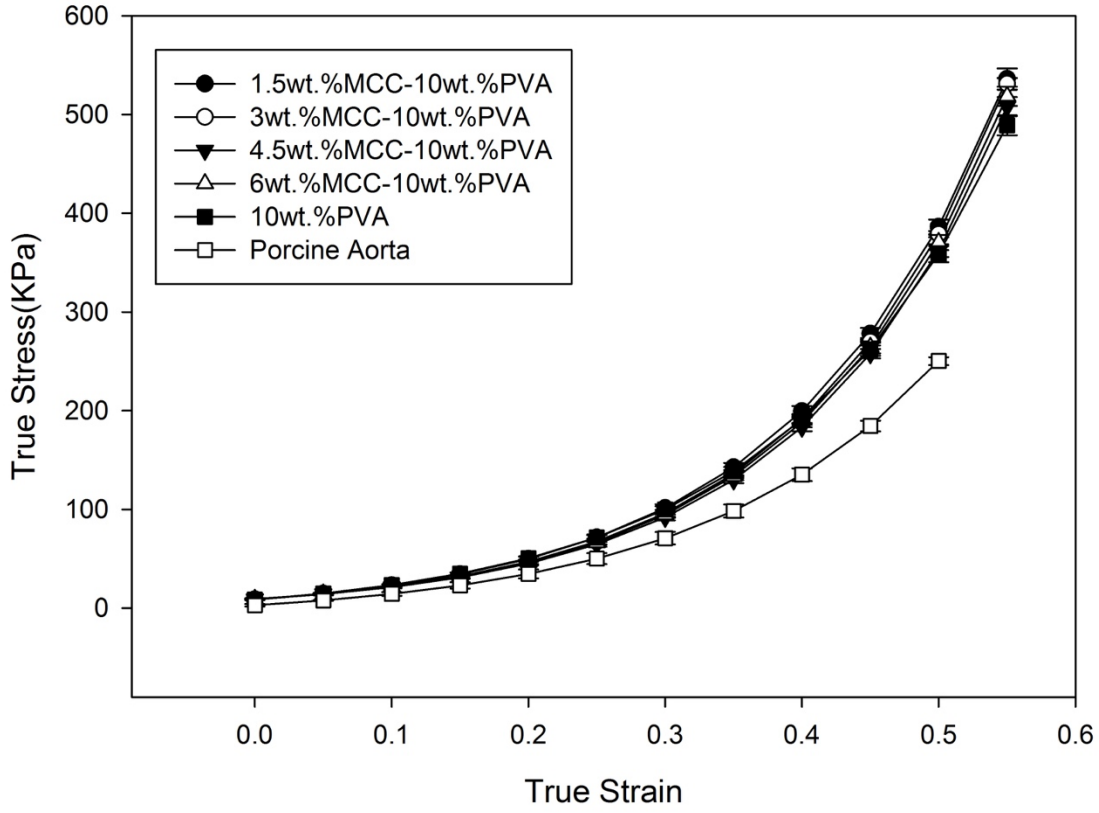

Figure 5.11 - Stress-strain curve for porcine aorta, PVA-MCC hydrogel composite and 10 wt. % PVA hydrogel on cycle 5.

In cycle 7, stress-strain curve for PVA-MCC hydrogel composites merge. By increasing number of freeze-thaw cycles, the weight loading of MCC in composite is not important; and all PVA-MCC hydrogel composites have the same stress-strain curve ($P>0.05$). By applying ANOVA, there is statistically significant difference between 10 wt. % PVA and PVA-MCC hydrogel composite. The stiffness of 10 wt. % PVA is higher than PVA-MCC hydrogels in cycle 7. Figure below shows stress-strain curve for PVA-MCC hydrogel composite for cycle 7. (Figure 5.12)

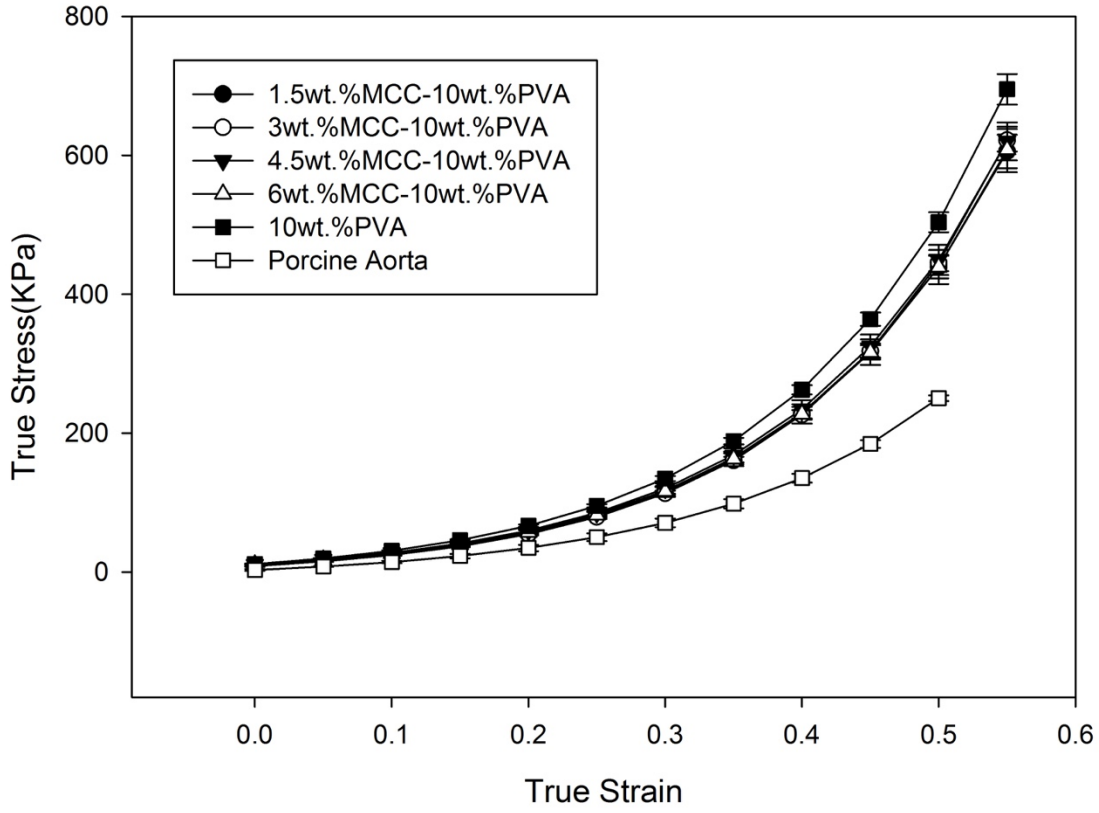

Figure 5.12 - Stress-strain curve for porcine aorta, PVA-MCC hydrogel composite and 10 wt. % PVA hydrogel on cycle 7.

5.5.2. PVA-Cotton Hydrogel Composite

5.5.2.1. Stress-strain

Different weight loadings of cotton (COT) fibers were added to PVA hydrogels to investigate their stress-strain curve in cycles 1, 3, 5, and 7. Figures 5.13, 5.14, 5.15, and 5.16 display stress-strain curve for cycles 1, 3, 5, and 7, respectively.

In cycle 1, as shown in Figure 5.13, PVA-cotton hydrogel composites with 6 wt.% cotton has higher stiffness than the control (P = <0.001). When ANOVA was applied at 30% and 50% strain, PVA-cotton hydrogels with 1.5%, 3%, and 4.5% weight loading show lower stiffness than the control.

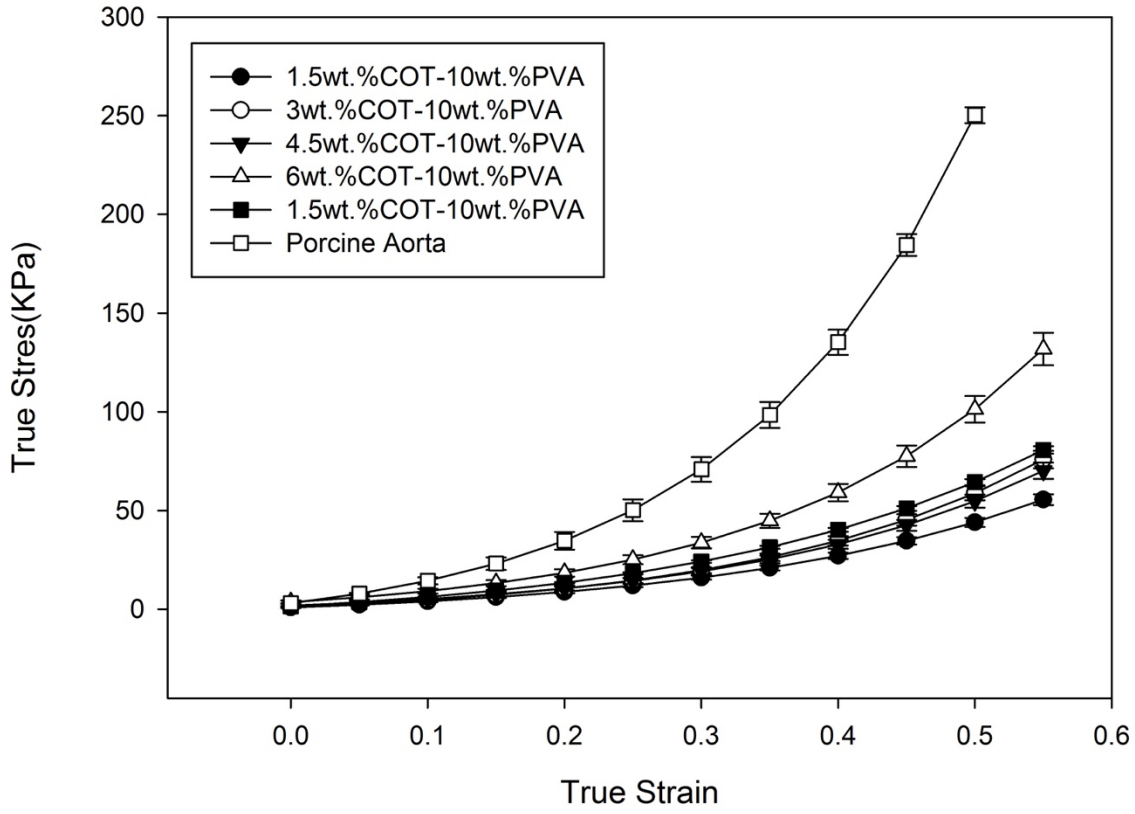

Figure 5.13 - Stress-strain curve for porcine aorta, PVA-cotton hydrogel composite and 10 wt. % PVA on cycle 1.

As shown in Figure 5.14, stiffness of all hydrogels improved from cycle 1. However, addition of cotton fibers did not affect stress-strain curve when compared to 10% wt. PVA. There is not statistically significant difference between PVA-cotton hydrogels and the control in cycle 3 (P>0.05). There was not statistically significant difference between porcine aorta and PVA-cotton hydrogel with 1.5 wt. % in cycle 3 at 30% and 50% strain.

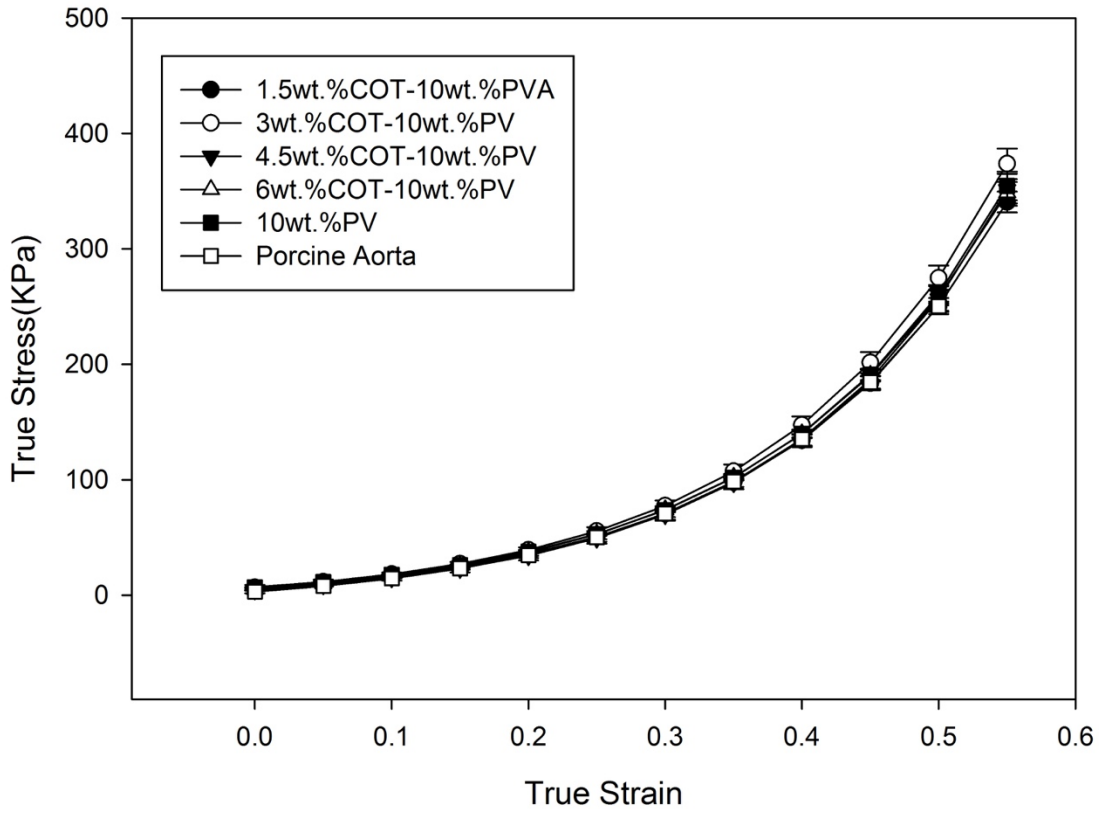

Figure 5.14 - Stress-strain curve for porcine aorta, PVA-cotton hydrogel composite and 10 wt. % PVA on cycle 3.

Stiffness Improved in cycle 5 and 7 when it was compared to lower cycles. Freeze-thaw cycling increase the stiffness of these hydrogels. Figures 5.15 and 5.16 show stress-strain curves for PVA-cotton hydrogel composites in cycles 5 and 7, respectively.

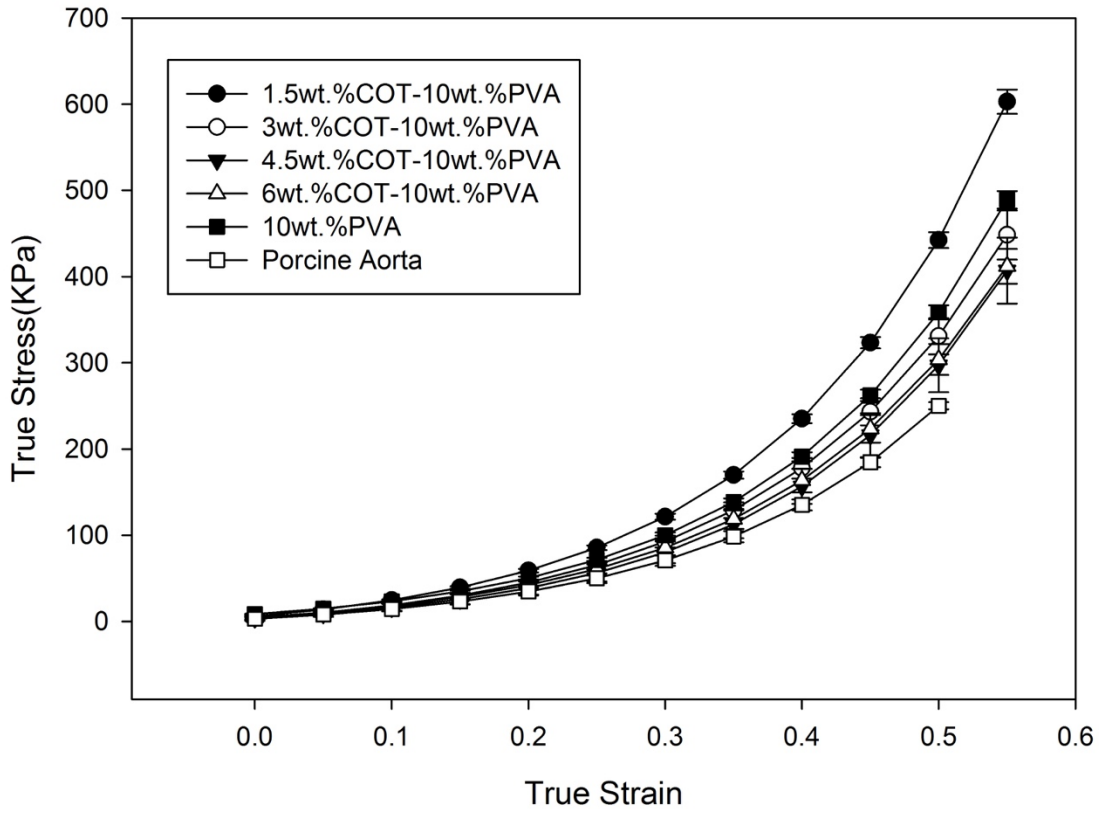

Figure 5.15 - Stress-strain curve for porcine aorta, PVA-cotton hydrogel composite and 10 wt. % PVA on cycle 5.

In cycle 5, PVA-cotton hydrogel with 1.5 wt. % cotton, has higher stiffness than the control at 30% and 50% strain (P= <0.001). However, in higher filler loadings, 10 wt. % PVA has higher stiffness than PVA-cotton hydrogel (P= <0.001). In cycle 7, PVA-cotton hydrogels have lower stiffness than the control at 30% and 50% strain (P= <0.001).

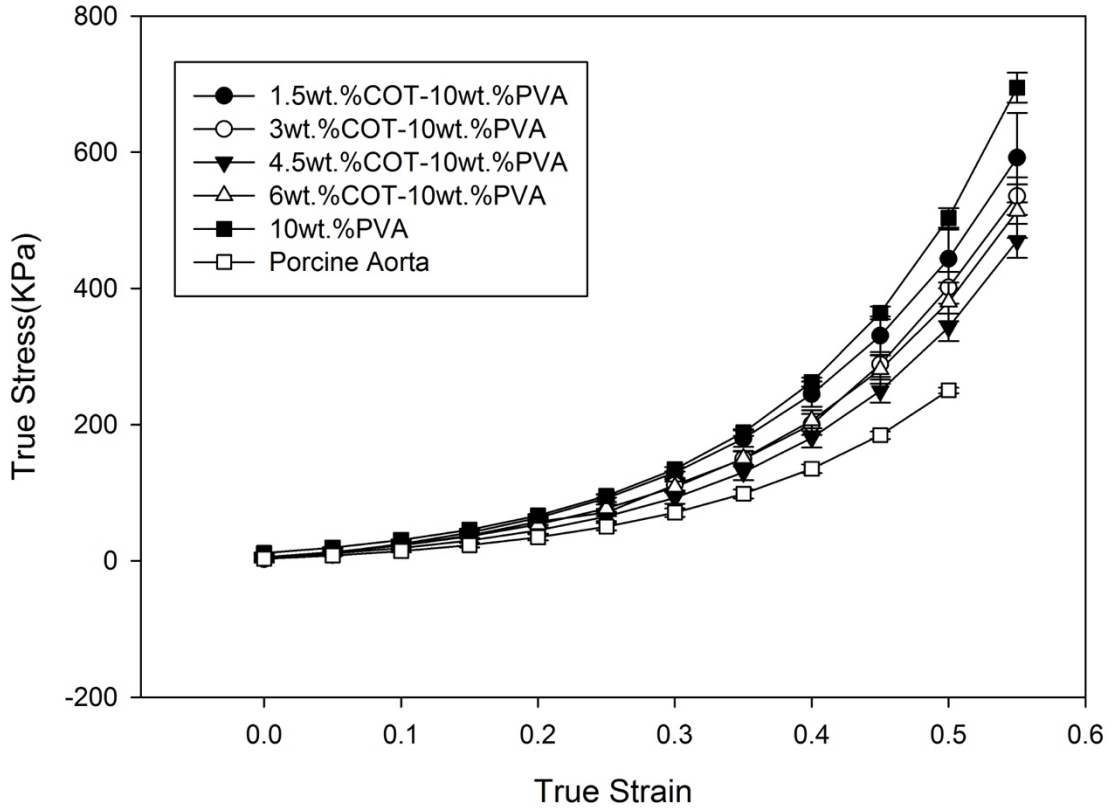

Figure 5.16 - Stress-strain curve for porcine aorta, PVA-cotton hydrogel composite and 10 wt. % PVA on cycle 7.

5.5.2.2. Maximum Force in Suture-tension Pull through Test

Mean maximum force for PVA-cotton hydrogel composites, which is observed at the initiation of tearing was measured for cycles 1, 3, and 5. The presence of cotton fibers made tearing less likely, meaning more force was needed to tear PVA-cotton hydrogel composites compared to the control. In all tests of PVA-cotton hydrogel composite samples and 10 wt. % PVA, sample failure at penetration hole was detected. The term sample failure in penetration hole means that the samples were torn at penetration hole.

As shown in Figure 5.17, the mean maximum force applied for PVA-cotton hydrogel composites in cycle 1 was significantly more than the control (P= <0.001). At the highest concentration of

cotton fibers (6 wt. %) the mean maximum force was around three times more than for 10 wt. % PVA. For other concentrations of cotton fiber, the mean maximum force increased for approximately twice the control. PVA-cotton hydrogel composite with 6 wt. % of cotton has the highest mean maximum force among all the hydrogels in cycle 1.

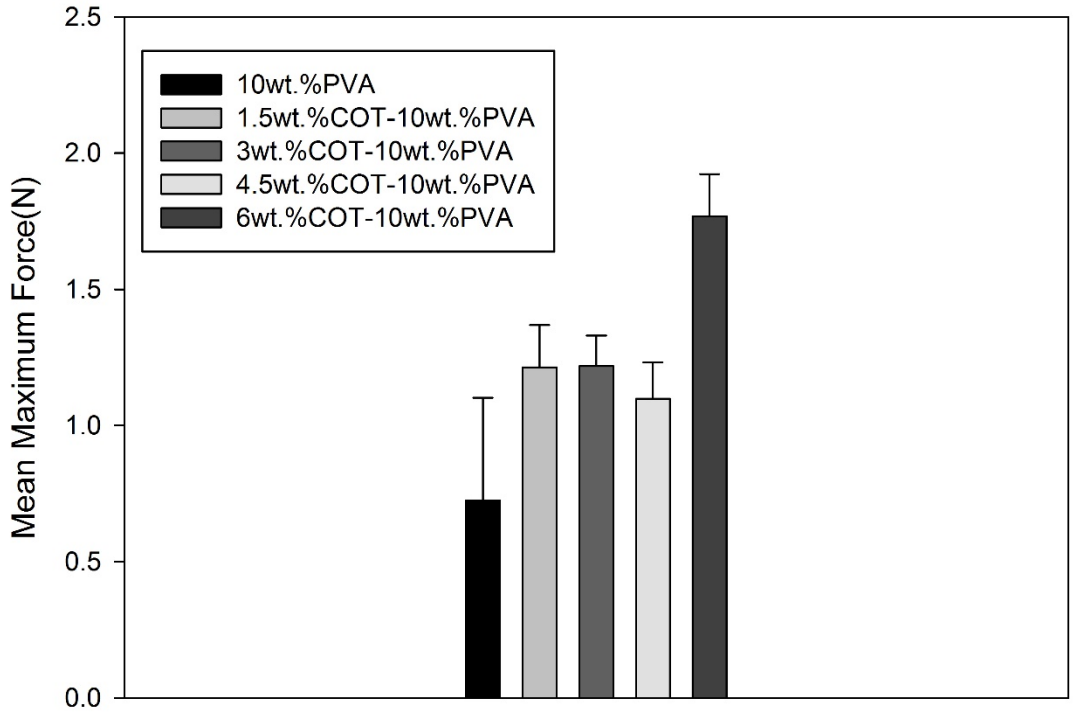

Figure 5.17 - Mean maximum force for tearing PVA-cotton hydrogel composites and 10 wt. % PVA on cycle 1.

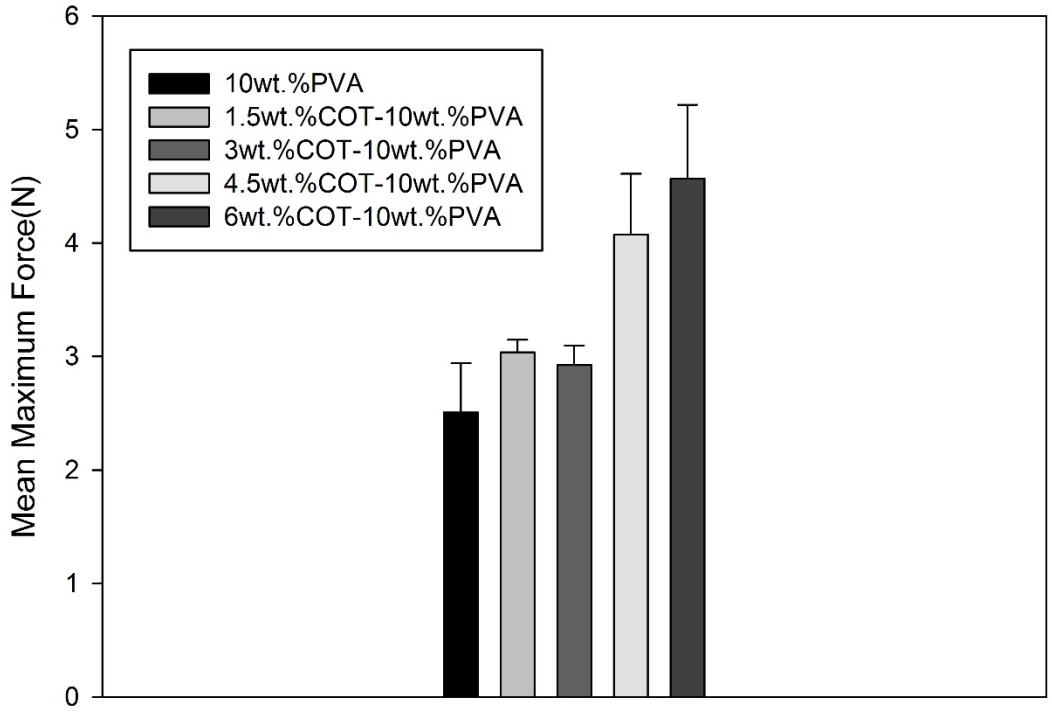

Figure 5.18 - Mean maximum force for tearing PVA-cotton hydrogel composites and 10 wt. % PVA on cycle 3.

By increasing the number of cycles the mean maximum force increased for cycle 3 (Figure 5.18). PVA-cotton hydrogel composites demonstrated higher mean maximum force for tearing compared to the control (P= <0.001). Generally, at higher fiber loading, mechanical properties of the composite improves [107]. By increasing the number of cycles and presence of additives, in cycle 3, 4.5 wt.% cotton-PVA and 6 wt.% cotton-PVA hydrogel composite had about two times higher maximum force than 10 wt.% PVA. There is no statistically significant difference between PVA-cotton hydrogel with 1.5 wt. % and 3 wt. % cotton (P=0.79, P>0.05). In addition, PVA-cotton hydrogel with 4.5 wt. % and 6 wt. % cotton are statistically the same (P=0.16, P>0.05).

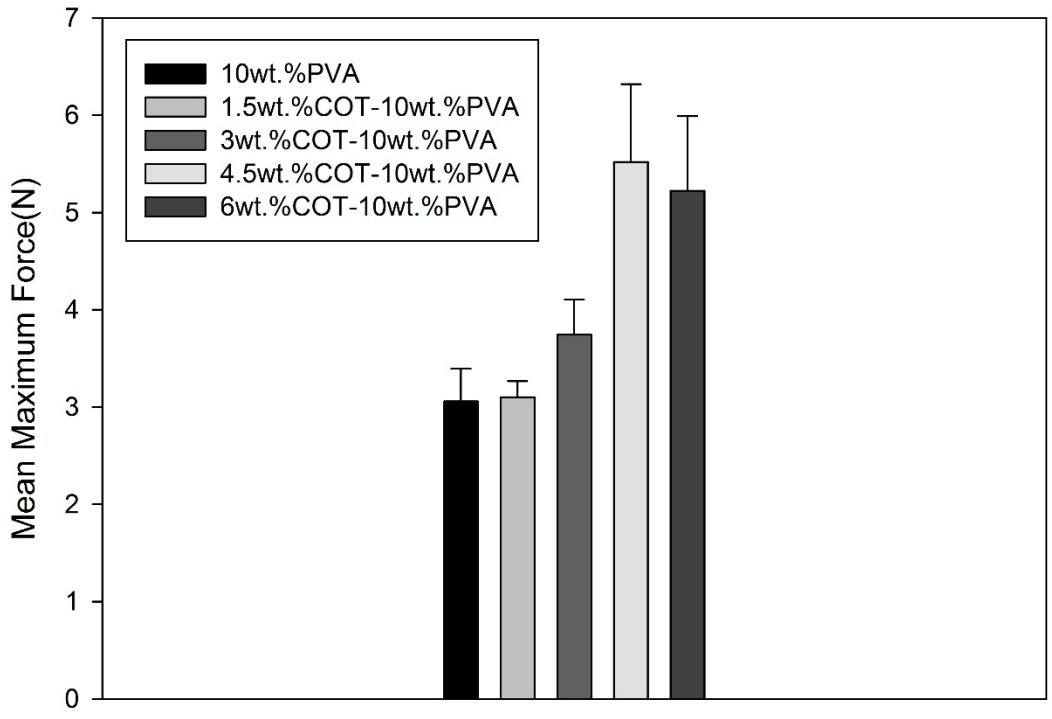

Figure 5.19 - Mean maximum force for tearing PVA-cotton hydrogel composites and 10 wt. % PVA on cycle 5.

In cycle 5, same pattern as cycle 3 was observed. When ANOVA was applied, there was no statistically significant difference between the control and PVA-cotton with 1.5 wt. % cotton ($P=0.82$, $P>0.05$). PVA-cotton hydrogels with 3, 4.5, and 6 wt. % had significantly higher mean maximum force ($P= <0.001$). PVA-cotton hydrogel with 4.5 and 6 wt. % cotton are also statistically the same ($P=0.49$, $P>0.05$). The mean force of tearing for PVA-cotton hydrogel composite with 6 wt. % was about two times more than 10 %wt. PVA. (Figure 5.19)

5.6. PVA Hydrogel Blends

5.6.1. PVA-Xanthan Gum Hydrogel

5.6.1.1. Stress-strain

Three different concentrations of xanthan gum (XG) were chosen: 0.5 wt. %, 1 wt. %, and 1.5 wt. %. Stress-strain curve of these hydrogels were examined for cycles 1, 3, 5, and 7.

Hydrogels with lower loading of xanthan gum (0.5 wt. % XG) are stiffer than other hydrogels in cycle 1. As shown in Figure 5.20, stress-strain curve for PVA-xanthan gum hydrogel with 0.5 wt. % xanthan gum is on top of other curves, followed by PVA-xanthan gum with 1 wt. % and 1.5 wt. %. The load curve for control is below the hydrogel blends. When ANOVA was applied, statistically significant difference between PVA-xanthan gum hydrogels and the control was observed ($P = <0.001$).

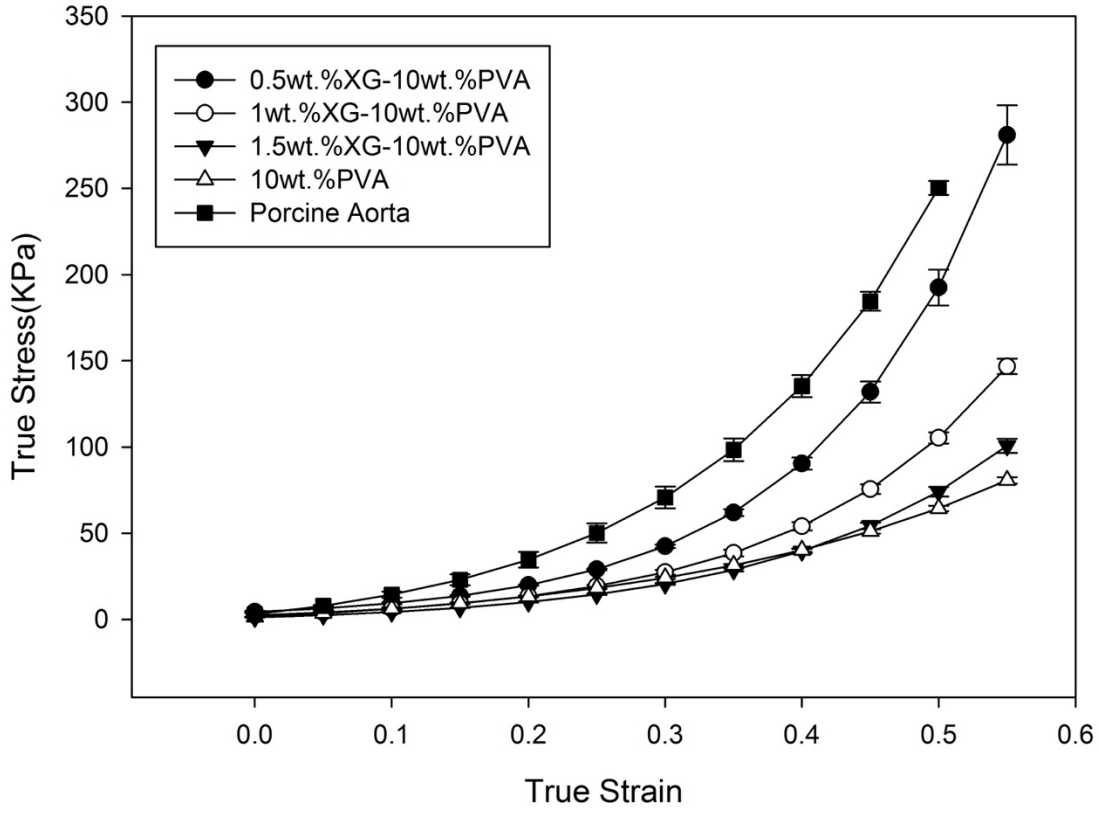

Figure 5.20 - Stress-strain curve for porcine aorta, PVA-xanthan gum hydrogel blend and 10 wt. % PVA hydrogel on cycle 1.

In cycle 3 there is statistically remarkable difference between PVA-xanthan gum hydrogel blend and the control. At 30% strain, 10 wt. % PVA shows higher stress than PVA-xanthan gum hydrogel (P= <0.001). At higher strain (50% strain), PVA-xanthan gum with 0.5 wt.% xanthan gum has higher stiffness than the control (P=0.004, P<0.05); while PVA-xanthan gum hydrogel with higher weight loading of xanthan gum (1 and 1.5 %) are less stiff than the control (P= <0.001). PVA-xanthan gum with highest weight loading of xanthan gum (1.5 wt. %) has the lowest stiffness among all other curves in cycle 3. Thermal cycling improved stiffness of 10 wt. % PVA more than PVA-xanthan gum hydrogel blends. There is no statistically significant difference between porcine aorta and PVA-xanthan gum hydrogel with 0.5 wt. % xanthan gum up to 40% strain. (Figure 5.21)

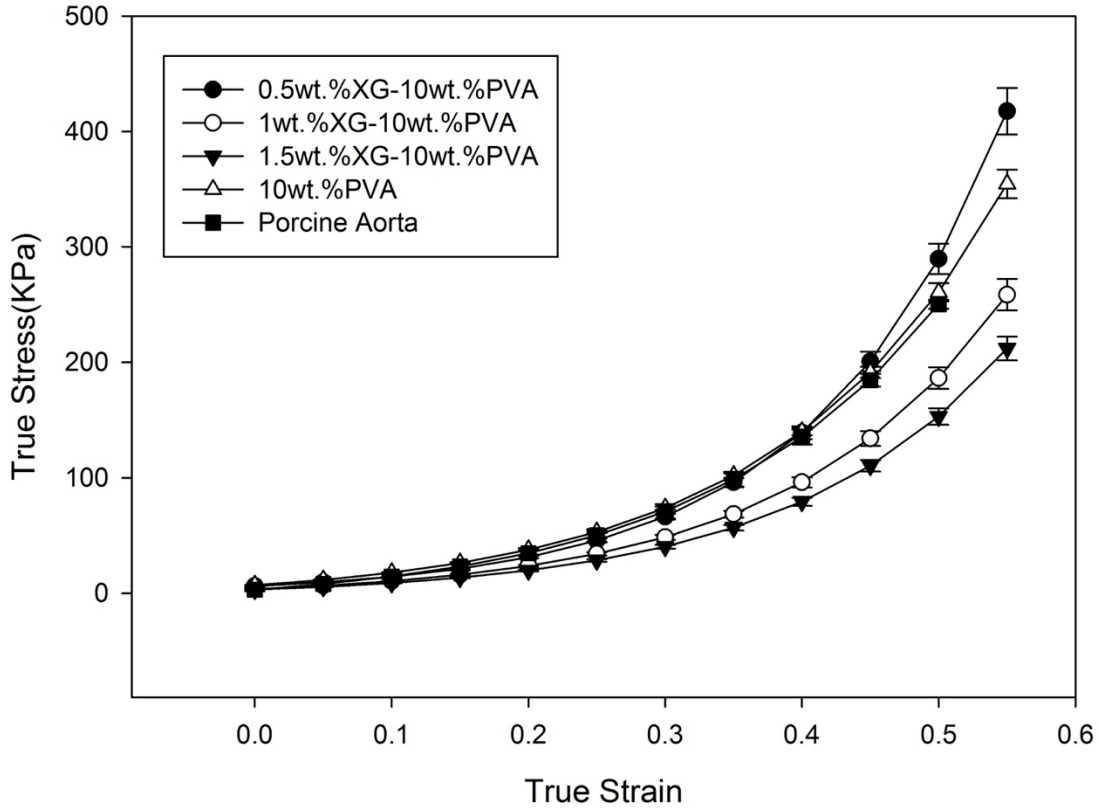

Figure 5.21 - Stress-strain curve for porcine aorta, PVA-xanthan gum hydrogel blend and 10 wt. % PVA hydrogel on cycle 3.

In 5th cycle, stiffness of PVA improved compared to 3rd cycle. On the other hand, PVA-xanthan gum hydrogel blends did not show dramatic growth in stiffness when it was compared to cycle 3. At 30% strain, there is a statistically significant difference between the control and PVA-xanthan gum hydrogel blends (P= <0.001). At 50% strain, PVA-xanthan gum hydrogel with 1 and 1.5 wt.% xanthan gum have lower stiffness (P= <0.001). Figure 5.22 shows PVA-xanthan gum hydrogel blends and 10 wt. % PVA stress-strain curve for cycle 5.

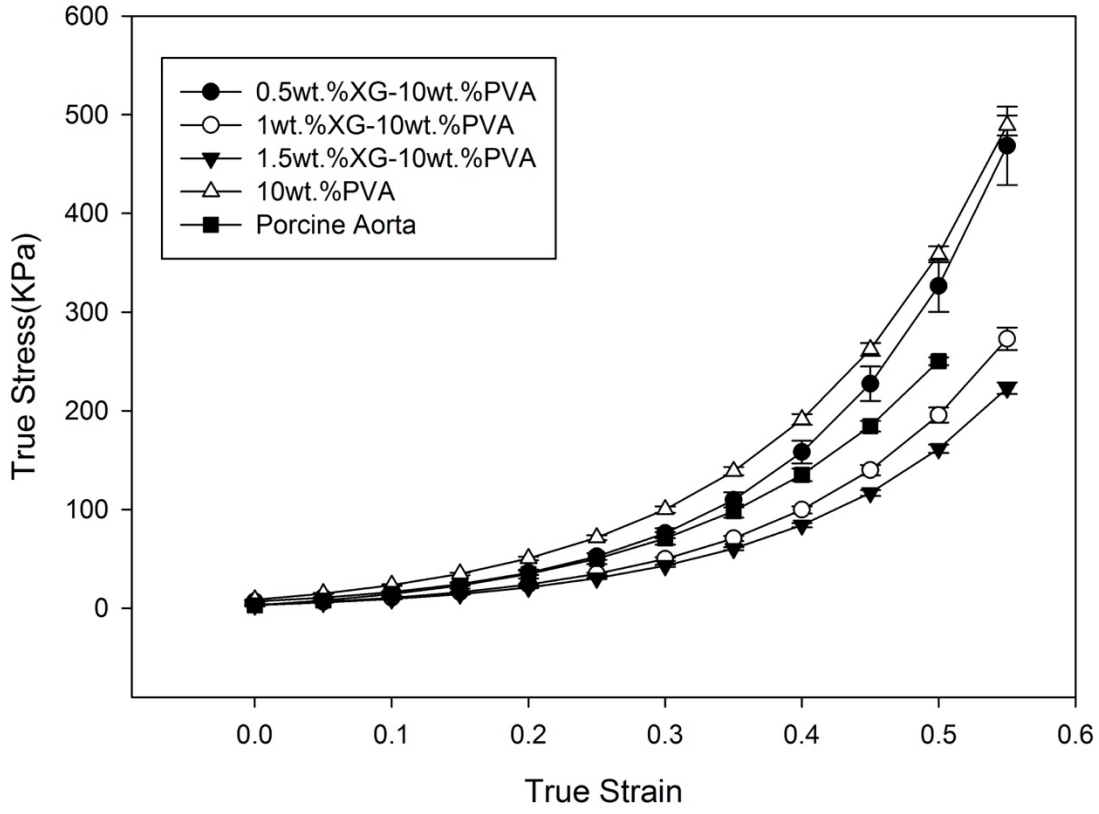

Figure 5.22 - Stress-strain curve for porcine aorta, PVA-xanthan gum hydrogel blend and 10 wt. % PVA hydrogel on cycle 5.

As shown in Figure 5.23, in cycle 7, 10 wt.% PVA is on top of other curves (PVA-xanthan gum hydrogel blends) followed by PVA-xanthan gum hydrogel with 0.5, 1, and 1.5 wt.%, respectively. One can conclude that thermal cycling does not enhance stiffness of PVA-xanthan gum hydrogel blends. When ANOVA was applied, there was a statistically significant difference between the control and PVA-xanthan gum hydrogels ($P = <0.001$). PVA-xanthan gum with 1 and 1.5 wt. % xanthan gum are statistically the same ($P=0.79$, $P>0.05$).

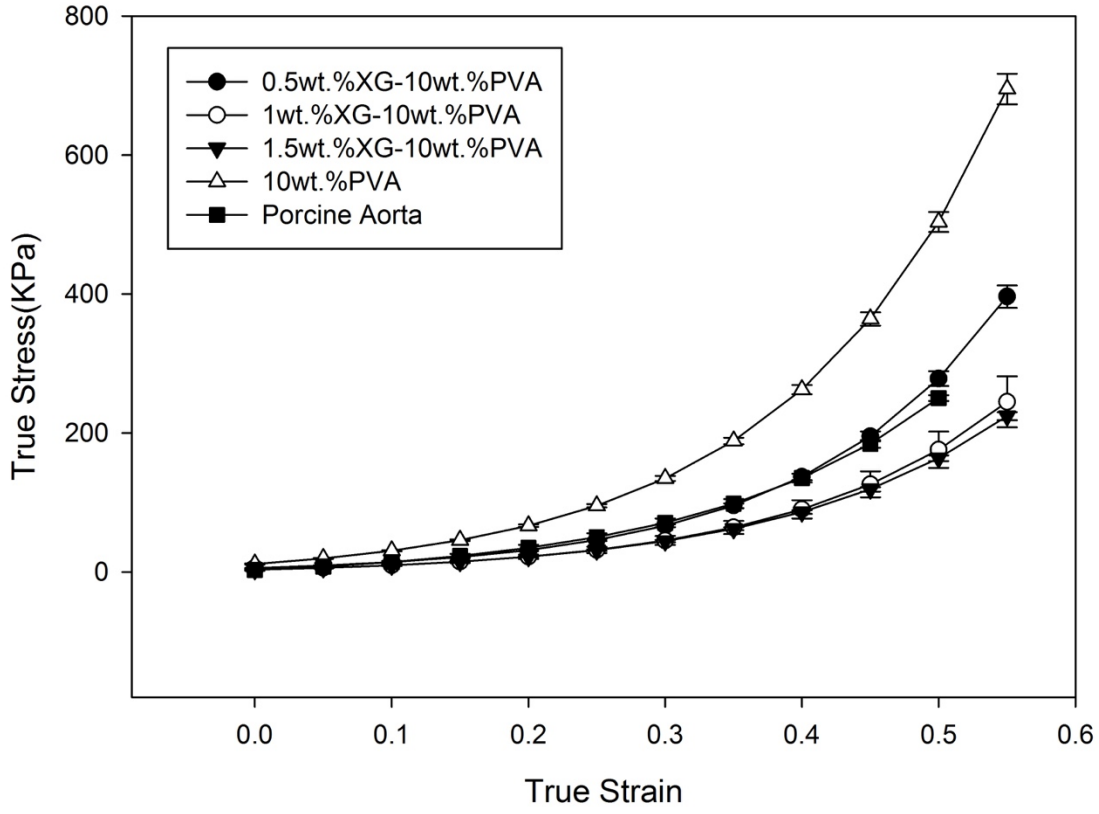

Figure 5.23 - Stress-strain curve for porcine aorta, PVA-xanthan gum hydrogel blend and 10 wt. % PVA hydrogel on cycle 7.

5.6.2. PVA-Sorbitol Hydrogel

5.6.2.1. Stress-strain

Sorbitol with different loadings was added to investigate the effect of addition of sorbitol (SOR) in PVA solution. The PVA-sorbitol hydrogel blends had four different concentrations of sorbitol: 2.5 wt. % SOR, 5 wt. % SOR, 7.5 wt. % SOR, and 10 wt. % SOR. The load curve for final hydrogels were studied in cycles 1, 3, 5, and 7.

For 1st cycle, there is statistically significant difference between PVA-sorbitol hydrogel blends and the control (P= <0.001). The control is stiffer than PVA-sorbitol composites in cycle 1. There is

no statistically significant difference between PVA-sorbitol hydrogels with different filler loadings (P>0.05). Figure 5.24 displays stress-strain curve of PVA-sorbitol hydrogel blend compared to the control.

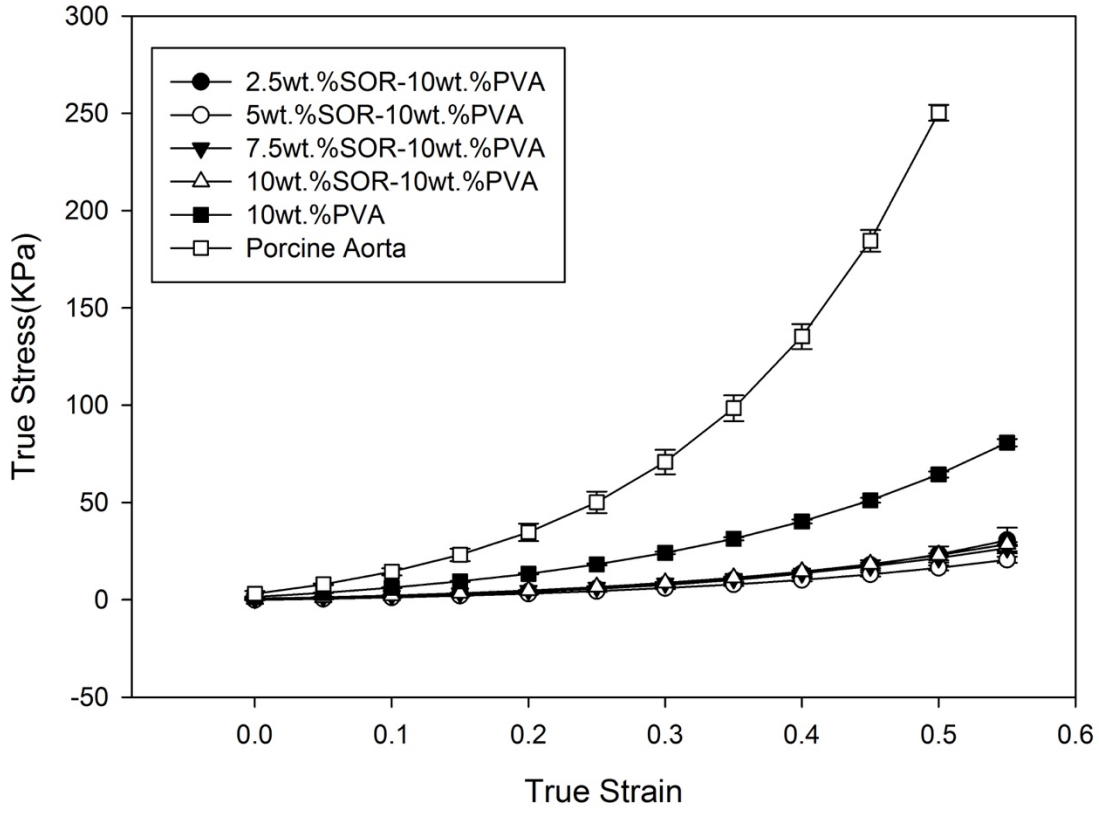

Figure 5.24 - Stress-strain curve for porcine aorta and PVA-sorbitol hydrogel blend and 10 wt. % PVA hydrogel on cycle 1.

Same pattern was observed in the 3rd cycle for PVA-sorbitol hydrogel blend and 10 wt. % PVA. As shown in Figure 5.25, 10 wt. % PVA is on top of all curves. There is a statistically significant difference between PVA-sorbitol hydrogels and the control in cycle 3 (P= <0.001). PVA-sorbitol hydrogel with 2.5 wt. % sorbitol is stiffer than PVA-sorbitol hydrogel with 7.5 and 10 wt. % sorbitol (P= <0.001). However, there is no statistically significant difference between PVA-sorbitol hydrogel with 2.5 and 5 wt. % sorbitol (P>0.05). While PVA-sorbitol with 5 and 7.5 wt.

% sorbitol are statistically the same (P>0.05); PVA-sorbitol with 5 wt. % sorbitol is stiffer than PVA-sorbitol with 10 wt. % sorbitol (P=0.009, P<0.05).

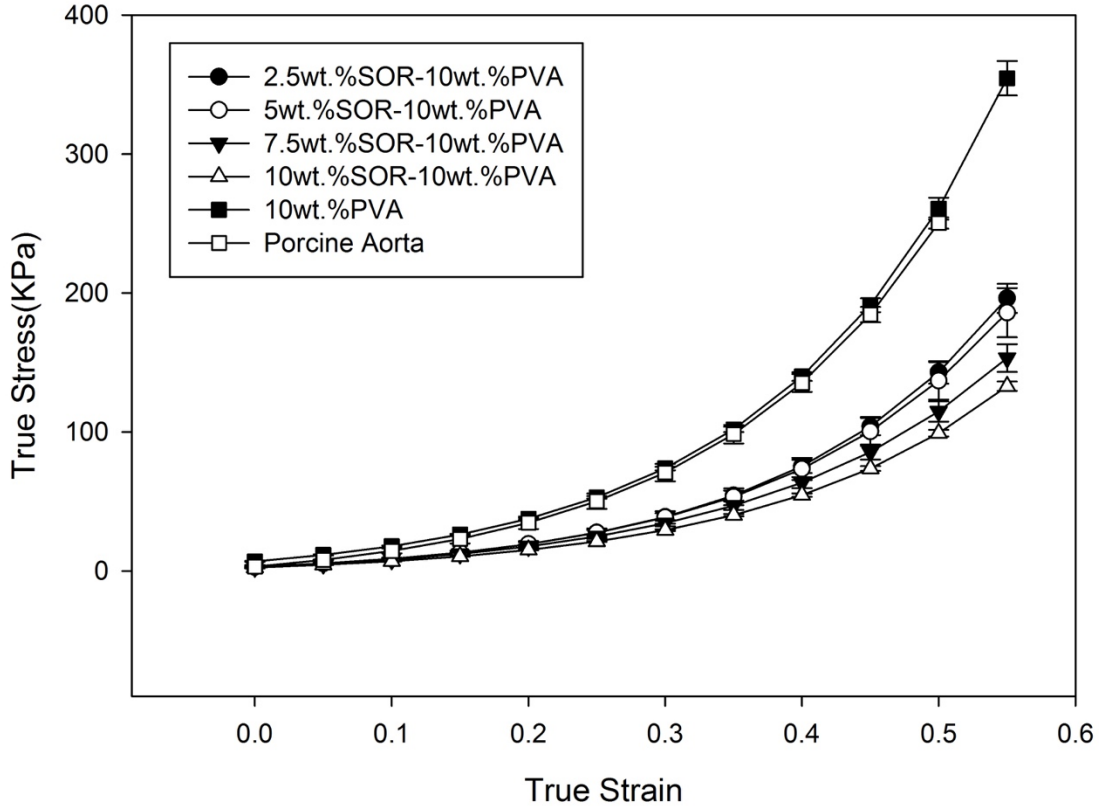

Figure 5.25 - Stress-strain curve for porcine aorta, PVA-sorbitol hydrogel blend and 10 wt. % PVA hydrogel on cycle 3.

Although stiffness increased by increasing the number of freeze-thaw cycles; thermal cycling had more influence in enhancing stiffness of 10 wt.% PVA compare to PVA-sorbitol hydrogels. The control has higher stiffness than PVA-sorbitol hydrogel in cycle 5 (P= <0.001). By applying ANOVA, there is no statistically significant difference between PVA-sorbitol in cycle 5 (P>0.05). Figures 5.26 and 5.27 present the stress-strain curve for PVA-sorbitol hydrogel blends and the control in cycle 5 and 7, respectively.

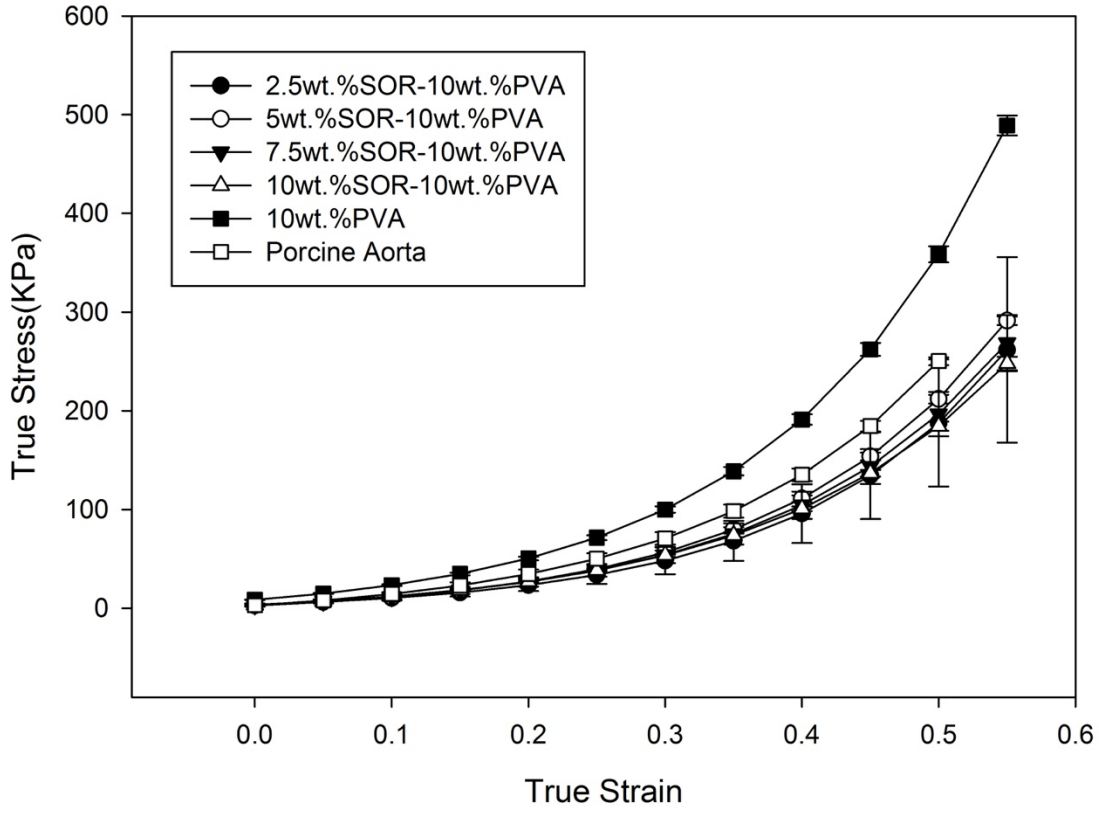

Figure 5.26 - Stress-strain curve for porcine aorta, PVA-sorbitol hydrogel blend and 10 wt. % PVA hydrogel on cycle 5.

In cycle 7, 10 wt. % PVA is stiffer than PVA-sorbitol hydrogel (P= <0.001). PVA-sorbitol with 7.5 and 10 wt. % sorbitol are statistically the same (P>0.05). At lower weight loadings of sorbitol (2.5 and 5 wt. %) there is statistically significant difference with PVA-sorbitol with 10 wt. % sorbitol (P= <0.001). At 50% strain, PVA-sorbitol with 2.5 wt. % sorbitol is statistically stiffer than PVA-sorbitol hydrogels with different sorbitol loadings (P<0.003).

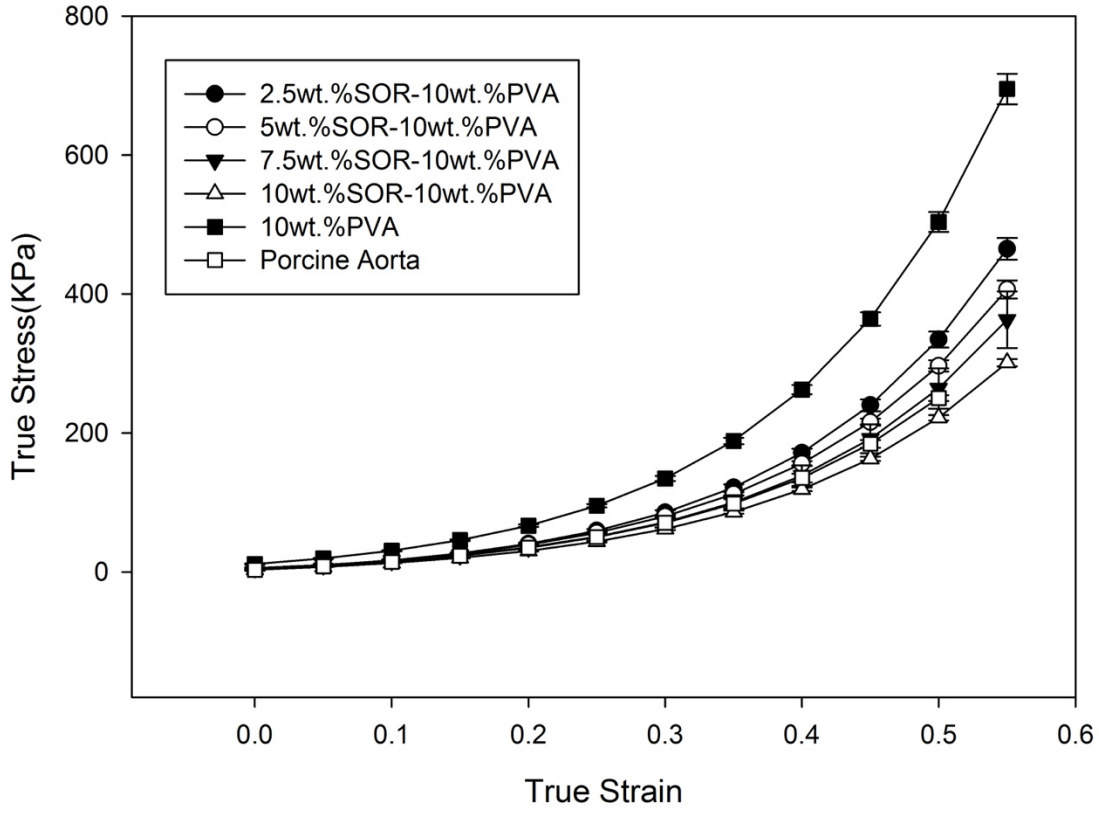

Figure 5.27 - Stress-strain curve for porcine aorta, PVA-sorbitol hydrogel blend and 10 wt. % PVA hydrogel on cycle 7.

5.6.2.2. Elongation at Break

5.6.2.2.1. Ultimate Elongation

Ultimate elongation was studied in PVA-sorbitol hydrogel blends for different number of thermal cycles. Figures 5.28, 5.29, 5.30, and 5.31 display ultimate elongation of PVA-sorbitol hydrogel blend in cycles 1, 3, 5, and 7, respectively.

In cycle 1, there was no statistically significant difference between 10 wt. % PVA and PVA-sorbitol blends. The soft and very delicate texture of 10 wt. % PVA and PVA-sorbitol with 2.5 wt.% sorbitol in cycle 1, made cutting process of samples hard. Most of these samples had defect;

and in few cases a fine sample was cut. High error bars for the control and PVA-sorbitol with 2.5 wt. % sorbitol is a proof of above mentioned statement. (Figure 5.28)

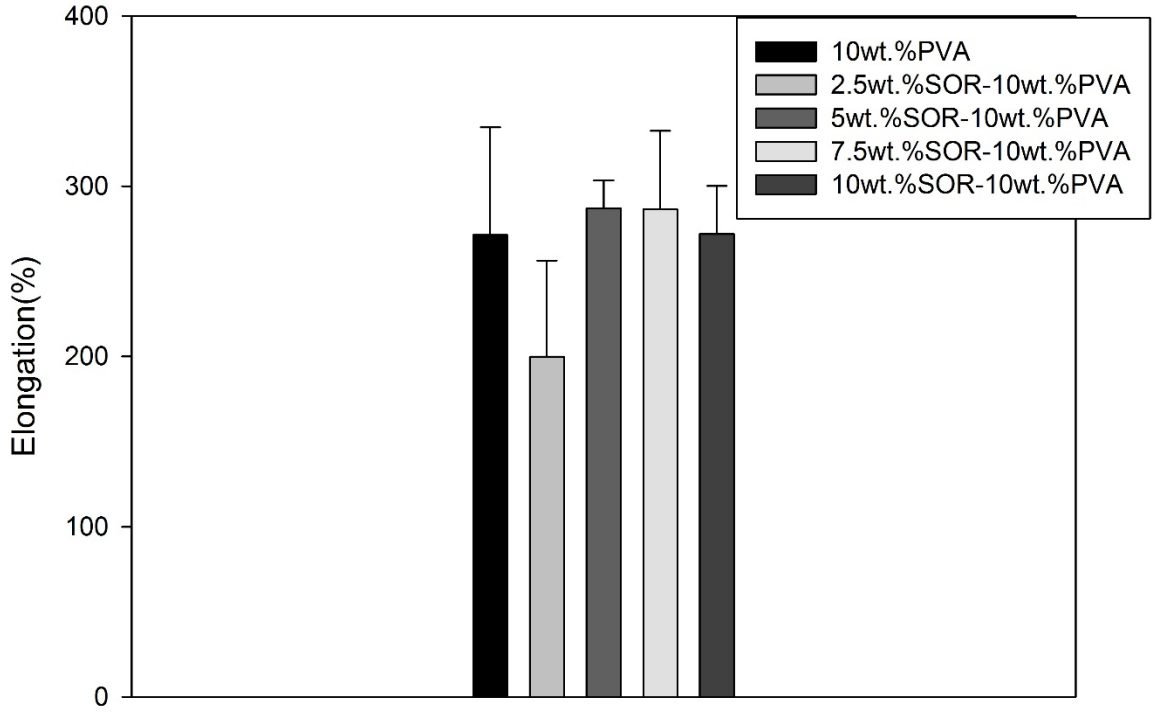

Figure 4.28 - Mean ultimate elongation for PVA-sorbitol hydrogel blend and 10 wt. % PVA hydrogel on cycle 1.

As displayed in Figure 5.29, ultimate elongation (%) increased by adding sorbitol to PVA in cycle 3. There is statistically significant difference between the control and PVA-sorbitol hydrogel with 5 and 10 wt. % sorbitol ($P<0.05$). However, there is not statistically significant difference between the control and PVA-sorbitol with 2.5 wt. % sorbitol ($P = 0.71$). The average ultimate elongation for the control and 5 wt. % SOR-PVA hydrogel blend has more than 30% improvement. Comparing Figures and 5.28 and 5.29, cryogenic treatment did not enhance elastic nature of hydrogels. By increasing the number of thermal cycles, these hydrogels become stiffer and less elastic.

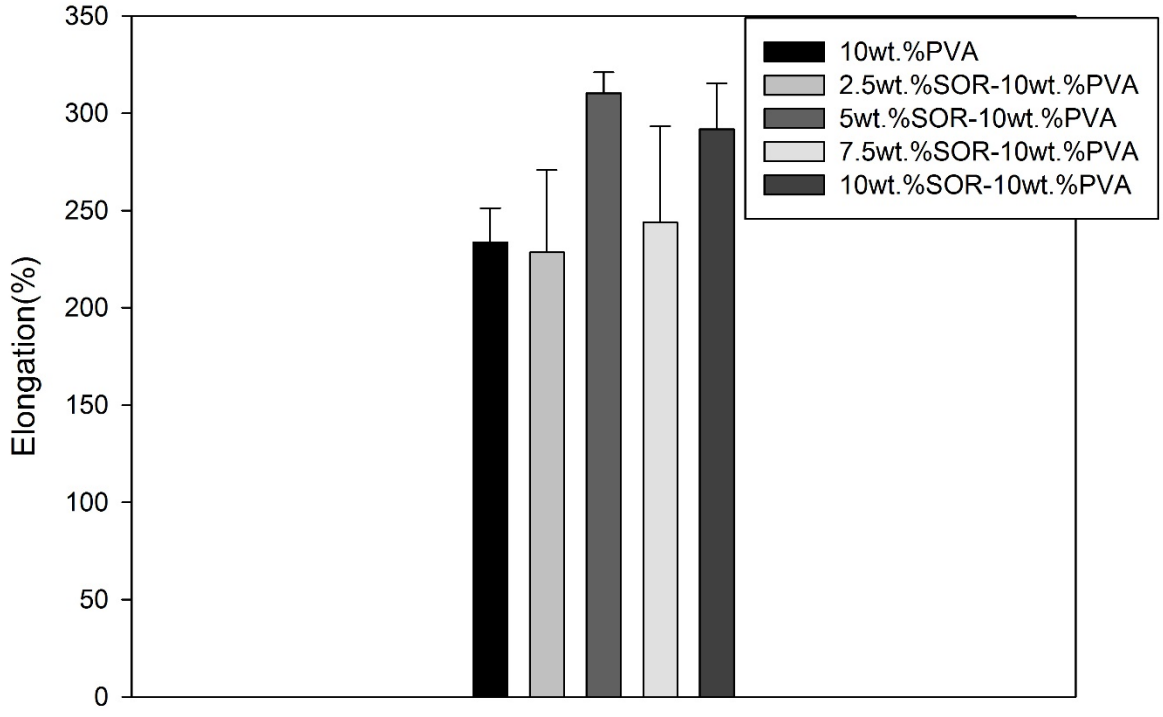

Figure 5.29 - Mean ultimate elongation for PVA-sorbitol hydrogel blend and 10 wt. % PVA hydrogel on cycle 3.

In cycle 5, same pattern in cycle 3 was observed. PVA-sorbitol blend with 2.5 and 7.5 wt. % sorbitol and the control were statistically the same. PVA-sorbitol with 5 and 10 wt. % sorbitol have higher ultimate elongation than the control. (Figure 5.30)

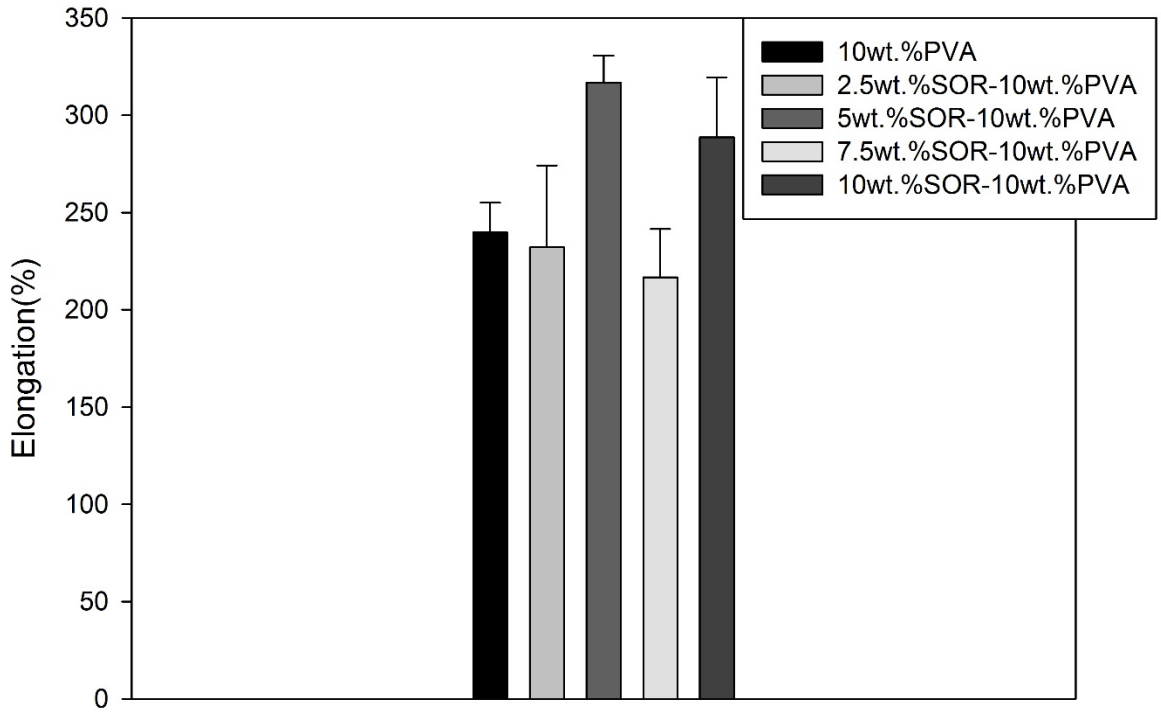

Figure 5.30 - Mean ultimate elongation of PVA-sorbitol hydrogel blend and 10 wt. % PVA on cycle 5.

Figure 5.31 shows the ultimate elongation of PVA-SOR hydrogel blends compared to the control in cycle 7. Thermal cycling weakens the elastic behavior of the hydrogels. When ANOVA was applied, PVA-sorbitol hydrogel with 5 wt. % 7.5 wt. %, 10 wt. % sorbitol were significantly different than 10 wt. % PVA hydrogel ($P<0.05$).

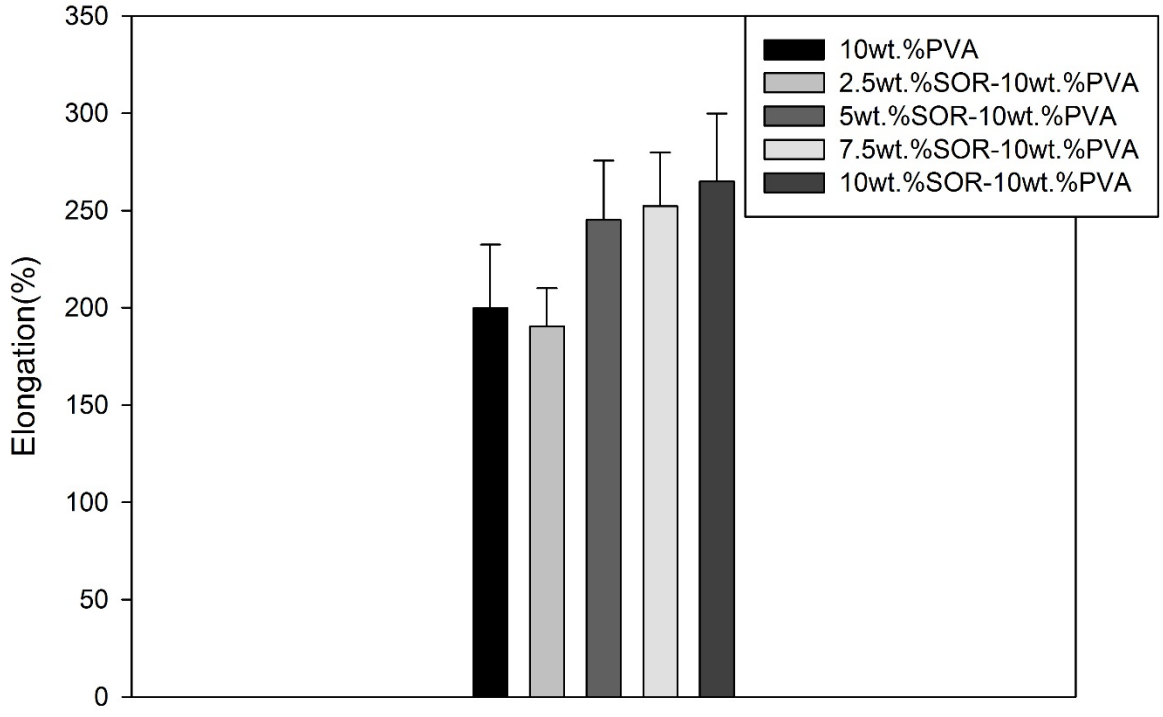

Figure 5.31 - Mean ultimate elongation for PVA-sorbitol hydrogel blend and 10 wt. % PVA hydrogel on cycle 7.

5.7. Relationship to Porcine Aorta Properties

5.7.1. Tensile Properties

The tensile properties of porcine aorta were compared to PVA-based hydrogel composites and PVA-based hydrogel blends to check if the stress-strain curves of these hydrogels match with porcine aorta for tissue phantom application. The stress-strain curve for porcine aorta was taken from Millon [79]. Figure 5.32 shows the load curve for porcine aorta.

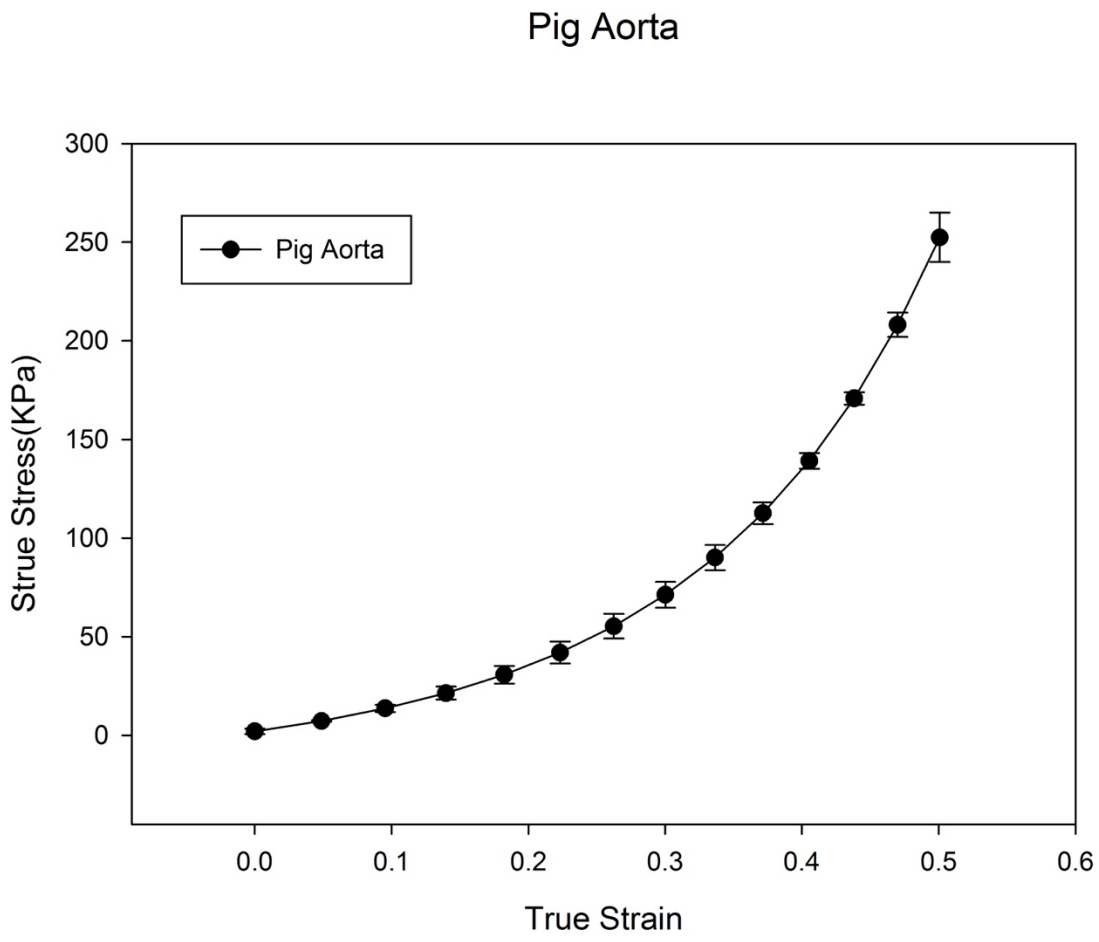

Figure 5.32 - Stress-strain curve for Pig Aorta from Millon.

Interestingly, the load curve closely matched, within physiological range, PVA-based hydrogels with 4.5 wt. % chitosan in cycle 5, 4.5 wt. % MCC, 1.5 wt. % cotton, and 0.5 wt. % xanthan gum in cycle 3. These hydrogels present the same tensile behavior up to 55% true strain. When ANOVA was applied to stress at every strain (up to 55%), these hydrogels and porcine aorta were found to be statistically the same.

Chapter 6 – Conclusions and Recommendations

The objective of this study was to develop mechanical testing procedures such as uniaxial tensile testing, elongation at break, and suture-tension pull through test for PVA-based hydrogel composites and blends. Prepared hydrogels were compared to porcine aorta load curve.

PVA-chitosan hydrogels were investigated to improve the stiffness of the material. However, addition of chitosan particles did not improve the stiffness of the final hydrogel. The presence of cotton fibers in the hydrogel, improved the strength of hydrogel. The weight loading of cotton fibers was proportional with tensile strength of these hydrogels.

Poly vinyl alcohol blended with sorbitol hydrogels have lower stiffness than 10 wt. % PVA in all cycles and weight loadings of sorbitol. Furthermore, PVA-sorbitol hydrogels showed more elastic behavior than 10 wt. % PVA. It is clear that addition of filler does not improve all properties of the material.

In order to successfully use the aforementioned hydrogels in tissue phantom applications, it is recommended that the mechanical properties of other tissues (tendon, ligament, skin, and articular cartilage) to be tested using the same procedure described in this thesis and then compared. Improving the mixing process will result in a better filler distribution in the matrix. Finally, the change in mechanical properties and crystallographic structure in PVA based hydrogels after the addition of fillers can be investigated further using X-ray diffraction (XRD) and SEM.

References:

[1] O. Okay, *Polymeric Cryogels*. 2014.

[2] V. I. Lozinsky, “Cryotropic gelation of poly (vinyl alcohol) solutions,” vol. 67, no. 7, 1998.

[3] R. M. Ottenbrite, *Biomedical Applications of Hydrogels Handbook*. 2010.

[4] V. I. Lozinsky, F. M. Plieva, I. Y. Galaev, and B. Mattiasson, “The potential of polymeric cryogels in bioseparation.,” *Bioseparation*, vol. 10, no. 4–5, pp. 163–188, 2001.

[5] K. Y. Lee and D. J. Mooney, “Hydrogels for Tissue Engineering,” vol. 101, no. 7, 2001.

[6] S. K. . Gulrez, S. Al-Assaf, and G. O. Phillips, “Hydrogels: Methods of Preparation, Characterisation and Applications in Molecular and Environmental Bioengineering,” *Prog. Mol. Environ. Bioeng. - From Anal. Moddelling to Technol. Appl.*, p. 646, 2011.

[7] L. E. Millon, *Isotropic and Anisotropic Polyvinyl Alcohol Based Hydrogels For Biomedical Applications*, no. August. 2006.

[8] H. Park and K. Park, “Hydrogels in bioapplications,” *ACS Symp. Ser.*, vol. 627, no. 2, pp. 2–10, 1996.

[9] Gordon Melissa J, *Controlling the Mechanical Properties of PVA Hydrogels for Biomedical Applications*. 1999.

[10] S. Monnerie, W. Suter, E. L. Thomas, and W. R. J. Young, *Biopolymers PVA Hydrogels Anionic Polymerisation Nanocomposites*. 2000.

[11] V. I. Lozinsky and F. M. Plieva, “Poly (vinyl alcohol) cryogels employed as matrices for cell immobilization . 3 . Overview of recent research and developments,” vol. 0229, no. 98, pp. 227–242, 1998.

[12] W. K. Wan, G. Campbell, Z. F. Zhang, A. J. Hui, and D. R. Boughner, “Optimizing the tensile properties of polyvinyl alcohol hydrogel for the construction of a bioprosthetic heart valve stent,” *J. Biomed. Mater. Res.*, vol. 63, no. 6, pp. 854–861, 2002.

[13] V. I. Lozinsky, “Cryogels on the basis of natural and synthetic polymers: preparation, properties and application,” *Russ. Chem. Rev.*, vol. 71, no. 6, pp. 489–511, 2002.

[14] A. S. Hoffman, “Hydrogels for biomedical applications ☆” *Adv. Drug Deliv. Rev.*, vol. 64, pp. 18–23, 2012.

[15] P. Taylor, M. Street, and L. Wt, “Access details : Access Details : [subscription number 927346821] Polymer Gels #,” no. 927346821, 2004.

[16] G. Śliwiński, A. Schneider, M. Schulz, M. Wolf, A. Fiolka, M. Meyer, H. Feußner, Z. Śliwiński, R. Poll, and C. Thiele, “Physical Organ Phantoms for Training in Minimal Invasive Surgery (MIS),” pp. 120–123, 2009.

[17] A. M. De Grand, S. J. Lomnes, D. S. Lee, M. Pietrzykowski, T. G. Morgan, R. G. Laurence, and J. V Frangioni, “Tissue-like phantoms for near-infrared fluorescence imaging system assessment and the training of surgeons,” vol. 11, no. February 2006, pp. 1–10, 2016.

[18] S. Gibson, “Simulating Arthroscopic Knee Surgery Using Volumetric Object Representation, Real-Time Volume Rendering and Haptic Feedback.”

[19] A. Sekhar, M. R. Sun, and B. Siewert, “A Tissue Phantom Model for Training Liver Biopsy,” *Acad. Radiol.*, vol. 21, no. 7, pp. 902–908.

[20] hiroyuki Abe, K. Hayashi, and M. Sato, “Data Book on Mechanical Properties of Living Cells , Tissues , and Organs,” 1996.

[21] V. I. Lozinsky, “Polymeric cryogels as a new family of macroporous and

supermacroporous materials for biotechnological purposes," *Russ. Chem. Bull.*, vol. 57, no. 5, pp. 1015–1032, 2008.

[22] M. U. S. Jhon, J. D. Andrade, and D. Materials, "Water and Hydrogels," vol. 7, pp. 509–522, 1973.

[23] J. E. Babensee, J. M. Anderson, L. V. McIntire, and A. G. Mikos, "Host response to tissue engineered devices," *Adv. Drug Deliv. Rev.*, vol. 33, no. 1–2, pp. 111–139, 1998.

[24] K. Y. Lee, E. Alsberg, and D. J. Mooney, "Degradable and injectable poly (aldehyde guluronate) hydrogels for bone tissue engineering," *J. Biomed. Mater. Res. Part A*, vol. 56, no. 2, pp. 228–233, 2001.

[25] B. Ríhová and B. Rihova, "Immunocompatibility and biocompatibility of cell delivery systems.," *Adv. Drug Deliv. Rev.*, vol. 42, no. 1–2, pp. 65–80, 2000.

[26] J. Kohn, "Trends in the Development of Bioresorbable Polymers for Medical Applications," pp. 216–250.

[27] A. A. Amini and L. S. Nair, "Enzymatically cross-linked injectable gelatin gel as osteoblast delivery vehicle," *J. Bioact. Compat. Polym.*, vol. 27, no. 4, pp. 342–355, 2012.

[28] K. P. Vercruysse, D. M. Marecak, J. F. Marecek, and G. D. Prestwich, "Synthesis and in vitro degradation of new polyvalent hydrazide cross-linked hydrogels of hyaluronic acid," *Bioconjug. Chem.*, vol. 8, no. 5, pp. 686–694, 1997.

[29] T. Andersen, P. Auk-Emblem, and M. Dornish, "3D Cell Culture in Alginate Hydrogels," *Microarrays*, vol. 4, no. 2, pp. 133–161, 2015.

[30] B. Soediono, "The influence of physical structure and charge on neurite extension in a 3D hydrogel scaffold," *J. Chem. Inf. Model.*, vol. 53, p. 160, 1989.

[31] W. R. Gombotz and D. K. Pettit, "Biodegradable polymers for protein and peptide drug

delivery.," *Bioconjug. Chem.*, vol. 6, no. 4, pp. 332–51, 1995.

[32] S. Pulapura and J. Kohn, "Trends in the development of bioresorbable polymers for medical applications.," *J. Biomater. Appl.*, vol. 6, pp. 216–250, 1992.

[33] L. Payne and A. Andrianov, "Protein release from polyphosphazene matrices.," *Adv. Drug Deliv. Rev.*, vol. 31, no. 3, pp. 185–196, 1998.

[34] P. Science, V. I. Lozinsky, G. E. Korotaeva, and S. V Rogozhin, "Study of cryostructurization of polymer systems," vol. 622, pp. 617–622, 1984.

[35] V. I. Lozinsky, L. G. Damshkaln, R. Brown, and I. A. N. T. Norton, "Study of Cryostructuration of Polymer Systems . XVI . Freeze – Thaw-Induced Effects in the Low Concentration Systems Amylopectin – Water," pp. 1740–1748.

[36] W. S. Chan and R. T. Toledo, "DYNAMICS O F FREEZING AND THEIR EFFECTS O N THE WATER-HOLDING CAPACITY O F A GELATINIZED STARCH GEL," vol. 41, pp. 301–303, 1976.

[37] S. Y. Chun and B. Yoo, "Effect of molar substitution on rheological properties of hydroxypropylated rice starch pastes," *Starch/Staerke*, vol. 59, no. 7, pp. 334–341, 2007.

[38] a. S. Navarro, M. N. Martino, and N. E. Zaritzky, "Viscoelastic properties of frozen starch-triglycerides systems," *J. Food Eng.*, vol. 34, no. 4, pp. 411–427, 1997.

[39] V. I. Lozinsky and L. G. Damshkaln, "Study of Cryostructuration of Polymer Systems . XVII . Poly (vinyl alcohol) Cryogels : Dynamics of the Cryotropic," pp. 2017–2023, 2017.

[40] H. Takeshita, T. Kanaya, K. Nishida, and K. Kaji, "Gelation process and phase separation of PVA solutions as studied by a light scattering technique," *Macromolecules*, vol. 32, no. 23, pp. 7815–7819, 1999.

[41] L. G. Damshkaln, I. A. Simenel, and V. I. Lozinsky, “Study of Cryostructuration of Polymer Systems . XV . Freeze – Thaw-Induced Formation of Cryoprecipitate Matter from Low-Concentrated Aqueous Solutions of Poly (vinyl alcohol),” pp. 1978–1986, 1999.

[42] V. I. Lozinsky, E. S. Vainerman, L. V Domotenko, A. M. Mamtsis, E. E. Titova, E. M. Belavtseva, and S. V Rogozhin, “Study of cryostructurization of polymer systems VII . Structure formation under freezing of poly (vinyl alcohol) aqueous solutions,” vol. 24, pp. 19–24, 1986.

[43] J. L. Valentín, D. López, R. Hernández, C. Mijangos, and K. Saalwächter, “Structure of Poly(vinyl alcohol) Cryo-Hydrogels as Studied by Proton Low-Field NMR Spectroscopy.,” *Macromolecules*, vol. 42, no. 1, pp. 263–272, 2009.

[44] R. Ricciardi, G. Mangiapia, F. Lo Celso, L. Paduano, R. Triolo, F. Auriemma, C. De Rosa, and F. Lauprêtre, “Structural organization of poly(vinyl alcohol) hydrogels obtained by freezing and thawing techniques: A SANS study,” *Chem. Mater.*, vol. 17, no. 5, pp. 1183–1189, 2005.

[45] Y. Osada, J. Ping Gong, and Y. Tanaka, “Polymer Gels,” *J. Macromol. Sci. Part C Polym. Rev.*, vol. 44, no. 1, pp. 87–112, 2004.

[46] E. Of, “S Tructural D Esign of O Ffshore S Hips F Ebruary 2002,” pp. 9–29, 2002.

[47] J. M. Rosiak and F. Yoshii, “Hydrogels and their medical applications,” *Nucl. Instruments Methods Phys. Res. Sect. B Beam Interact. with Mater. Atoms*, vol. 151, no. 1–4, pp. 56–64, 1999.

[48] M. I. Baker, S. P. Walsh, Z. Schwartz, and B. D. Boyan, “A review of polyvinyl alcohol and its uses in cartilage and orthopedic applications,” *J. Biomed. Mater. Res. Part B Appl.*

Biomater., vol. 100B, no. 5, pp. 1451–1457, 2012.

[49] G. Paradossi, F. Cavalieri, E. Chiessi, C. Spagnoli, and M. K. Cowman, "Poly(vinyl alcohol) as versatile biomaterial for potential biomedical applications," *J. Mater. Sci. Mater. Med.*, vol. 14, no. 8, pp. 687–691, 2003.

[50] A. J. Hui, *Hydroge-Based Artificial Heart Valve Stent Material*. 1998.

[51] N. Kashyap, N. Kumar, and M. N. V. R. Kumar, "Hydrogels for pharmaceutical and biomedical applications.," *Crit. Rev. Ther. Drug Carrier Syst.*, vol. 22, no. 2, pp. 107–149, 2005.

[52] V. I. Lozinsky and F. M. Plieva, "Poly(vinyl alcohol) cryogels employed as matrices for cell immobilization. 3. Overview of recent research and developments," *Enzyme Microb. Technol.*, vol. 23, no. 3–4, pp. 227–242, 1998.

[53] C. U. Devi, R. M. Vasu, and a K. Sood, "Design, fabrication, and characterization of a tissue-equivalent phantom for optical elastography.," *J. Biomed. Opt.*, vol. 10, no. 4, p. 44020, 2005.

[54] N. a. Peppas and N. K. Mongia, "Ultrapure poly(vinyl alcohol) hydrogels with mucoadhesive drug delivery characteristics," *Eur. J. Pharm. Biopharm.*, vol. 43, no. 1, pp. 51–58, 1997.

[55] F. M. Plieva, M. Karlsson, M. R. Aguilar, D. Gomez, S. Mikhalovsky, I. Y. Galaev, and B. Mattiasson, "Pore structure of macroporous monolithic cryogels prepared from poly(vinyl alcohol)," *J. Appl. Polym. Sci.*, vol. 100, pp. 1057–1066, 2006.

[56] R. Ricciardi, F. Auriemma, C. De Rosa, and F. Lauprêtre, "X-ray Diffraction Analysis of Poly(vinyl alcohol) Hydrogels, Obtained by Freezing and Thawing Techniques," *Macromolecules*, vol. 37, no. 5, pp. 1921–1927, 2004.

[57] C. M. Hassan and N. A. Peppas, “Structure and Morphology of Freeze / Thawed PVA Hydrogels,” pp. 2472–2479, 2000.

[58] R. Ricciardi, C. Gaillet, and G. Ducouret, “Investigation of the relationships between the chain organization and rheological properties of atactic poly (vinyl alcohol) hydrogels,” vol. 44, pp. 3375–3380, 2003.

[59] S. R. Stauffer and N. a. Peppast, “Poly(vinyl alcohol) hydrogels prepared by freezing-thawing cyclic processing,” *Polymer (Guildf).*, vol. 33, no. 18, pp. 3932–3936, 1992.

[60] M. Aider and D. De Halleux, “LWT - Food Science and Technology Cryoconcentration technology in the bio-food industry : Principles and applications,” *LWT - Food Sci. Technol.*, vol. 42, no. 3, pp. 679–685, 2009.

[61] V. I. Lozinsky, L. G. Damshkaln, I. N. Kurochkin, and I. I. Kurochkin, “Study of cryostructuring of polymer systems. 33. Effect of rate of chilling aqueous poly(vinyl alcohol) solutions during their freezing on physicochemical properties and porous structure of resulting cryogels,” *Colloid J.*, vol. 74, no. 3, pp. 319–327, 2012.

[62] K. Masuda, “H CRAMPS Measurements of Different Types of OH Groups in Poly (vinyl alcohol) Films.” 1998.

[63] M. Kobayashi, “Structural and dynamix studies of poly (vinyl alcohol) gels by high-resolution solid-state C NMR spectroscopy.” 1997.

[64] S. Ramakrishna, J. Mayer, E. Wintermantel, and K. W. Leong, “Biomedical applications of polymer-composite materials: A review,” *Compos. Sci. Technol.*, vol. 61, no. 9, pp. 1189–1224, 2001.

[65] F. Hussain, “Review article: Polymer-matrix Nanocomposites, Processing, Manufacturing, and Application: An Overview,” *J. Compos. Mater.*, vol. 40, no. 17, pp. 1511–1575,

2006.

[66] M. Dash, F. Chiellini, R. M. Ottenbrite, and E. Chiellini, “Chitosan - A versatile semi-synthetic polymer in biomedical applications,” *Prog. Polym. Sci.*, vol. 36, no. 8, pp. 981–1014, 2011.

[67] M. G. Cascone, N. Barbani, C. C. P.Giusti, G. Ciardelli, and L. Lazzeri, “Bioartificial polymeric materials based on polysaccharides,” *J. Biomater. Sci. Polym. Ed.*, vol. 12, no. 3, pp. 267–281, 2012.

[68] M. G. Cascone and S. Maltinti, “Hydrogels based on chitosan and dextran as potential drug delivery systems,” *J. Mater. Sci. Mater. Med.*, vol. 10, no. 5, pp. 301–307, 1999.

[69] B. Duan, X. Yuan, Y. Zhu, Y. Zhang, X. Li, Y. Zhang, and K. Yao, “A nanofibrous composite membrane of PLGA–chitosan/PVA prepared by electrospinning,” *Eur. Polym. J.*, vol. 42, no. 9, pp. 2013–2022, 2006.

[70] M. G. Cascone, N. Barbani, C. Cristallini, P. Giusti, G. Ciardelli, and L. Lazzeri, “Review article Bioarti cial polymeric materials based on polysaccharides,” *J. Biomater. Sci. Polym.*, vol. 12, no. 3, pp. 267–281, 2001.

[71] D. T. Mathews, “Mechanical and Morphological Characteristics of Poly (vinyl alcohol)/Chitosan Hydrogels,” *J. Appl. Phys.*, vol. 113, pp. 1763–1772, 2009.

[72] Y. Liu, N. E. Vrana, P. A. Cahill, and G. B. McGuinness, “Physically crosslinked composite hydrogels of PVA with natural macromolecules: Structure, mechanical properties, and endothelial cell compatibility,” *J. Biomed. Mater. Res. Part B Appl. Biomater.*, vol. 90B, no. 2, pp. 492–502, 2009.

[73] E. S. Costa-Júnior, E. F. Barbosa-Stancioli, A. A. P. Mansur, W. L. Vasconcelos, and H. S. Mansur, “Preparation and characterization of chitosan/poly(vinyl alcohol) chemically

crosslinked blends for biomedical applications," *Carbohydr. Polym.*, vol. 76, no. 3, pp. 472–481, 2009.

[74] I. S. Arvanitoyannis, "Totally and Partially Biodegradable Polymer Blends Based on Natural and Synthetic Macromolecules : Preparation , Physical Properties , and Potential as Food Packaging Materials," *Polymer (Guildf).*, vol. 39, no. 2, pp. 205–271, 1999.

[75] Y. T. Jia, J. Gong, X. H. Gu, H. Y. Kim, J. Dong, and X. Y. Shen, "Fabrication and characterization of poly (vinyl alcohol)/chitosan blend nanofibers produced by electrospinning method," *Carbohydr. Polym.*, vol. 67, no. 3, pp. 403–409, 2007.

[76] J. Bonilla, E. Fortunati, L. Atarés, a. Chiralt, and J. M. Kenny, "Physical, structural and antimicrobial properties of poly vinyl alcohol-chitosan biodegradable films," *Food Hydrocoll.*, vol. 35, pp. 463–470, 2014.

[77] I. Siró and D. Plackett, "Microfibrillated cellulose and new nanocomposite materials: a review," *Cellulose*, vol. 17, no. 3, pp. 459–494, 2010.

[78] L. E. Millon, "The Polyvinyl Alcohol-Bacterial Cellulose System As A New Nanocomposite for Biomedical Applications," *J. Biomed. Mater. Res. B. Appl. Biomater.*, vol. 83, no. 2, pp. 340–344, 2007.

[79] L. E. Millon, G. Guhados, and W. Wan, "Anisotropic polyvinyl alcohol-Bacterial cellulose nanocomposite for biomedical applications.," *J. Biomed. Mater. Res. B. Appl. Biomater.*, vol. 86, no. 2, pp. 444–52, 2008.

[80] D. Klemm, F. Kramer, S. Moritz, T. Lindström, M. Ankerfors, D. Gray, and A. Dorris, "Nanocelluloses: A New Family of Nature-Based Materials," *Angew. Chemie Int. Ed.*, vol. 50, no. 24, pp. 5438–5466, 2011.

[81] T. Abitbol, T. Johnstone, T. M. Quinn, and D. G. Gray, "Reinforcement with cellulose

nanocrystals of poly(vinyl alcohol) hydrogels prepared by cyclic freezing and thawing," *Soft Matter*, vol. 7, no. 6, p. 2373, 2011.

[82] A. Mihranyan, "Viscoelastic properties of cross-linked polyvinyl alcohol and surface-oxidized cellulose whisker hydrogels," *Cellulose*, vol. 20, no. 3, pp. 1369–1376, 2013.

[83] L. a. Utracki, "History of Commercial Polymer Alloys and Blends (From a Perspective of the Patent Literature)*," *Polym. Eng. Sci.*, vol. 35, no. 1, pp. 2–17, 1995.

[84] F. García-Ochoa, V. E. Santos, J. a. Casas, and E. Gómez, "Xanthan gum: Production, recovery, and properties," *Biotechnol. Adv.*, vol. 18, no. 7, pp. 549–579, 2000.

[85] B. Katzbauer, "Properties and applications of xanthan gum," *Polym. Degrad. Stab.*, vol. 59, no. 1–3, pp. 81–84, 1998.

[86] A. Palaniraj and V. Jayaraman, "Production, recovery and applications of xanthan gum by Xanthomonas campestris," *J. Food Eng.*, vol. 106, no. 1, pp. 1–12, 2011.

[87] P. Giannouli and E. R. Morris, "Cryogelation of xanthan," *Food Hydrocoll.*, vol. 17, no. 4, pp. 495–501, 2003.

[88] S. K. H. Gulrez, S. Al-Assaf, and G. O. Phillips, "Hydrogels : Methods of Preparation , Characterisation and Applications," *Prog. Mol. Environ. Bioeng.*, vol. 51, pp. 117 – 150, 2003.

[89] I. C. Alupei, M. Popa, M. Hamcerencu, and M. J. M. Abadie, "Superabsorbant hydrogels based on xanthan and poly(vinyl alcohol)," *Eur. Polym. J.*, vol. 38, no. 11, pp. 2313–2320, 2002.

[90] S. Ray, S. Banerjee, S. Maiti, B. Laha, S. Barik, B. Sa, and U. K. Bhattacharyya, "Novel interpenetrating network microspheres of xanthan gum-poly(vinyl alcohol) for the delivery of diclofenac sodium to the intestine--in vitro and in vivo evaluation.," *Drug*

Deliv., vol. 17, no. 7, pp. 508–19, 2010.

[91] S. S. Bhattacharya, A. Mishra, D. Pal, A. K. Ghosh, A. Ghosh, S. Banerjee, and K. K. Sen, "Synthesis and Characterization of Poly(acrylic acid)/Poly(vinyl alcohol)-xanthan Gum Interpenetrating Network (IPN) Superabsorbent Polymeric Composites," *Polym. Plast. Technol. Eng.*, vol. 51, no. 9, pp. 878–884, 2012.

[92] T. Bhunia, A. Giri, T. Nasim, D. Chattopadhyay, and A. Bandyopadhyay, "Uniquely different PVA-xanthan gum irradiated membranes as transdermal diltiazem delivery device," *Carbohydr. Polym.*, vol. 95, no. 1, pp. 252–261, 2013.

[93] M. Grembecka, "Sugar alcohols—their role in the modern world of sweeteners: a review," *Eur. Food Res. Technol.*, vol. 241, no. 1, pp. 1–14, 2015.

[94] S. M. and J. R., "The biotechnological production of sorbitol," *Appl. Microbiol. Biotechnol.*, vol. 59, no. 4–5, pp. 400–408, 2002.

[95] R. G. Loughlin, M. M. Tunney, R. F. Donnelly, D. J. Murphy, M. Jenkins, and P. a. McCarron, "Modulation of gel formation and drug-release characteristics of lidocaine-loaded poly(vinyl alcohol)-tetraborate hydrogel systems using scavenger polyol sugars," *Eur. J. Pharm. Biopharm.*, vol. 69, no. 3, pp. 1135–1146, 2008.

[96] I. Arvantoyannis, "Physico-chemical studies od chitosan-poly(vinyl alcohol) blends plasticized with sorbitol sucrose." 1997.

[97] A. Lazaridou, H. Vaikousi, and C. G. Biliaderis, "Effects of polyols on cryostructurization of barley beta-glucans," *Food Hydrocoll.*, vol. 22, no. 2, pp. 263–277, 2008.

[98] Y.-H. Yun, Y.-H. Na, and S.-D. Yoon, "Mechanical Properties with the Functional Group of Additives for Starch/PVA Blend Film," *J. Polym. Environ.*, vol. 14, no. 1, pp. 71–78, 2006.

[99] A. N. Frone, “Preparation and characterization of PVA composites with cellulose nanofibers obtained by ultrasonication,” vol. 6, pp. 487–512, 2011.

[100] C. B. Manufacturing, C. R. Specimens, T. Determina-, and S. V. Sheets, “Standard Test Methods for Vulcanized Rubber and Thermoplastic Elastomers —,” pp. 1–14, 2016.

[101] R. Burkhardt, A. Preiss, A. Joss, and N. P. Lang, “Influence of suture tension to the tearing characteristics of the soft tissues: An in vitro experiment,” *Clin. Oral Implants Res.*, vol. 19, no. 3, pp. 314–319, 2008.

[102] D. Askeland, P. Fulay, and W. Wright, “The science and engineering of materials,” *Sci. Eng. Mater.*, pp. 650–651, 2010.

[103] R. De Santis, F. Sarracino, F. Mollica, P. A. Netti, L. Ambrosio, and L. Nicolais, “Continuous fibre reinforced polymers as connective tissue replacement,” *Compos. Sci. Technol.*, vol. 64, no. 6, pp. 861–871, 2004.

[104] T. C. Doehring, E. O. Carew, and I. Vesely, “The effect of strain rate on the viscoelastic response of aortic valve tissue: A direct-fit approach,” *Ann. Biomed. Eng.*, vol. 32, no. 2, pp. 223–232, 2004.

[105] I. M. Ward and P. R. Pinnock, “The mechanical properties of solid polymers,” *Br. J. Appl. Phys.*, vol. 17, no. 1, pp. 3–32, 2002.

[106] D. Palomba, G. E. Vazquez, and M. F. Díaz, “Prediction of elongation at break for linear polymers,” *Chemom. Intell. Lab. Syst.*, vol. 139, pp. 121–131, 2014.

[107] L. Mohammed, M. N. M. Ansari, G. Pua, M. Jawaid, and M. S. Islam, “A Review on Natural Fiber Reinforced Polymer Composite and Its Applications,” vol. 2015, 2015.

Appendix A: Dilution Method for PVA-Composite

For accurate comparison with control, the PVA concentration in the composite or blends must be kept constant at 10 wt. %. As a result, the concentration of PVA in initial solution must be sufficiently high so that by adding water and fillers (particles or fibers) it will drop to target value (10 wt. % PVA). The target value is $C_{p,2}$ which is concentration of PVA in final solution. There were two assumptions in calculations. First, the mass of water will be constant for solution "1" and solution "2" (no water is lost): $M_{w,1} = M_{w,2}$. Second, the concentration of polymer (matrix and filler) will be higher in final solution due to water loss. Solution "1" and solution "2" refer to just PVA solution and PVA and filler solution, respectively.

$$M_{s,1} = M_{s,1} \times C_{p,1} + M_{w,1}$$

$$M_{w,1} = M_{s,1} - M_{s,1} \times C_{p,1}$$

$$M_{w,1} = M_{s,1}(1 - C_{p,1}) \qquad \text{Eq.1}$$

$$M_{s,2} = M_P + M_F + M_{w,2}$$

$$M_{w,2} = M_{s,2} - M_P - M_F \qquad \text{Eq.2}$$

$$M_{w,1} = M_{w,2} \qquad \text{Eq.3}$$

By substituting Eq.1 and Eq.2 into Eq.3:

$M_{s,1}(1 - C_{P,1}) = M_{s,2} - M_P - M_F$ *And* $M_{P,2} = C_{P,2} \times M_{s,2}$

$$M_{s,1}(1 - C_{P,1}) = M_{s,2}(1 - C_{P,2}) - M_F$$

$$\frac{M_{s,1}(1 - C_{p,1})}{M_{s,2}(1 - C_{p,2})} = 1 - \frac{M_F}{M_{s,2}(1 - C_{p,2})}$$

$$\frac{M_{s,1}(1 - C_{P,1})}{M_{s,2}(1 - C_{p,2})} = 1 - \frac{M_F}{M_{s,2}(1 - C_{P,2})}$$

$$C_F = \frac{M_F}{M_{s,2}} \; and \; \frac{M_{s,1}}{M_{s,2}} = \frac{C_{P,2}}{C_{P,1}}$$

$$\frac{C_{P,2}(1-C_{P,1})}{C_{P,1}(1-C_{P,2})} = 1 - \frac{C_F}{(1-C_{P,2})}$$

$$\frac{C_{P,2}}{C_{P,1}}\left(1-C_{P,1}\right) = \left(1-C_{P,2}\right) - C_F$$

$$\frac{C_{P,2}}{C_{P,1}} - C_{P,2} = 1 - C_{P,2} - C_F$$

$$C_{P,1} = \frac{C_{P,2}}{(1-C_F)} \qquad \text{Eq.4}$$

Where:

$M_{s,1}$ mass of solution "1", g,

$M_{s,2}$ mass of solution "2", g,

$C_{P,1}$ concentration of PVA in solution "1", wt.%,

$C_{P,2}$ concentration of PVA in solution "2" (which is 0.1), wt.%,

$M_{w,1}$ mass of water in solution "1", g,

$M_{w,2}$ mass of water in solution "2", g

M_P mass of PVA, g,

M_F mass of fibers, g.

The initial solution was made with 15 wt. % PVA as described in section 3.2.1. The actual concentration of solution was determined by the following procedure. A small piece of aluminum foil was cut and weighed, and the PVA solution was poured on aluminum foil and weighed. The aluminum foil with PVA was put in the oven at 185 degrees of Celsius for one hour. After one hour, the sample was weighed and the value recorded. Consequently, the sample was weighed every 10 minutes until the weight was constant for two consecutive measures. At this level, all water is evaporated and the actual concentration of PVA was found. The actual concentration of PVA was calculated by the following equation:

$$(C_{P,1})_{Actual} = \frac{(M_n - M_{Al})}{(M_1 - M_{Al})} \qquad \text{Eq.5}$$

Where:

$(C_{p,1})_{Actual}$ actual concentration of PVA, wt. %,

M_n final mass of the sample, g,

M_1 initial mass of the sample, g,

M_{Al} mass of aluminum foil, g.

After calculating $(C_{P,1})_{Actual}$ and $C_{P,1}$ values, initial PVA solution was poured in four different containers. The amount of poured PVA solution in each container was weighed and recorded. For reaching to target concentration of PVA, distilled water and filler must be added to solution. By considering $(C_{P,1})_{Actual}$ and $C_{P,1}$ values, the amount of added water can be calculated with following equation:

$$(C_{P,1})_{Actual} \times M_{RS} = C_{P,1}(M_{RS} + (M_w)_{add})$$

$$(C_{P,1})_{Actual} \times M_{RS} = C_{P,1} \times M_{RS} + C_{P,1} \times (M_w)_{add}$$

$$(M_w)_{add} = M_{RS}\left(\frac{(C_{P,1})_{Actual}}{C_{P,1}} - 1\right) \quad \text{Eq.6}$$

Where:

$(M_w)_{add}$ mass of added water, g,

M_{RS} mass of poured PVA solution in each container, g,

$(C_{P,1})_{Actual}$ actual concentration of PVA, wt. %.

By adding water to the solution, mass of solution will increase:

$$(M_{s,1})^{After} = M_{RS} + (M_w)_{add} \quad \text{Eq.7}$$

$$(M_{s,1})^{After} \times C_{P,1} = (M_{s,2})^* \times (C_{P,2})^*$$

$$(M_{s,2})^* = \frac{(M_{s,1})^{After} \times C_{p,1}}{(C_{P,2})^*} \quad \text{Eq.8}$$

Where:

$(M_{s,1})^{After}$	mass of solution after water is added, g,
M_{RS}	mass of poured PVA solution in each container, g,
$(M_w)_{add}$	mass of added water, g,
$C_{P,1}$	concentration of PVA in just PVA solution, wt.%,
$(C_{P,2})^*$	concentration of PVA in final solution (which is 10 wt. %), wt. %,
$(M_{s,2})^*$	mass of final solution, g.

Mass of filler can be calculated by following equation:

$$M_F = C_F \times (M_{s,2})^* \quad \text{Eq.9}$$

Where:

M_F	mass of filler, g,
C_F	concentration of filler, wt. %,
$(M_{s,2})^*$	mass of final solution.

The calculated value for water and filler was added to initial PVA solution and mixed properly. Mixing continues until fully dispersed solution with Chitosan is obtained.

For PVA-MCC solution preparation:

The initial solution with 15 wt. % of PVA was prepared using the same procedure described in section 3.2.1; And followed by same methodology for calculating actual concentration of PVA $(C_{p,1})_{Actual}$. The prepared solution was transferred into four different containers. The weight of each solution in the container was recorded. Each container was labeled by name and weight of PVA solution. Mass of added water for four different fiber concentrations (1.5, 3, 4.5, 6 wt. %) was calculated by utilizing Eq.6. Distilled water based on calculated values form Eq.6 were poured into four different jars. These jars were marked with an identification name, mass of added distilled

water, and concentration of filler. Mass of filler was measured by Eq.9. Calculated value for mass of filler were dispersed and stirred in each jar.